UILU-ENG-72-2005

Annual Report

on

INFLUENCE OF PORE WATER PRESSURE ON THE ENGINEERING PROPERTIES OF ROCK

Submitted to

Advanced Research Project Agency, ARPA
and its agent
Bureau of Mines, Department of Interior

by

G. Mesri

R.A. Jones K. Adachi

Department of Civil Engineering
University of Illinois
Urbana, Illinois

February 1972

Unclassified
Security Classification

3200.8 (Att 1 to Encl 1)
Mar 7, 66

DOCUMENT CONTROL DATA - R & D

(Security classification of title, body of abstract and indexing annotation must be entered when the overall report is classified)

1. ORIGINATING ACTIVITY (Corporate author)

Department of Civil Engineering
University of Illinois, Urbana, Illinois

2a. REPORT SECURITY CLASSIFICATION

Unclassified

2b. GROUP

3. REPORT TITLE

INFLUENCE OF PORE WATER PRESSURE ON THE ENGINEERING PROPERTIES OF ROCK

4. DESCRIPTIVE NOTES (Type of report and inclusive dates)

Annual Report, Nov. 1970 - Nov. 1971

5. AUTHOR(S) (First name, middle initial, last name)

Gholamreza Mesri
Ronald Jones
Kakuichiro Adachi

6. REPORT DATE

February 1972

7a. TOTAL NO. OF PAGES

109

7b. NO. OF REFS

41

8a. CONTRACT OR GRANT NO.

H0110085

b. PROJECT NO.

ARPA Order No. 1579

c. Program Code No. 0F10
Work Unit No. F53213

d.

9a. ORIGINATOR'S REPORT NUMBER(S)

3

9b. OTHER REPORT NO(S) (Any other numbers that may be assigned this report)

10. DISTRIBUTION STATEMENT

Distribution of this document is unlimited

11. SUPPLEMENTARY NOTES

12. SPONSORING MILITARY ACTIVITY

Advanced Research Project Agency, ARPA

13. ABSTRACT

Five series of unconfined compression tests were performed on intact samples of Barre Granite, Berea Sandstone, Clinch Sandstone, Nevada Tuff and Yule Marble, with strain rates varying from 0.0001 inch/inch/min. to 10/0 inch/inch/min. In each series tests were performed on dry and saturated specimens. The test results are summarized and correlations were presented between unconfined compression strength and strain rate. The results indicated that the presence of pore water may produce effects on the shear strength of rock in terms of pore pressures which change effective normal stresses and/or deleterious physico-chemical interaction with mineral grains.

A special triaxial cell was designed and constructed. This cell was used to saturate rock specimens, measure rock permeabilities, and measure rock pore water pressures under changes in all-around confining pressures.

A comprehensive literature survey was made in order to review and summarize published theoretical and experimental studies of pore pressure effects in rock and other porous materials. Most previous results confirm the applicability of Terzaghi's effective stress equation to rock.

DD FORM 1 NOV 65 1473

Unclassified
Security Classification

14. KEY WORDS	LINK A		LINK B		LINK C	
	ROLE	WT	ROLE	WT	ROLE	WT
pore water pressure						
rock						
engineering properties						
unconfined compression strength						
strain rate						
compressibility						
porosity						

UILU-ENG-72-2005

Annual Report

on

INFLUENCE OF PORE WATER PRESSURE ON THE ENGINEERING PROPERTIES OF ROCK

Submitted to

Advanced Research Project Agency, ARPA
and its agent
Bureau of Mines, Department of Interior

by

G. Mesri

R.A. Jones K. Adachi

Department of Civil Engineering
University of Illinois
Urbana, Illinois

February 1972

Annual Report

on

INFLUENCE OF PORE WATER PRESSURE ON THE ENGINEERING PROPERTIES OF ROCK

Sponsored by
Advanced Research Projects Agency
ARPA Order No. 1579

Monitored by

Bureau of Mines, Department of Interior
under Contract No. H0110085
Program Code Number 0F10

Effective Date of Contract	November 1, 1970
Contract Expiration Date	November 1, 1971
Amount of Contract	$ 34,000

Report Submitted by
Department of Civil Engineering
University of Illinois
Urbana, Illinois

Principal Investigator	G. Mesri, Ext. 217-333-6934
Project Scientist	G. Mesri, Ext. 217-333-6934

February 1972

CONTENTS

ILLUSTRATIONS

TABLES

SECTION 1

INTRODUCTION

1.1 Statement of Problem

In rock, resistance to deformation and failure is developed by the intrinsic shear strength of minerals and shearing resistance at mineral contacts. The shearing resistance at mineral contacts is controlled by the frictional characteristics of mineral surfaces and intergranular contact stresses as well as by the cohesive bonds at the contacts. Pore water as a component of rock could alter the shearing resistance at mineral contacts in two distinct ways. The pressure in pore water can either decrease or increase intergranular contact stresses. Pore water could interact with mineral surfaces and alter their surface properties as well as the nature of bonding (Horn and Deere, 1962). The pore water pressure in rock could be due to a static water head, due to steady state seepage, or generated by a permanent or transient change in the state of total stress. The pore water (or joint-water) pressures can develop and be controlled by both the jointed and intact portions of the rock mass. Under many field conditions, the permeability, compressibility, and dilatancy of the joints control the maximum pore pressures which can develop during compression or distortion of the rock mass. However, under other conditions significant pore pressures can develop in the intact portion of the rock mass, particularly when the intact specimen has a relatively high compressibility, a low dilatancy during shear, and is loaded rapidly (for example, at the load rates for which a protective structure is

designed or rates corresponding to rapid excavations).

1.2 Literature Survey

The importance of the influence of pore water and pore water pressure on the engineering properties of rock has been recognized by many investigators, and the problem has been studied by theoretical and experimental means. A literature survey was made in order to review and summarize all published theoretical and experimental studies of pore pressure and effective stress in rock and other similar porous media. A summary of each study follows.

Zisman (1933) measured the linear compressibilities of twenty-eight rock types on both jacketed and unjacketed samples, measurements being taken at $30^{o}C$ and up to pressures of 840 kg/cm^2. He computed the cubic compressibilities by tripling the mean of the linear compressibilities measured on three mutually perpendicular samples for each rock type. The samples were eight inches in length and five-eighths of an inch in diameter. Kerosene was used to supply the confining pressure, jacketed samples being enclosed in 0.0002-inch annealed copper foil. The compressibility of jacketed samples was shown to be much greater than that of unjacketed samples at low pressures. At high pressures the values of the compressibility of jacketed samples tended to reduce those of the unjacketed samples, which showed only slight reductions in compressibilities with increase in pressure. He noted that smaller amounts of permanent set were observed in unjacketed tests compared to jacketed tests, and the more porous rocks exhibited the greatest amount of permanent set. Zisman stated the likely errors in the results to be of the order of 2% for compact rocks, with errors up to 5% for values obtained when the rock showed a rapid change in compresibility with

pressure. Several of the rocks tested, namely Sudbury norite, peridotite, orthogneiss, quartzitic sandstone and Vermont marble and limestone showed no change in linear compressibility in either one or two of the directions measured, when tested in the unjacketed state.

Griggs (1936) carried out a series of unjacketed tests on Solenhofen limestone and marble samples at confining pressures up to 11,000 atmospheres. Sample size was 1 inch long and 1/2 inch diameter. Two jacketed tests on the limestone were also carried out. The samples subjected to unjacketed tests showed an appreciable increase in compressive strength with increase in confining pressure. The jacketed samples indicated much greater compressive strengths than unjacketed samples at the same confining pressure. The pressures used in the unjacketed tests were exceptionally high compared to those considered in rock mechanics problems. Skempton (1960) shows results of the unjacketed tests as a plot of compressive strength against confining pressure. This is the only reference which has shown an increase of compressive strength with increase in confining pressure in unjacketed tests.

Terzaghi (1945) considered mechanisms of failure on a shear surface through a porous rock or concrete material, when the pores are filled with a fluid under pressure, to postulate the effect of the water pressure on the applied stresses. From the results of jacketed triaxial compression tests on dry samples by von Karman (1911), Richart, Brandzaeg and Brown (1928), and Ros and Eichinger (1928), he concluded that failure occurred in the bonds joining grains of the rock or concrete, based on the consistent increase in strength obtained with increase in confining pressure. From the results of unjacketed triaxial compression tests on concrete by Terzaghi (1934)

and on marble by Griggs (1936), he concluded that no appreciable increase in compressive strength was observed when the confining pressure was increased. He postulated that a sinuous failure surface through the points of contact of the bonds would allow pore fluid to act almost over the entire area of the failure surface and thus reduce the normal force on the failure surface by a proportion of the pore pressure. He used the term 'boundary porosity, n_b' to describe this area of pore fluid contact and concluded that n_b must be close to unity to explain the results of the unjacketed tests. Thus in this case, $\bar{\sigma} = \sigma - u$, defined the effective stress, where σ = total applied stress and u = pore fluid pressure.

For the general case of pore pressure at a lower value than confining pressure in a triaxial compression test, he postulated that up to confining pressures of 20 tons/ft^2 the principle of effective stress $\bar{\sigma} = \sigma - u$ would approximately determine the effective stress. Beyond this value, he stated that triaxial tests would be required to determine a suitable relationship. This conclusion was based on compressibility tests carried out by Zisman (1933) on jacketed and unjacketed samples of rock which showed that up to 20 tons/ft^2, the compressibility of a jacketed sample was still much greater than that of an unjacketed sample and thus the boundary porosity would still be close to unity. Beyond this arbitrary value of 20 tons/ft^2 the compressibility of the jacketed sample gradually decreased and approached that of the unjacketed sample at very high pressures. At this stage the boundary porosity of the jacketed sample was considered to be close to zero. Although not stated, the approach by Terzaghi appears to assume that the effective stress controlling shear strength is the same as that controlling volume change.

Skempton (1954) introduced the concept of the pore pressure coefficients A and B to describe the change in pore pressure in a soil resulting from a change in applied total principal stresses under undrained loading. Skempton expressed the change in pore pressure for undrained loading as

$$\Delta u = B[\Delta\sigma_3 + A(\Delta\sigma_1 - \Delta\sigma_3)]$$

where Δu = change in pore pressure
$\Delta\sigma_1$ = change in total major principal stress
$\Delta\sigma_3$ = change in total minor principal stress
A = pore pressure coefficient describing change in pore pressure for applied shear stress (Deviator Stress)
B = pore pressure coefficient describing change in pore pressure for an equal all-round confining pressure increase.

A and B can be measured experimentally in an undrained triaxial test. Ignoring the compressibility of the soil grains, the value of B was shown to be

$$B = \frac{1}{1-nC_r/C_c}$$

where n = porosity
C_r = compressibility of the void fluid
C_c = compressibility of the soil skeleton

For saturated soils it was pointed out that B would be equal to 1 as $\frac{C_r}{C_c} \to 0$. For a soil behaving in accordance with elastic theory, A would have the value 1/3. However it was noted that in general this would not be the case, and A would vary with stress and strain and would not have a constant value.

The assumption of the applicability of the principal of effective stress is included in the derivation of the above equations. Until the effective stresses acting in rock are known it will not be possible to derive equations which can be tested by experimental measurements, other than by comparing postulated equations to experimental results which do not require effective stress analyses.

One other variable required to derive meaningful relations for rock pore pressure coefficients is the compressibility of the soil grains.

Bredthauer (1957) tested various rock samples 1" long by 1/2" diameter at various confining pressures up to 15,000 psi. The samples were tested dry and jacketed, with the exception of tests run on a sandy shale, where unjacketed and saturated-jacketed tests were carried out. Increases in compressive strength with increasing confining pressure were obtained on all formations tested dry and jacketed. Brittle to ductile transitions were obtained on anhydrite, Carthage marble, the sandy shale, coarse Chico limestone and shale specimens. The remainder of the rocks experienced brittle failure for the range of confining pressure used. These included White dolomite, fine Chico limestone, Rush Springs sandstone, Knippa basalt, and Virginia limestone. Samples subjected to unjacketed tests showed virtually no increase in compressive stress compared to dry samples tested at atmospheric pressure. In the case of the sandy shale, two specimens were tested saturated and jacketed. Lower yield stresses were obtained for these specimens compared to dry jacketed specimens at the same confining pressures (5,000 psi and 10,000 psi). Both series of samples showed ductile failure. The only conclusion that can be drawn from the results is that the effective confining pressure was reduced due to pore pressure in the samples. The samples were probably reducing in volume at the yield stage of the test and allowing a positive pore pressure to be generated.

Robinson (1959) carried out triaxial tests on Indiana limestone, Carthage marble, two sandstones and a shale in which pore pressure was controlled at different values independently of confining pressure. Samples were 1.5" long by 0.75" in diameter, and axial load was applied

at a constant rate of 0.15% per second. Pore fluid pressure was held at a constant value throughout each test. The yield point was arbitrarily selected as the stress level necessary to deform the specimen 0.2% beyond the proportional limit. Using the above mentioned criteria of failure, he noted that the mode of failure was controlled by the difference between the confining pressure and the lower pore pressure, with a gradual change from brittle to malleable failure occurring as the difference increased from zero to 10,000 psi. Microscopic examination of the Indiana limestone samples showed conically shaped regions adjacent to the top and bottom platens. These regions did not yield during deformation. Plastic deformations occurred after yielding in the zones outside the cones of fracture, the crystals shearing apart as deformation increased. He noted that at equal pore and confining pressures, failure was generally characterized by one distinct failure plane, whereas as the differential pressure increased, an increasing number of failure planes were observed. Samples decreased in volume during the linear part of the stress strain curve and increased in volume beyond the yield stress.

That the mode of deformation changed, as the difference between confining pressure and pore pressure was increased, is clear evidence that the effective stress was increased. For the Pictured Cliff sandstone (brittle failures) the results show that the principle of effective stress, $\bar{\sigma} = \sigma - u$, is operative, as essentially constant strengths were obtained at constant effective confining pressure. For the remainer of the results no definite conclusions can be drawn owing to the arbitrary failure criteria chosen and the fact that pore pressure distribution in the failure zone cannot be assumed to be the same as that applied. This is inferred as a result of testing the

samples at constant strain and the observation that non-uniform stress distributions occurred in the samples during ductile failure as evidenced by the formation of cones at the platens.

Heard (1960) conducted more than 115 triaxial compression and extension tests on mechanically isotropic, homogeneous Solenhofen limestone to determine the transition from brittle fracture to ductile flow as a function of temperature, confining pressure, and interstitial fluid pressure. The tests were carried out at a constant strain rate of 0.01% per second, on samples with a 0.5-inch diameter by 1-inch length. The temperature range was 25°C and the confining pressure range 1 to 5,000 atmospheres.

Heard concluded: (1) that for a given temperature and confining pressure corresponding to a ductile mode of failure for a sample tested dry, the behavior of the limestone changed from ductile to brittle as the interstitial fluid pressure was increased. (2) The effects of interstitial fluids at any pressure on the strength of the Solenhofen limestone may be neglected provided the sample fails in a ductile mode. This applied to any temperature less than 480°C and confining pressure greater than 1000 atmospheres. (3) Brittle-ductile transitions did not occur at constant effective confining pressure at any one temperature. Thus the principle of effective stress was not valid in this case. He noted that brittle failure was characterized by wedge splitting, with shearing localized on one or occasionally two planes and prominent slickensides being formed on the shear fractures. Near the brittle ductile transition the shear fractures were observed to be coated with a friable mylonite layer. In ductile failure, nearly homogeneous flow occurred. Fluid saturation of the samples was not

definitely proven by the author in his discussion of this point. A correlation of principal effective stresses at failure for brittle samples was not presented although this relation could be determined from the data presented.

Skempton (1960) derived expressions for effective stress in soils or porous solids in relation to changes in shear strength and compressibility, by considering two dimensional conditions of equilibrium at particle contacts. Three theories of shear strength were postulated to apply at the contact; the resulting three expressions for effective stress being tested against published data to determine the most correct expression. In considering compressibility, he applied two of the foregoing expressions for effective stress to the basic compressibility equation and derived a third expression from basic principles. He then compared the predictions of these three expressions to published data as was done for shear strength.

The equations concluded to be the most accurate were

for shear strength, $\bar{\sigma} = \sigma - \left(1 - \frac{a \tan \psi}{\tan \phi'}\right) u_w$ (1)

for compressibility, $\bar{\sigma} = \sigma - \left(1 - \frac{C_s}{C}\right) u_w$, (2)

where a is the area of contact between the particles per unit of gross area, ψ and C_s are the angle of intrinsic friction and the compressibility of the solid substance comprising the particles, ϕ' and C are the angle of shearing resistance and the compressibility of the porous material, and u_w is the pore water pressure.

The expressions for shear strength rejected were

$$\bar{\sigma} = \sigma - (1-a)u_w$$

$$\bar{\sigma} = \sigma - u_w$$

These two adopted expressions were also used to represent the effective stress in the compressibility equation $-\frac{\Delta V}{V} = C_s \bar{\sigma}$.

The assumptions used to determine the above expressions for effective stress, i.e., eqs. (1) and (2), were that shear strength of the particles could be defined by $\tau_i = K + \sigma \tan \psi$, the shear strength at the contact being defined by $\tau_s = \beta K + \sigma_s \tan \psi_s$, where β is a factor less than 1 and ψ_s less than ψ. σ_s is the normal stress at the contact, and K is the intrinsic cohesion.

Although not stated specifically, the effective stress controlling shear strength appears to have been derived for conditions of no volume change. The effective stress equation for compressibility has been derived for conditions of uniform all round effective stress change. The shear strength-effective stress equation was compared to published data of failure conditions. The derivations assume that failure occurs at the particle contacts. In the case of compressibility, void ratio is not explicitly considered although it is a function of C.

Boozer, Hiller and Serdenegecti (1963) carried out triaxial compression tests on samples of Navajo sandstone (1" long by 0.5" diameter) and Indiana limestone (1.5" long by 0.75" diameter) in which the pore fluids were oleic acid, oleylamine, distilled water and n-hexadecane. Samples were tested up to 20,000 psi confining pressures, temperatures between 78 and 300°F , and applied strain rates in the range 0.001% to 13% per second. Tests were run with pore pressure lower than confining pressure in one series on limestone, the remainder of the samples being tested with zero pore pressure.

The conclusions regarding each rock type were as follows:

Indiana limestone. The predominant effect of the fluids, with the exception of n-hexadecane, was a decrease in the yield stress of

the limestone. Above 1000 psi confining pressure, all samples failed in a ductile manner, except when saturated with oleic acid when brittle failure occurred to confining pressures above 1000 psi. They postulated that these results were due to ductile yield being dependent on free surface energy which is affected by the adsorption of the saturation fluid. Ionic bonding was the mechanism stated to be operative in accomplishing adsorption on the calcite surface of the grains.

Navajo sandstone. The ultimate strength of the sandstone was decreased by the saturating fluids. They postulated that adsorption of fluids by hydrogen bonding, on the quartz surfaces of the grains, was the mechanism responsible for the reduction of free surface energy and reduced strength. At high temperature ($260^{o}F$ or more), the fluids had little effect on the strength of the sandstone due to a reduction of hydrogen bonding.

The order of strength reduction lay in the range 0 to 24% for the limestone and 0 to 13% for the sandstone, depending on the saturating fluid, level of confining pressure and temperature. The results of the series of tests on the limestone with 10,000 psi confining pressure and 5,000 psi pore pressure, indicated an effective confining pressure intermediate between 5,000 and 10,000 psi to be operative.

The authors refer to P. A. Rebinder and V. Likhtman (1957) for a detailed discussion of the nature of the phenomenon of the reduction of free surface energy on various solids brought about by adsorption. The results of the tests carried out show that effective stress is not just a function of the mechanical effects of the pore fluid on the rock structure.

Handin et al (1963) reported the results of triaxial compression tests on 1/2" diameter by 1" long samples of Hasmark dolomite, Marianna limestone, Berea sandstone, Muddy shale and Repetto siltstone. For shale samples only unjacketed tests were carried out. The remaining rock types were tested with independently applied confining and pore pressures within the range 0 to 2 kilobars (0 to $\simeq 29 \times 10^3$ psi), with both pressures being held constant throughout a test. A constant strain of 1% per minute was used, and the samples were loaded perpendicular to bedding planes.

They concluded: (1) The concept of effective stress (Terzaghi, 1923) is applicable to rocks and controls the ultimate strength and ductility of the rock, provided (a) the interstitial fluid is inert relative to the rock minerals, (b) the permeability of the rock is sufficient to allow pervasion of the fluid and to permit the fluid to flow freely through the rock during deformation so that the pore pressure remains constant. This second requirement was found valid when rock was a sand-like aggregate with connected pore space, the configuration of which insured that the pore pressure was transmitted fully throughout the solid phase. The results for sandstone and limestone showed that the principle of effective stress was valid. The siltstone also behaved in this manner when (a) was satisfied, i.e., when kerosene was used instead of water. Shale was not tested with differing confining and pore pressures, but partial pore pressure effects were deduced from the unjacketed tests. In the case of crystalline rocks of low porosity such as Hasmark dolomite, the principle of effective stress was not found to be valid. The authors assumed that condition (b) had not been fulfilled in this rock. (2) The permanent shortening of porous sedimentary rocks is accompanied by a

reduction of porosity wherever the ratio of pore pressure to confining pressure is of the order of 0.6 or less. At ratios of 0.6 to 0.8, the pore volume remains essentially constant, but above 0.8 the porosity increases and the rocks are dilatant. The conclusions with respect to the application of the principle of effective stress were deduced from plots of effective principal stresses at failure, on which the results of dry samples and those with pore pressure were plotted.

A Fracture Index was defined and used to estimate the degree of grain fracturing occurring at various levels of effective confining pressure. For sandstone the greatest degree of fracture occurred for samples exhibiting a decrease in porosity. Ultimate compressive strengths were measured in all samples. In the case of the Hasmark dolomite, ductile failure was not observed in the range of pressures used in the tests.

Schwartz (1964) reported triaxial tests with constant pore pressure lower than confining pressure as part of a general investigation into the shear strength of rock. A review of previous experimental work is included in this paper. Triaxial tests were carried out with a constant confining pressure of 5,000 psi and with constant pore pressures of 1,000, 3,000 and 5,000 psi. The rocks tested were a limestone and sandstone with void ratios of 0.2, and a marble and granite with void ratios of 0.02. Sample size was 7/8" diameter by 1 3/4" height. All the samples were reported to have failed in a brittle manner. The strengths of the sandstone and limestone, $\sigma_1-\sigma_3$, were essentially the same as when tested dry at the same effective confining pressure, whereas the strengths of the granite and marble were reduced compared to dry specimens at the same effective confining pressure, the reductions in each case being essentially constant ir-

respective of the value of pore pressure. Deformation rates were in the range of 0.005 to 0.002 inches/minute. The results obtained for the granite and marble samples are anomalous. If the pore pressure did not communicate through the sample, the effect would be to increase the effective confining pressure and thus the strength, due to a reduction in pore pressure produced by volume increase during shear.

Colback and Wiid (1965) presented the results of the effect of moisture content on the uniaxial and triaxial compressive strengths of a quartzitic shale and a quartzitic sandstone. The porosities of these rocks were 0.28% and 15% respectively. Sample size was either 0.845" diameter by 1.7" length or 1" diameter by 2" length. Samples tested uniaxially were loaded at 100 psi/second to failure, and samples in triaxial testes were loaded to failure by increasing σ_1 and σ_3 at a constant ratio of σ_1/σ_3. Samples were stored at a relative humidity of 50% $\pm$ 5% and a constant temperature of 20°C $\pm$ 1.1°C , until they attained a stable moisture content. This was the datum to which test moisture content was referred. Both rocks showed a 50% reduction in uniaxial compressive strength over a moisture content range representing 'dry' and 'saturated' conditions. The results of the triaxial tests gave a constant Mohr fracture envelope whether tested dry or saturated but with the 'cohesive' intercept for the saturated samples being lower than that obtained for dry samples.

A series of uniaxial tests was carried out on 'saturated' quartzitic sandstone samples in which the strength of the samples, with differing pore fluid, was compared to the surface tension of the fluids. A linear relationship was obtained showing a reduction in strength with increasing surface tension of the fluid.

It was concluded that for a quartzitic rock there is a reduction in uniaxial compressive strength, from the dry to the saturated condition, that is dependent on the reduction of the surface free energy of quartz produced by the presence of the fluid. The rate of decrease in strength with increasing moisture content was attributed to the differences in porosity of the two materials.

The importance of moisture content with respect to compressive strength test results is clearly shown by the results of the experiments. The reductions in strength observed were postulated to be only a function of surface energy effects of the pore fluid. As the time to failure was relatively short in the uniaxial tests, the effects of pore pressures would be a factor to be considered in explaining the reductions in strength observed.

Brace and Byerlee (1966) summarized four areas of interest in the study of brittle fracture of rock: (1) the volume changes which accompany brittle fracture, (2) the propogation of cracks in compression, (3) frictional characteristics of rocks and minerals at high pressure, and (4) the law of effective stress for crystalline rocks.

The following conclusions were reached: Dilation is due to the formation of cracks beginning at a stress level of one-third to two-thirds of the fracture stress appropriate to the confining pressure of the test. Brittle fracture is due to the growth and interaction of cracks. Stress concentration in a single crack decreases with crack growth under compression and thus interaction must be of importance in the process of sample fracture. Formation of arrays of cracks seems to be a possibility, although the mechanisms of final fracture are not known. Friction is dependent on the roughness of the sliding

surfaces, the failure of asperities being postulated to be the result of brittle failure. The effective normal stress is the other factor on which the value of friction is most dependent.

Results were presented to show that the relationship at fracture between the maximum and minimum principal stresses was essentially the same for samples of granite tested triaxially with and without pore pressure. They reviewed the work of Heard and Handin and suggested the conclusion that the law of effective stress holds for all rocks except carbonate rocks of low porosity. They were of the opinion that the carbonate minerals flowed plastically under compressive stress and thus would impede the flow of water through the sample where this occurred. They noted that the law would not appear to hold where the deformation rate exceeded the rate at which pore pressure can be transmitted through the rock. They raised the question as to what proportion of porosity found in laboratory samples was a result of removal of the sample from the rock body. This comment applied particularly to the dense crystalline rocks.

The possibility of porosity arising as a result of cracks which do not have access to pore fluid was raised by the authors, as a result of measurements on marble which showed an increase in resistivity when the rock was dilatant. Any theoretical treatment of effective stress would require taking this phenomenon into account. The extent to which this occurs in various rocks and the proportion of porosity due to such cracks at differing stress levels requires investigation. Presumably when fracture finally occurs, pore fluid has access to the fracture surface, or else the experimental results surrporting the law of effective stress would not have been obtained.

Kjaernsli and Sande (1966) presented unconfined compression tests for syenite tested dry, saturated, and submerged. They concluded that the strengths of saturated, and saturated-submerged specimens are 94% and 85% respectively of the dry strength. The unconfined compression test samples referred to as saturated were recognized by the authors to be probably only partially saturated. Samples were placed in a water bath for 3 days at a temperature of 20°C to obtain 'saturation'. Rate of incremental loading was 100 kg/cm^2 every 2 minutes, which gave 28 to 40 minutes to failure. Sample size was 5 x 5 cm. square by 10 to 14 cm. high. The mechanisms causing reduction in strength were not discussed.

Kowalski (1966) proposed equations to correlate the compressive strength and void ratio for limestones and marls. He concluded that equations of the form $R = de^{-c}$ could express the relationship between strength, R, and void ratio, e, where d and c were constants for the type of strength considered, the rock type, and the test conditions. Thus d and c would differ for air-dried as opposed to saturated samples, and for samples tested perpendicular to bedding planes rather than parallel to bedding planes.

The type of strength considered was not clarified in the paper, although it would appear that uniaxial compressive strength was the strength referred to in the results presented for limestone and marl. The equations presented are purely empirical and show, as would be anticipated, that the compressive strength reduces as the void ratio increases, i.e., less grain connections with increased void ratio.

Trollope and Brown (1966) considered that intermolecular forces constituted a component of effective stress. They presented the equation of shear strength at failure on any plane of a two phase

system as

$$\tau_f = (\sigma_f - u_f + \rho_f) \tan \phi_f$$

where τ_f = shear strength at failure
σ_f = normal stress at failure
u_f = water pressure at failure
ρ_f = intermolecular force at failure
ϕ_f = friction angle determined at failure

For a granular material they considered that three fundamental modes of failure were possible at the particle contacts and presented equations describing shearing strength for each mode. These were:

Mode 1 - tensile failure, $\tau = f(\rho_f)$

Mode 2 - particle slip at the contact, $\tau_f = (\sigma_f - u_f + \rho_f) \tan \phi_f$

Mode 3 - shearing through a polycrystalline material with a positive pore pressure developed in the external voids, $\tau_f = C = (\rho_f + u_w) \tan \phi_f$

They were of the opinion that in a real granular rock material modes 2 and 3 occur together, and that splitting failure in uniaxial compression samples was a result of mode 1 failure. The treatment takes no account of void ratio and assumes that the principle of effective stress holds, in that the full water pressure is subtracted from the normal stress. The main point of interest in this paper is the concept that intermolecular forces are involved in shearing, although the mechanisms of the involvement are not explained.

Walsh and Brace (1966) discussed in general terms the character of porosity in rock and how the behavior of rock is determined by the type of porosity present. They noted that porosity in rock typically varies from 0.1 to 0.2 down to 0.001 to 0.002. In general the higher porosity rocks have voids as a result of the presence of pores, whereas low porosity rocks have porosity as a result of cracks. Pores tend to be equidimensional while cracks are postulated to have a maximum length to width ratio of 1000. The type of porosity present

in a rock was noted to be a function of its geological formation. While some rocks may have cracks and pores, the cracks would proportionally influence the bulk properties of the rock to the greater extent. They also discussed the differences in behavior of granite subjected to all round pressure compared to a uniaxial stress. It was noted that linear stress-strain behavior occurred under hydrostatic loading, whereas under uniaxial compression hysteresis was observed. It was concluded that this was caused by loss of energy in the system, due to friction opposing motion on the faces of cracks which had closed. They considered that a rock with porosity due to pores would behave as a linear elastic body, whereas a rock containing cracks may not.

Brace and Martin (1968) presented the results of triaxial tests, including pore pressure measurements, on crystalline silicate rocks to establish if the law of effective stress held for these materials. Rocks tested were granite, diabase, fine grained dolomite, gabbro, partly sepentised dunite and silica cemented sandstone. The experimental approach was to compare fracture strengths of each rock type at two different effective confining pressures. The confining pressures used were 1.56 kilobars and 3.12 kilobars with respective pore pressures of 0 and 1.56 kilobars. Pore pressure was maintained constant throughout the test and applied to one end of the sample. The sample size was 1.58 cm. diameter by 3.81 cm. length. Strain rates were varied over the range 10^{-1} to 10^{-6} percent per second for samples tested with and without pore fluid.

The strength of samples tested dry was observed to increase with increasing strain rate although the reason for this was not given. Samples with pore pressure were observed to have the same strength at low strain rate, but as the strain rate increased, an increase was

observed in the strength above a critical strain rate. This increase in strength was termed dilatancy hardening, and was ascribed to a drop in pore pressure within the sample due to dilatancy and a consequent increase in the effective confining pressure. Although the pore pressure was maintained constant during the test, it was noted that a lag in pore pressure equilibrium could occur between the exterior and interior of the sample as the strain rate increased and thus account for the unmeasured drop in pore pressure. A method of calculating the pore pressure within the sample under the above conditions was presented in the appendix to the paper. Estimated sample strengths based on this approach approximated the measured strengths in the case of granite. The authors concluded that the law of effective stress was applicable to low porosity crystalline rocks as long as loading rates were kept below the critical strain rates. The hypothesis presented by the authors to explain dilatancy hardening is really based on the principle of effective stress being valid, provided the correct pore pressure values are used.

Lane (1969), as part of a summary of the state of art with respect to effective stress controlling shear strength, presented the results of research undertaken by the Corps of Engineers, Missouri River Division. Specifically the results of load induced pore pressure tests (undrained tests) were presented for a porous sandstone. Current testing procedures of the Corps of Engineers (Miss. R. Div.) were outlined as: (1) sample size 2 1/8" diameter, 4 - 4 1/2" in height (i.e., NX core size), (2) measurement of pore pressure at both ends of the sample, and (3) use of back pressuring techniques to obtain full saturation. The details of the testing equipment have been presented by Neff (1966).

A Mohr failure envelope for Berea Sandstone (porosity 19%) for undrained tests plotted on the basis of effective stress (i.e., $\bar{\sigma} = \sigma - u$) was presented, and shown to be identical to the envelope obtained for drained tests. Samples tested air dry showed a slightly higher envelope at higher normal stresses. The axial stress-strain relationship and the pore pressure values obtained in undrained tests on Berea Sandstone were correlated with the fracture concepts of Bieniawski (1967). Thus the initial concave upward section of the stress-strain curve corresponded to the closing of microcracks at low stress levels. A linear section of the stress strain curve followed, corresponding to the propogation of microcracks, termed stable fracture propogation. Pore pressure increase was measured up to this stage of the test, although at a decreasing rate. This corresponded to the volume decrease shown by Bieniawski to occur in dry samples. A reduction in the slope of the stress strain curve followed, corresponding to unstable propogation of cracks, progressive failure, and finally rupture. Pore pressure decrease occurred during this latter phase of the test, becoming negative near rupture at the same point when the volume in a dry specimen would increase above the original volume. This is the first reference in which load induced pore pressures in rock are discussed. The test results confirm the principal of effective stress to be applicable to Berea Sandstone, however the porosity of this rock is very high and results on lower porosity rocks would be of more interest.

Wissa (1969) discussed the errors arising in pore pressure measurement in soils of low compressibility. He presented an expression for the pore pressure parameter B which included the compressibility of the pressure measuring system. This was :

$$B = \frac{\Delta u}{\Delta \sigma} = \frac{1}{1 + n\frac{C_w}{C_{sk}} + \left(\frac{V_L}{V_o}\right)\left(\frac{C'_w}{C_{sk}}\right) + \frac{(C_L + C_M)}{C_{sk}\ V_o}}$$

where V_o is the total volume of the test specimen, V_L the volume of fluid in the back pressure lines, C'_w the compressibility of the fluid in the pore water lines, C_L the compressibility of the pore water lines equal to the change in total internal volume of the lines per unit change in pressure, and C_M the compressibility of the pore pressure measuring element equal to the change in total volume for a unit change in pressure. He recommended that to minimize the errors in the measurement of pore pressures in saturated cemented soils the following modifications to standard procedure be specified:

(1) reduce the total volume of the pore pressure lines in the triaxial cell base to be at most 3% of the pore volume of the test specimen,

(2) measure pore pressures with a transducer having a compressibility no larger than 1.6×10^{-5} cc per kg/cm^2,

(3) seal the test specimen in a 0.04 cm. thick rubber membrane,

(4) use zero volume change, low leakage valves in the pore pressure lines,

(5) check for complete saturation by measuring the pore pressure response at several back pressures, keeping the effective consolidation pressure approximately constant (the pore pressure reponse should be constant), and

(6) for cemented soils the minimum consolidation pressure should be sufficiently high to prevent lateral surface drainage during the initial stages of undrained shear.

As noted by the author when the soil skeleton has a low

compressibility, it is required that the compressibility of the measuring system be taken into account. This factor is of even greater importance when dealing with rocks.

Robinson and Holland (1969) presented an expression for boundary porosity, n_b, (Terzaghi 1945) using a force analysis and Mohr's condition of failure. The equation presented was then tested against published data (Robinson 1959). He derived the following equation:

$$S = \frac{P_v}{3} + P_c - P_p\left(1 - \frac{A_G}{A_s}\right)$$

where

S = matrix octahedral stress = $\frac{\sigma_1+\sigma_2+\sigma_3}{3}$
A_G = area of grains on a section
A_s = area of section of failure surface considered
P_v = vertical piston force
P_c = confining pressure
P_p = pore pressure

This equation was obtained by a force analysis on two planes, perpendicular and parallel to the major axis of a triaxial sample. The above equation was then amended to

$$S = \frac{P_v}{3} + P_c - n_b P_p \qquad \text{where } n_b = 1 - \frac{A_G}{A_s}$$

Assuming that boundary porosity is the same for two samples failing at the same axial load and shear stress, for two different combinations of pore and confining pressure they obtained:

$$n_b = \frac{P_c - P'_c}{P_p - P'_p}$$

The equation was applied to the results presented by Robinson (1959). Pictured Cliffs sandstone was determined to have a boundary porosity of 100%, while Indiana limestone showed a decrease in n_b with increasing

confining pressure. They concluded that this latter result indicated a decreasing amount of the failure plane passed between the grains. It should be noted that the equation is only valid at failure and assume n_b is a constant for different combinations of pore and confining pressure for the same shear stress and axial load at failure.

Lee, Morrison and Haley (1969) discussed the reasons why the B coefficient values (Skempton 1954) have been measured less than one for saturated stiff soils. They concluded that values of B less than one were possible due to the term C_d, the compressibility of the soil structure, becoming relatively close to or even smaller than C_w, the compressibility of water. Normally C_d is much greater than C_w and hence B approaches unity. The value of C_s, the compressibility of the soil grains, is ignored in the calculation of B, which is allowable for soils.

They presented results of isotropic compressibility tests on various sands, which showed compressibility to decrease with increase in confining pressure. The lowest values were obtained for Ottawa sand, 20 to 9 x 10^{-6} in^2/lb for the pressure range 0 to 1000 psi. Tests carried out to measure B coefficients in Ottawa sand and Sacramento sand gave caluculated values of C_d which correlated to measured values.

In the case of a compacted Kaol in clay it was concluded that the small increment of effective stress applied in measuring B coefficinets led to the clay displaying a pseudo-preconsolidation effect with associated low compressibility. Values of B coefficients calculated using values of C_d obtained from small-increment loading compressibility tests gave results close to those measured. The compressibility of clay was also found to decrease with increasing confining pressure. They also concluded that the value of B, determined using the above

procedure, remained essentially constant throughout a subsequent undrained triaxial test conducted to measure values of the pore pressure parameter A. The value of C_d for kaolin was quoted to be in the range 10^{-4} to 10^{-6} in^2/lb over the pressure range of 0 to 1000 psi.

As the compressibility of a rock skeleton will be low, e.g., 3 to 4 x 10^{-7} in^2/lb for quartzitic sandstone over the pressure range 0 to 1000 psi (Zisman 1933), C_d will have to be taken into account in any expression derived to determine B-values for rock. The value of C_w is 3.3 x 10^{-6} in^2/lb and thus is greater than that of a rock skeleton. Mineral grain compressibility is of the order of 10^{-7} in^2/lb and will also have to be included in an expression for B for rock.

1.3 Objectives of the Research Program

The influence of water on the engineering properties of rock may be as follows:

(1) Mechanical - pore water pressures developing due to static water head or due to strains in the rock mass.

(2) Physico-chemical - adsorbed water changing the surface properties of the mineral grains or crystals and chemical reaction of the water and rock minerals, such as solutioning, etc.

The physico-chemical effects would generally not be significant in engineering work unless the ground water regime is significantly altered, i.e., unless a significant change in water table elevation and degree of saturation of the rock, and/or chemical composition of the ground water is anticipated in association with the engineering project. However in a laboratory study of the mechanical effects of pore water, using dry and saturated specimens, the physico-chemical effects of pore water also needs to be considered in order to isolate the effects of pore water pressures.

The mechanical effects could result from a changing stress state within the rock and are thus intimately associated with engineering works. These mechanical effects might be considered in terms of the A and B coefficients proposed by Skempton (1954) as considered earlier in the literature survey.

The magnitude of the A and B coefficients for rock depend upon such factors as:

(1) degree of saturation of the rock mass,

(2) relative bulk compressibilities of water, the minerals composing the grains, and the aggregate structure of the rock,

(3) porosity and nature of the pores of the rock aggregate structure,

(4) permeability of the rock aggregate structure,

(5) nature of the bonds and forces between the grains,

(6) rate of change of the stress state, and

(7) boundary drainage conditions.

Several of the above factors may be interdependent, but as long as the functional relationships are not known, each factor must be considered separately. The testing program described below was undertaken to measure A and B coefficients for various rock types.

1.3.1 Study of A coefficient by means of unconfined compression tests

Five series of unconfined compression tests were performed on Barre granite, Clinch sandstone, Nevada tuff, Yule marble, and Berea sandstone. In all a total of 112 unconfined compression tests were performed with rates of strain varying from 0.0001 inch/inch/min. to 10 inch/inch/min. Tests were performed on dry and saturated specimens.

If the rock aggregate structure is very porous, so that the rock

tends to decrease in volume during shear, it would be expected in saturated specimens that positive pore water pressures develop during shear, decreasing the rock strength. This effect would be more pronounced at higher rates of loading since less drainage and dissipation of pore water pressure could occur. But if the rock aggregate structure were dense enough so that it tends to dilate during shear, negative pore pressures would develop and the specimen would be stronger when saturated. This effect would also be more pronounced at higher rates of loading because of less drainage. The results of unconfined compression tests on the dry and saturated specimens were compared at various strain rates and Skempton's A coefficients were calculated for all five rock types.

If the strength of the saturated specimens are less than the strength of the dry specimens, even at long times to failure, this would indicate that the presence of water in the voids had some deleterious effect on the strength of the rock. The possibility of performing a limited number of tests using a pore fluid other than water was considered, but based on the results of the tests on water-saturated specimens, the conclusions of the literature survey, and other reasons to be considered later, these tests were not performed.

1.3.2 Study of B coefficient by means of hydrostatic compression tests

Skempton's B coefficients were measured for four rock types in a specially designed triaxial cell (see later discussion). Tests were performed on Barre granite, Clinch sandstone, Yule marble, and Berea sandstone. The rock specimens were saturated using large hydraulic gradients and when necessary by means of high back pressures. B coefficients were measured under increasing increments of all around

total pressure. Skempton's equation for B coefficient includes the compressibilities of the pore fluid and aggregate structure. For soils the compressibility of the soil skeleton is generally much higher than the compressibility of the water and this leads to a B equal to unity for most soils. For rocks the compressibility of the aggregate structure may become very small, in some cases possibly approaching the compressibility of the rock minerals, such that both have to be taken into account in a theoretical derivation.

1.3.3 Design and construction of the triaxial cell

The saturation of very low porosity rock and measurements of B coefficients in rocks of low bulk compressibilities would require special equipment and techniques. Initially it was intended to build a permeameter to be used for the saturation of the rock specimens. Since a pressure cell was also required for B coefficient measurements and since during the second and third years of the study triaxial compression tests with pore water pressure control or measurement will be performed, an all-purpose triaxial compression cell was designed and built which can serve all of the above needs. The triaxial cell was successfully used to saturate rock specimens, to measure rock permeabilities, and to measure B coefficients.

SECTION 2

DESCRIPTION OF ROCKS TESTED

2.1 Barre Granite

Barre granite is a uniform, gray, black,and white, medium-grained, dense rock with an interlocking, crystalline texture. The specimens were obtained from a quarry in Barre, Vermont. The petrographic description (Deere and Miller, 1966), based on thin-section micrographs is as follows: "The sections show the typical hypidiomorphic granular texture of granite. Brown biotite (7 percent), altering in places to penninite, contains small crystals of zircon. Quartz (29 percent) exhibits undulatory extinction and is interstitial to the subhedral grains of plagioclase (An_7, 15 percent), orthoclase, and microcline (36 percent combined). Perthitic intergrowths of microcline and plagioclase make up 9 percent of the rock. Muscovite (4 percent) has developed in cleavage planes, or as irregular masses on the orthoclase. Accessory apatite, zircon, and magnetite, make up less than one percent of the total." Barre granite has a dry unit weight of 165 pcf, a porosity of 2.1 percent, a specific gravity of solids of 2.70, an unconfined compression strength of 23,500 psi (1% strain/min. load rate), an initial tangent modulus of 5.2×10^6 psi, and a tangent modulus at a stress level of 50 percent of failure of 8.7×10^6 psi.

2.2 Berea Sandstone

Berea sandstone is a light gray, fine-grained, massive porous rock with a cemented, partially interlocking texture of subangular grains. The rock samples came from Amherst, Ohio. The petrographic description (Deere and Miller, 1966), based on thin-section micrographs is as follows: "This rock consists of tightly packed subangular grains of quartz, and small amounts of plagioclase and microcline, all having a well sorted average grain size of 0.15 to 0.20 mm. Secondary quartz growth serves as the predominant cementing material; however, in places, a fine-grained calcite cement holds the detrital quartz grains in place." Berea sandstone has a dry unit weight of 136 pcf, a porosity of 18.4 percent, a specific gravity of solids of 2.66, an unconfined compressive strength of 8,300 psi (1% strain/min. load rate), an initial tangent modulus of 0.45×10^6 psi, and a tangent modulus at a stress level of 50 percent of failure of 3.0×10^6 psi.

2.3 Clinch Sandstone

Clinch sandstone is a pale orange, poorly sorted, very fine-grained, dense, orthoquartzite, with a highly cemented structure. The predominant cementation is from secondary growth. The samples were obtained from Morristown, Tennessee. Clinch sandstone has a dry unit weight of 158 pcf, a porosity of 5.6 percent, a specific gravity of solids of 2.67, an unconfined compressive strength of 31,600 psi (1% strain/min. load rate), an initial tangent modulus of 2.6×10^6 psi, and a tangent modulus at a stress level of 50 percent of failure of 8.8×10^6 psi.

2.4 Nevada Tuff

Nevada tuff is a very light pink, porous tuff, containing randomly distributed white, gray, and brown lithic fragments with a cemented texture. The tuff specimens were obtained from the Atomic Energy Commision Nevada Test Site. The petrographic description (Deere and Miller, 1966), based on thin-section micrographs is as follows: "This tuff contains numerous fragments of welded plagioclastic material (up to 4 mm. in length) with elongate vesicles and partially devitrified spherulites. Some fragments of very fine-grained recrystallized quartz are laced with secondary white mica. Euhedral crystals and crystal chips of zoned plagioclase and quartz are scattered throughout. All are enclosed in a fine-grained dark, dusty, red matrix of devitrified glass and shards which are rimmed with black iron dust and small amounts of chlorite." Nevada tuff has a dry unit weight of 101 pcf, a porosity of 36.2 percent, a specific gravity of solids of 2.50, an unconfined compressive strength of 2,000 psi (1% strain/min. load rate), an initial tangent modulus of 0.80×10^6 psi, and a tangent modulus at a stress level of 50 percent of failure of 0.75×10^6 psi.

2.5 Yule Marble

Yule marble is a very pure white, uniform fine-grained, massive, saccharsidal marble with tightly interlocking, crystalline texture. The samples were obtained from West Rutland, Vermont. The petrographic description (Deere and Miller, 1966) based on thin-section micrographs is as follows: "A coarse-grained calcite marble with interlocking calcite grains (2 mm.), some containing round quartz crystals." The marble has a dry unit weight of 169 pcf, a porosity of

2.0%, a specific gravity of solids of 2.75, an unconfined compressive strength of 9,600 psi (1% strain/min. load rate), an initial tangent modulus of 0.52×10^6 psi, and a tangent modulus at a stress level of 50 percent of failure of 7.3×10^6 psi.

SECTION 3

UNCONFINED COMPRESSION TESTS

3.1 Preparation of Rock Specimens

The rock samples of Barre granite, Berea sandstone, Clinch sandstone, and Yule marble were obtained by coring six-inch thick quarry blocks. The blocks were drilled with a 2 1/8-inch diameter, water-cooled diamond bit core barrel. Nevada tuff was furnished in 1.75-inch diameter cores by the Atomic Energy Commission from the Nevada Test Site. The samples were then cut to a length which gave a height-diameter ratio of two, using a water-cooled diamond saw. Next the sample ends were polished using a Crane Lapmaster until the variation in height was less than 0.005 inches. The Crane lapping device uses special molds to hold the samples to insure that ends are lapped to give surfaces at right angles to the longitudinal axes of the samples.

After lapping, the samples were cleaned with benzene to remove the lapping fluid and any particles of rock or lapping abrasive which may have accumulated on the ends of the samples. The samples were then scrubbed with soap and water and rinsed thoroughly.

Several cores of Nevada tuff had been sealed to prevent dehydration when sampled in the field. These cores were used for the tests on saturated specimens. Care was taken not to allow drying of the samples during the steps described above. These samples were stored in a humidity room or in distilled water between the various steps of the procedure.

3.2 Saturation of Rock Specimens

Several procedures were used in an attempt to saturate the rock samples. The low porosities of Clinch sandstone, Barre granite, and Yule marble contributed to the difficulties of fully saturating these samples by the available techniques.

Samples of Clinch sandstone and Yule marble were saturated by various procedures to determine the best method of saturation for these rocks. In the first procedure, the rock specimens were oven dried to remove hygroscopic moisture which could block pores, thus preventing saturation. The specimens were then cooled in a vacuum dessicator, placed in a vacuum chamber, and saturated by allowing water to slowly enter the bottom of the chamber until the rock specimens were fully submerged. In the second procedure the samples were boiled in water for two hours. In the third method, the samples were oven dried and cooled in a vacuum dessicator. Then the samples were jacketed with a rubber membrane and set up in triaxial cells. The samples were subjected to cell pressures of 100 psi which sealed the jackets against the sample surfaces and helped to prevent flow of water around the samples. Then a back pressure of 80 psi was applied to one end of the specimens while the other ends were in contact with atmospheric pressure. In this way water was forced to flow under a pressure gradient through the samples and saturate them. All these procedures resulted in about the same degree of saturation as is shown in Table 3.1.

	Degree of Saturation, percent		
Rock Type	1	2	3
Clinch Sandstone	71.2	69.4	68.1
Yule Marble	17.9	21.6	20.9

Table 3.1 Average Degrees of Saturation for Various Methods of Saturation

As the values indicate, total degrees of saturation are low. These results indicate the effective porosities of these rocks are rather small, particularly in the case of Yule marble, or none of the procedures could fully saturate these rocks. The third procedure appeared to be the most promising method of saturating the samples. The failure of this method may be partially due to regeneration of air bubbles in the rock sample after pore pressure is reduced (air coming out of solution). This problem will be further considered in connection with the saturation of the rock specimens for B coefficient measurements.

The procedure for saturation of samples for unconfined compression tests finally adopted was as follows:

(a) Oven dry samples for forty-eight hours to remove hygroscopic moisture which could block pores.

(b) Cool samples to room temperature under a vacuum dessicator.

(c) With samples standing on end in a vacuum chamber, allow distilled-deaired water to slowly fill chamber, reaching top of samples in approximately thirty minutes.

(d) Allow samples to soak under vacuum for six hours.

(e) Boil samples for thirty minutes.

(f) Store under deaired water until tested.

Since drying could produce mineralogical changes in the clay minerals of the tuff, steps (a) and (b) were omitted for the tuff samples. The average and range in degrees of saturation are shown in Table 3.2.

Rock Type	Average Porosity (%)	Average Degree of Saturation (%)	Range in Degree of Saturation (%)
Barre granite	2.10	56.9	42.5 - 72.6
Berea sandstone	18.40	98.1	92.4 - 100.0
Clinch sandstone	5.58	82.2	71.0 - 98.1
Nevada tuff	36.20	68.9	35.0 - 100.0
Yule marble	2.03	51.3	39.2 - 68.5

Table 3.2. Degrees of Saturation for Unconfined Compression Test Specimens

The data show that the Berea sandstone has a large porosity and interconnected voids (i.e., a large effective porosity) and was effectively saturated. The Nevada tuff has the largest porosity but the presence of clay minerals may indicate that most of the voids are small in size and are not easily saturated, especially since steps (a) and (b) were omitted. The degree of saturation for the tuff is actually higher than calculated. This difference is due to the porphyritic nature of the tuff. The coring process sometimes left large voids on the surfaces of the samples where phenocrysts were plucked loose. Also the ash minerals form a honeycomb structure leaving additional surface voids. These voids could not be maintained in a saturated state and produced a good deal of scatter in the computed degrees of saturation. More meaningful values could have been obtained if lower sample volumes had been determined by submersion techniques, rather than calculating bulk volumes from overall sample dimensions. Conclusions concerning the low porosity rocks are difficult to predict. A major attempt would have to be made first to delineate the total and effective porosities of the intact rock structures.

3.3 Experimental Procedure

The unconfined compression testing was conducted using an MTS servo-hydraulic testing system with 600-kip capacity. The tests were all performed at constant rates of deformation. The control system includes a linear variable displacement transducer (LVDT) to measure axial deformations and a load cell system to measure total load. The test system is shown in Figure 3.1 and the control system in Figures 3.2 and 3.3. The maximum load at full range could be varied from 60 kips to 600 kips to a full scale voltage output of 10 volts. This

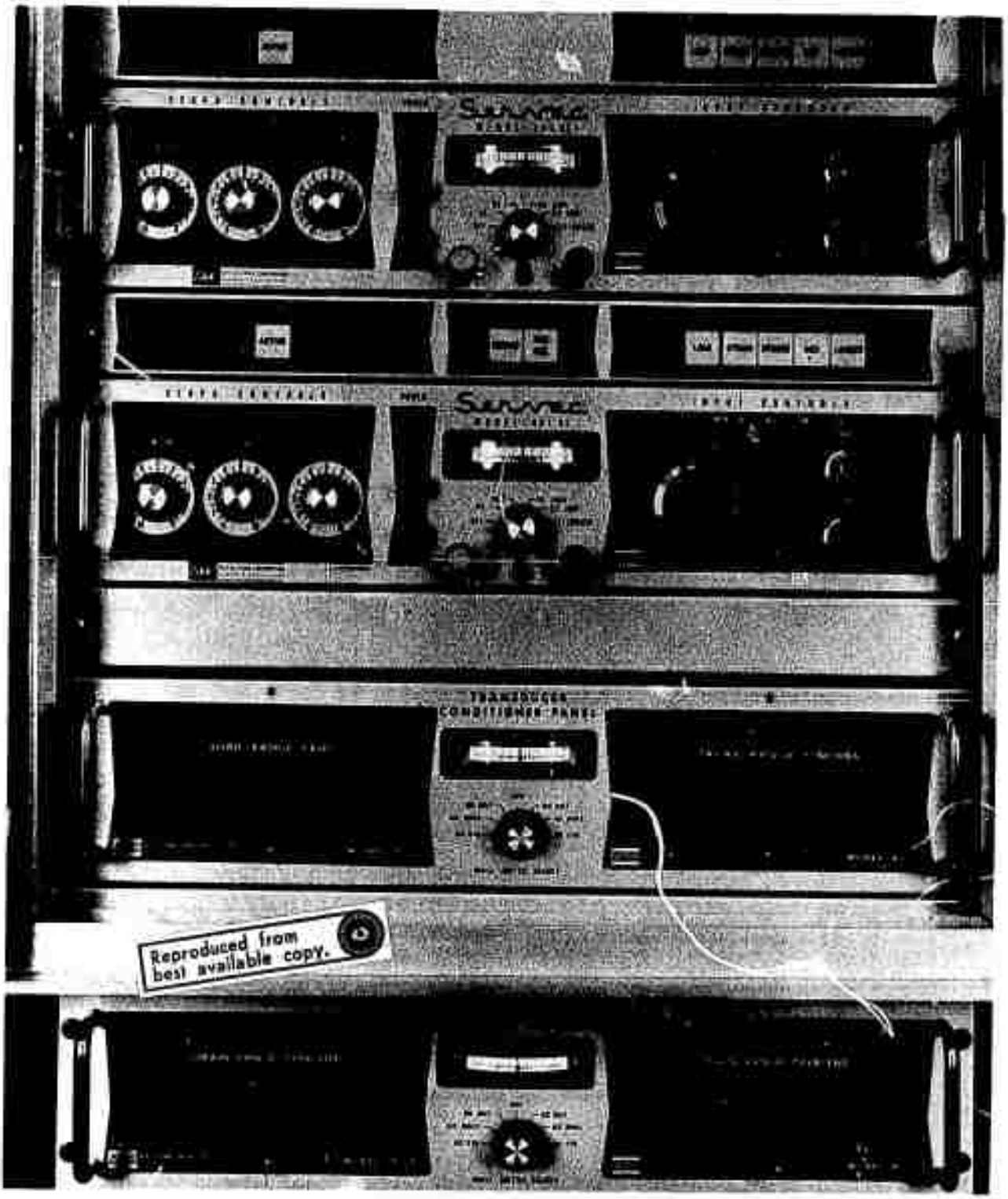

Fig. 3.1. Model 904.58 Materials Testing System

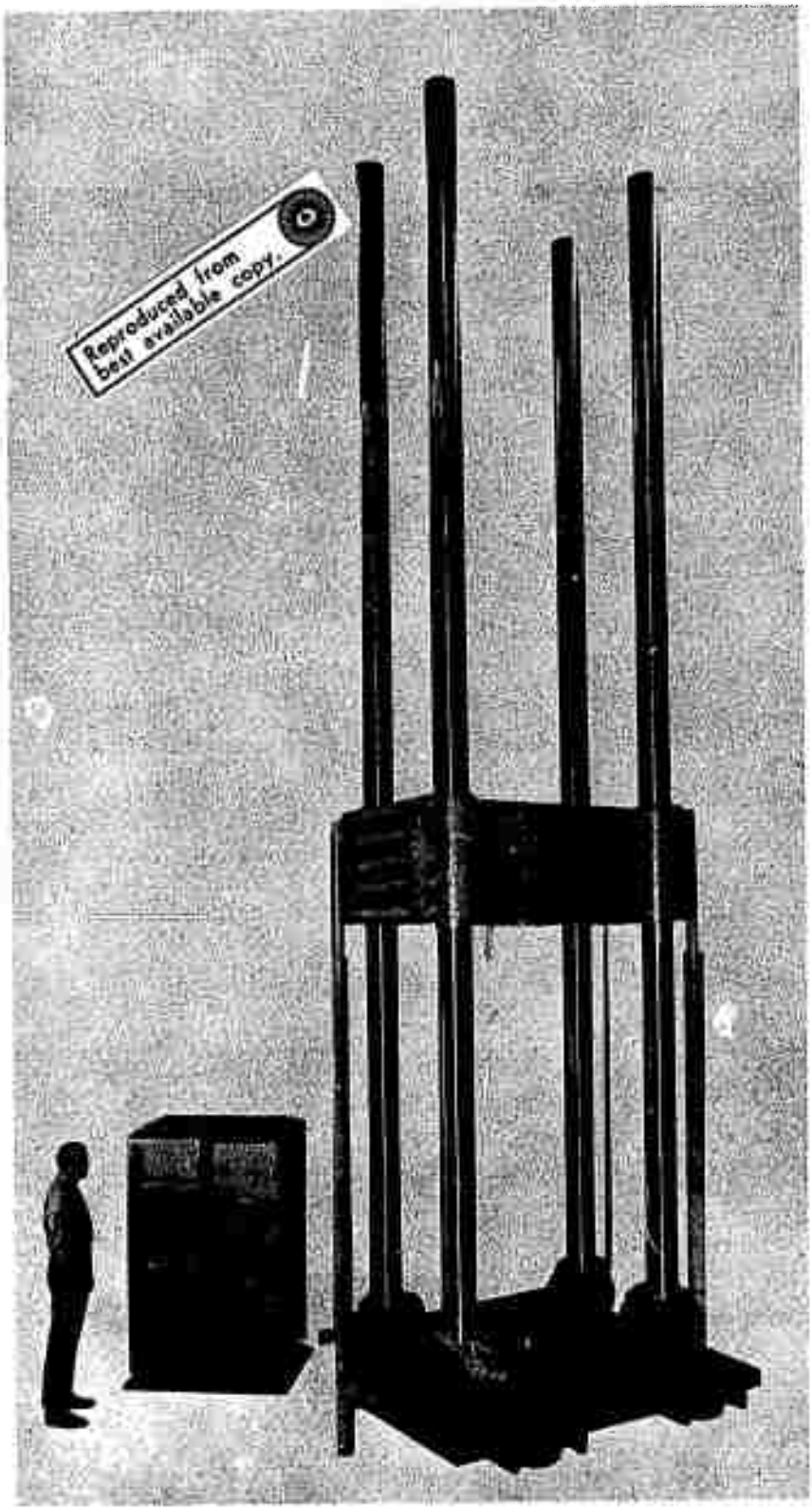

Fig. 3.2. Controls and Indicators, Panel 1

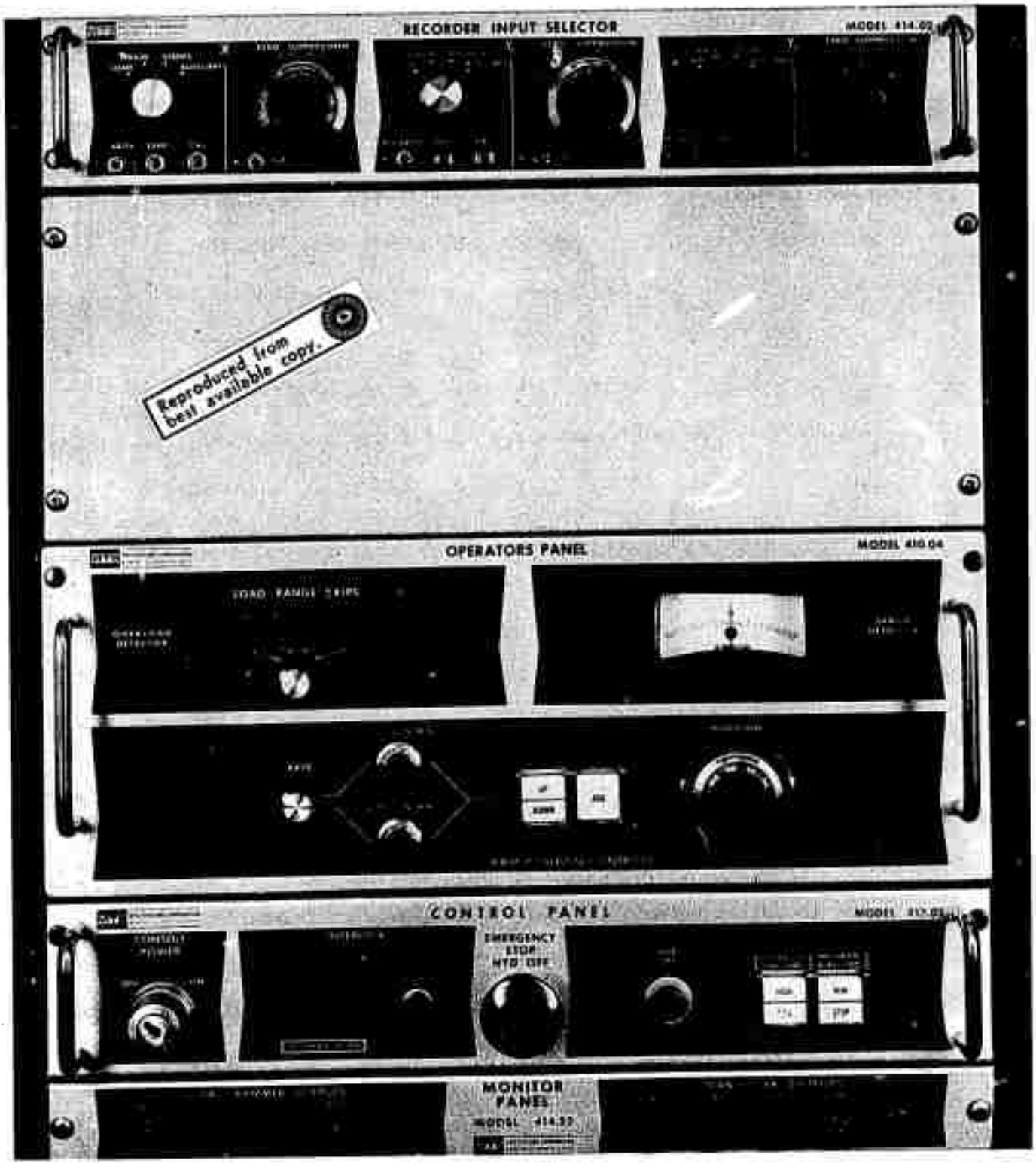

Fig. 3.3. Controls and Indicators, Panel 2

capability was important because of the wide range of failure loads encountered for the rock types used. The LVDT used is an MTS Long-Stroke LVDT Model No. 661.04 which is mounted in the hydraulic ram and is controlled by an MTS Model 425.31 a.c. Transducer Conditioner. This gage has the following characteristics: ten inch maximum stroke, ± 1 percent linearity, and ± 0.1 percent sensitivity. The load cell is a LeBow 1000-Kip Load Cell controlled by an MTS Model 425.41 d.c. Transducer Conditioner and has a sensitivity of ± 0.1 percent of full scale.

Before testing, the compression heads of the load frame were seated in their hydraulic grips under a 300-Kip load to insure proper alignment of the heads. To further reduce eccentricity in loading, a movable six-inch diameter by one-half inch thick steel plate was placed between the top platen and the sample, and a swivel-head, four-inch diameter steel plate with ball-bearing linkage was placed below the sample. The sample set-up is shown in Figure 3.4. In addition to the LVDT, two independent strain measurements were made on the samples. Two MTS Model 632.13 Extensiometers were placed to measure the longitudinal strain on opposite sides of a sample. Averaging of the two readings gave the net longitudinal strain in a sample, and comparison of the difference in the two readings gave an indication of the degree of eccentricity of loading. These gages had the following characteristics: 2.000 inch gage length, 0.150 inch range, ± 0.1 percent sensitivity, 0.3 percent hysteresis over operating range, 100 Hertz maximum operating frequency with negligible distortion, 20 gm. weight and 120 gm. operating force at full scale. The extensiometers were controlled by MTS Transducer Conditioners Model Nos. 425.31 or 425.41. The gages contacted the samples along knife-edge

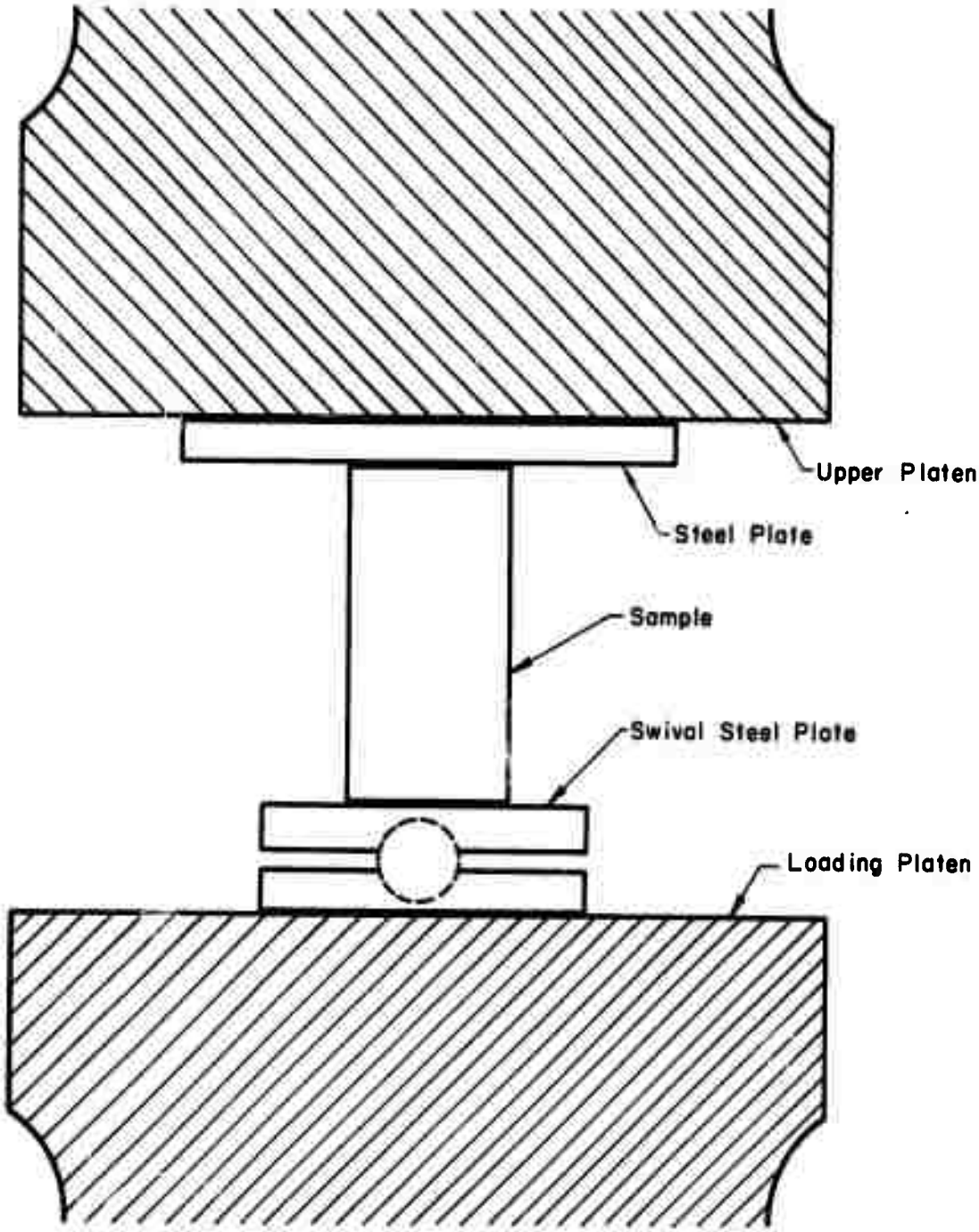

Fig. 3.4. Sample set-up for Unconfined Compression Test

supports and were held in place by elastic bands.

To prevent surface drying of the saturated samples in the slow tests, loose saturated gauze was wrapped around the samples and intermittently sprayed with water during testing. No similar precautions were necessary for the fast tests where failure was reached in less than one minute.

For the slower tests, load vs. deformation and strain vs. deformation were plotted directly on analog plotters. For the faster tests the data was recorded on magnetic tape at high speed. The tape was then run through an analog-digital converter and stored on digital tape. This tape was then played at slow speed through a digital-analog converter and plotted on an analog plotter.

Since the LVDT in the ram recorded total deformation of the sample plus machine components above the gage, a machine deflection curve was also made by loading the system without a sample on the platens. This deflection was subtracted from the LVDT readings to give the net sample deflection. This net deflection gave sample strains which compared reasonably with the direct strain measurements and were used to assist in the interpretation of the plotted strain results. The net deformation was also used to compute the actual deformation rates and strain rates for each test.

3.4 Description of Failure

The primary mode of failure exhibited by the majority of the samples of each rock type was that of a conic shear rupture. The marble, tuff, and Berea sandstone failed by a progressive shear rupture as the ultimate strength was reached and some plastic yielding simultaneously occurred. In contrast, the granite and Clinch sandstone

exhibited a brittle fracture by violent rupture. Several samples (30% of the tuff and 10% of the others) failed along a single shear plane. Also approximately 30% of the marble samples failed by tensile splitting longitudinally, followed by the development of secondary shear planes in the separate portions of the split samples.

3.5 Experimental Results

The maximum loads and deformations at failure were used to determine the unconfined compressive strengths, given in Tables 3.3 to 3.7. Also shown are the porosities and degrees of saturation computed from measurements of dry and saturated weight, total volume, and specific gravity of solids.

The unconfined compressive strength was then plotted as a function of strain rate to observe the effect of saturation. These plots are shown in Figures 3.5 to 3.9. The scatter in the results is typical of rock tests of this type because of minor geologic discontinuities in the samples and eccentricities in loading.

Using the values of unconfined strength predicted by these curves, Skempton's A coefficients were computed by the procedure illustrated in Figure 3.10. The results of these computations are given in Table 3.8.

Table 3.3. Unconfined Compression Test Data For Barre Granite

Sample No.	Porosity n (%)	Degree of Saturation (%)	Strain Rate (in/in/min)	Strain at Failure (%)	Unconfined Compression Strength (psi)
1	2.06	56.4	0.000109	0.432	16,300
2	2.15	50.7	0.000822	0.433	21,200
3	2.03	70.3	0.0142	0.516	23,400
4	2.01	42.5	5.37	1.07	23,500
5	2.02	47.5	0.452	0.638	23,900
7	2.13	0	0.0000802	0.501	21,500
8	2.05	0	0.000746	0.499	22,000
9	1.97	0	0.0154	0.439	21,300
10	1.95	0	5.85	0.972	27,100
11	2.02	0	0.447	0.730	24,200
12	2.09	72.6	0.000071	0.327	18,000
14	2.07	61.2	0.000076	0.302	15,400
15	2.29	59.4	0.00078	0.319	17,000
16	2.27	53.7	0.016	0.373	19,600
17	2.10	58.7	0.61	0.616	22,600
18	2.05	52.4	6.35	0.654	29,400
19	2.17	0	0.000081	0.385	20,500
20	2.02	0	0.00076	0.393	22,600
21	2.35	0	0.0168	0.559	24,700
22	2.23	0	0.585	0.608	27,400
23	2.17	0	5.38	0.414	28,800

Table 3.4. Unconfined Compression Test Data For Berea Sandstone

Sample No.	Porosity n (%)	Degree of Saturation (%)	Strain Rate (in/in/min)	Strain at Failure (%)	Unconfined Compression Strength (psi)
1	18.3	97.9	0.000134	0.572	6,700
2	18.0	100.0	0.00014	0.592	6,640
3	18.3	99.3	0.00132	0.581	6,670
4	18.6	99.7	0.0013	0.566	7,040
5	18.1	100.0	0.0251	0.577	7,640
6	18.2	97.5	0.0277	0.620	7.640
7	18.3	97.1	11.45	0.824	7,700
8	18.2	100.0	10.92	0.806	9,170
9	18.6	97.1	0.98	0.858	8,170
10	18.8	92.4	0.94	0.835	6,960
11	18.6	0	0.000135	0.581	6,810
12	18.6	0	0.000126	0.876	6,050
13	18.0	0	0.00055	0.341	7,730
14	18.3	0	0.0014	0.546	7,220
15	18.7	0	0.026	0.645	6,280
16	18.6	0	0.026	0.564	8,730
17	18.1	0	10.34	0.835	10,490
18	18.3	0	11.27	0.879	10,510
19	18.1	0	1.02	0.808	9,970
20	18.4	0	1.02	0.808	9,930

Table 3.5. Unconfined Compression Test Data For Clinch Sandstone

Sample No.	Porosity n (%)	Degree of Saturation (%)	Strain Rate (in/in/min)	Strain at Failure	Unconfined Compression Strength (psi)
2	4.82	98.1	0.000215	0.867	24,200
3	5.86	75.0	0.00171	0.888	26,300
4	5.24	94.7	0.0295	0.725	27,300
5	5.33	90.1	7.02	1.05	27,800
8	5.32	0	0.000215	1.03	29,700
9	5.79	0	0.00175	0.803	28,500
10	5.65	0	0.0405	0.889	31.500
11	5.35	76.6	0.645	1.09	23,800
12	5.53	0	5.91	0.986	37,600
13	5.34	0	0.564	0.934	34,300
14	5.33	0	0.00114	0.715	24,300
19	5.79	77.5	0.000108	0.700	23,100
20	5.76	77.8	0.00106	0.717	25,200
21	5.66	80.2	0.021	0.731	26,900
22	6.07	71.1	0.830	0.930	24,600
23	5.68	80.6	8.06	0.919	23,600
24	5.67	0	0.000098	0.706	28,700
25	5.86	0	0.00100	0.775	32,400
26	5.80	0	0.0207	0.869	33,400
28	5.75	0	7.99	1.047	35,500

Table 3.6 Unconfined Compression Test Data For Nevada Tuff

Sample No.	Porosity n (%)	Degree of Saturation (%)	Strain Rate (in/min/min)	Strain at Failure (%)	Unconfined Compression Strength (psi)
1	32.9	56.6	0.000156	0.299	1,090
2	32.9	69.0	0.00147	0.437	1,570
3	32.9	35.0	0.0227	0.447	880
4	32.9	100.0	8.97	0.389	2,280
5	32.9	55.8	0.905	0.534	1,140
6	29.4	0	0.000247	0.359	1,920
7	30.8	0	0.00179	0.442	3,690
8	34.8	0	0.00191	0.617	2,400
9	33.5	0	0.0388	0.438	2,860
10	36.1	0	9.02	0.677	3,480
11	36.4	0	0.978	0.570	1,870
12	40.3	0	0.0175	0.418	5,750
13	33.3	0	0.000147	0.486	1,630
14	31.3	0	0.0164	0.286	1,710
16	35.7	0	0.000178	0.579	1,670
17	38.1	0	0.0019	0.437	1,910
18	42.2	0	0.0825	1.370	1,460
19	40.1	0	14.80	0.678	1,780
20	38.1	0	1.33	0.576	1,820
21	40.1	0	1.43	0.543	1,550
23	39.2	73.3	0.00043	0.645	200
24	39.2	70.3	0.0019	0.456	340
25	39.2	75.2	0.060	0.708	710
26	39.2	80.0	12.57	0.996	480
27	39.2	56.8	1.18	0.557	990
28	39.2	85.6	1.37	0.434	830

Table 3.7. Unconfined Compression Test Data For Yule Marble

Sample No.	Porosity n (%)	Degree of Saturation (%)	Strain Rate (in/min/min)	Strain at Failure (%)	Unconfined Compression Strength (psi)
2	1.91	39.2	0.0000920	0.445	7.090
3	1.86	68.5	0.00131	0.403	7,860
4	1.75	48.0	0.0208	0.428	11,400
5	1.98	65.7	8.03	0.611	13,500
7	1.86	0	0.000128	0.418	10,400
8	1.94	0	0.00145	0.638	8,600
9	1.77	0	0.0260	0.577	10,400
10	1.93	0	7.67	0.478	9,950
11	1.89	56.6	0.646	0.646	14,100
12	1.86	0	0.887	0.621	10,100
13	1.70	0	0.00093	0.417	9,150
14	1.80	0	0.00010	0.350	8,270
15	2.38	42.6	0.000100	0.234	3,280
16	2.20	49.6	0.00096	0.262	4,870
17	2.18	45.4	0.0152	0.263	9,270
18	2.25	45.9	8.69	0.471	6,220
20	2.36	0	0.000110	0.636	4,280
21	2.32	0	0.0020	0.600	5,490
22	2.25	0	0.018	0.317	9,500
23	2.24	0	7.32	0.518	9,320
24	2.21	0	0.78	0.494	7,610

Rock Type		$\dot{\epsilon}$ (in/in/min/) 0.0001	0.001	0.01	0.1	1.0	10.0	Assumed ϕ
Barre Granite	q_d	18,900	20,400	22,000	23,500	25,100	26,600	
	q_s	15,500	17,000	18,500	20,000	21,600	23,100	50°
	A	0.077	0.071	0.065	0.060	0.046	0.043	
Berea Sandstone	q_d	6,800	7,500	8,300	9,000	9,700	10,400	
	q_s	6,600	6,900	7,200	7,500	7,900	8,200	40°
	A	0.018	0.017	0.035	0.044	0.048	0.061	
Clinch Sandstone	q_d	28,200	30,000	31,600	33,300	35,000	36,700	
	q_s	26,000	26,000	26,000	26,000	26,000	26,000	40°
	A	0.013	0.031	0.050	0.065	0.077	0.092	
Nevada Tuff	q_d	2,000	2,000	2,000	2,000	2,000	2,000	
	q_s	800	800	800	800	800	800	30°
	A	0.51	0.51	0.51	0.51	0.51	0.51	
Yule Marble	q_d	9,600	9,600	9,600	9,600	9,600	9,600	
	q_s	6,500	8,000	9,600	11,200	12,700	14,300	40°
	A	0.10	0.038	0.0	-0.036	-0.071	-0.078	

Table 3.8. Experimental Results

$\dot{\epsilon}$ = strain rate
ϕ = effective angle of internal friction
q_d = unconfined strength of dry sample in psi
q_s = unconfined strength of wet sample in psi
A = Skempton A-coefficient

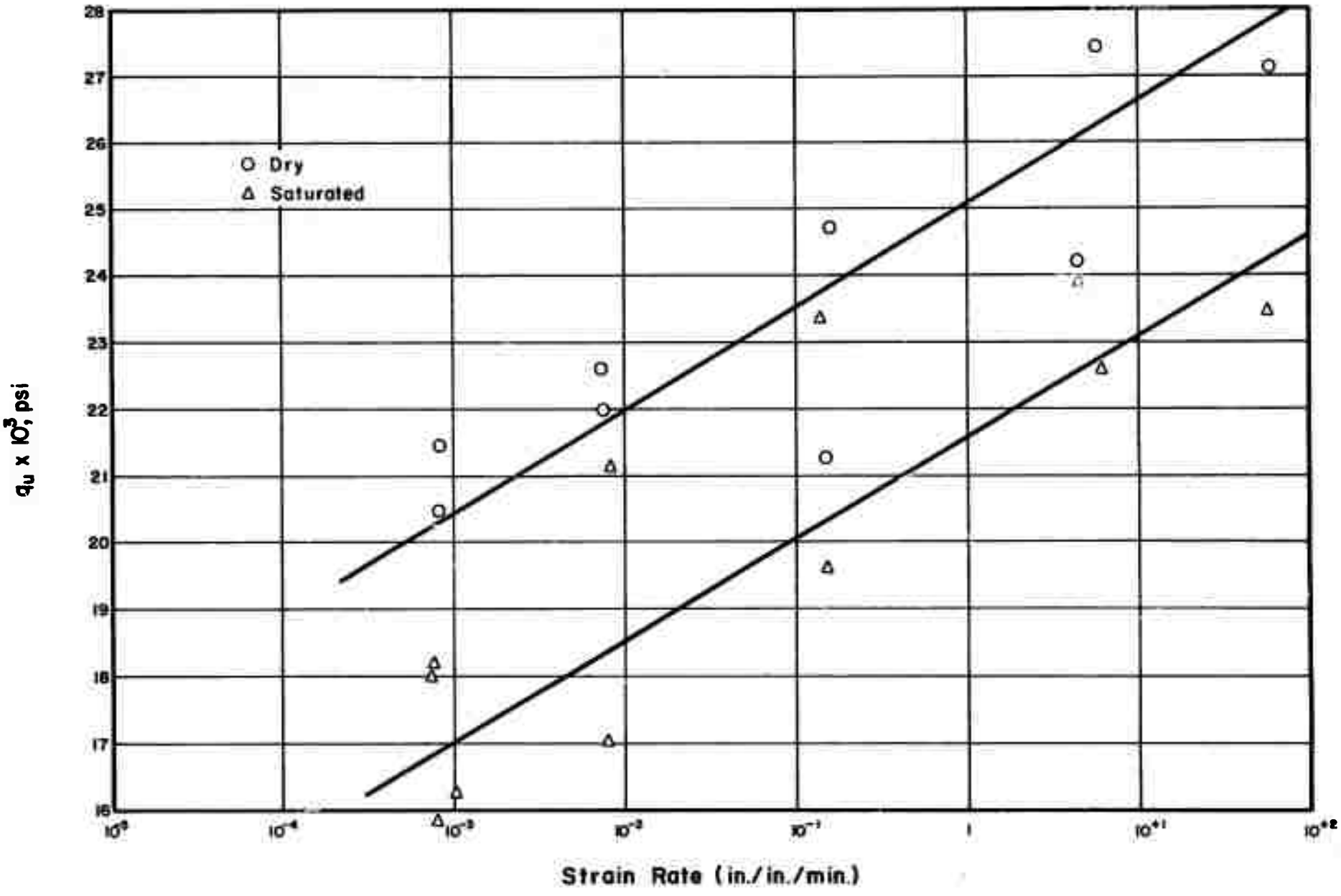

Fig. 3.5. Unconfined Compression Strength - Strain Rate Relation for Barre Granite

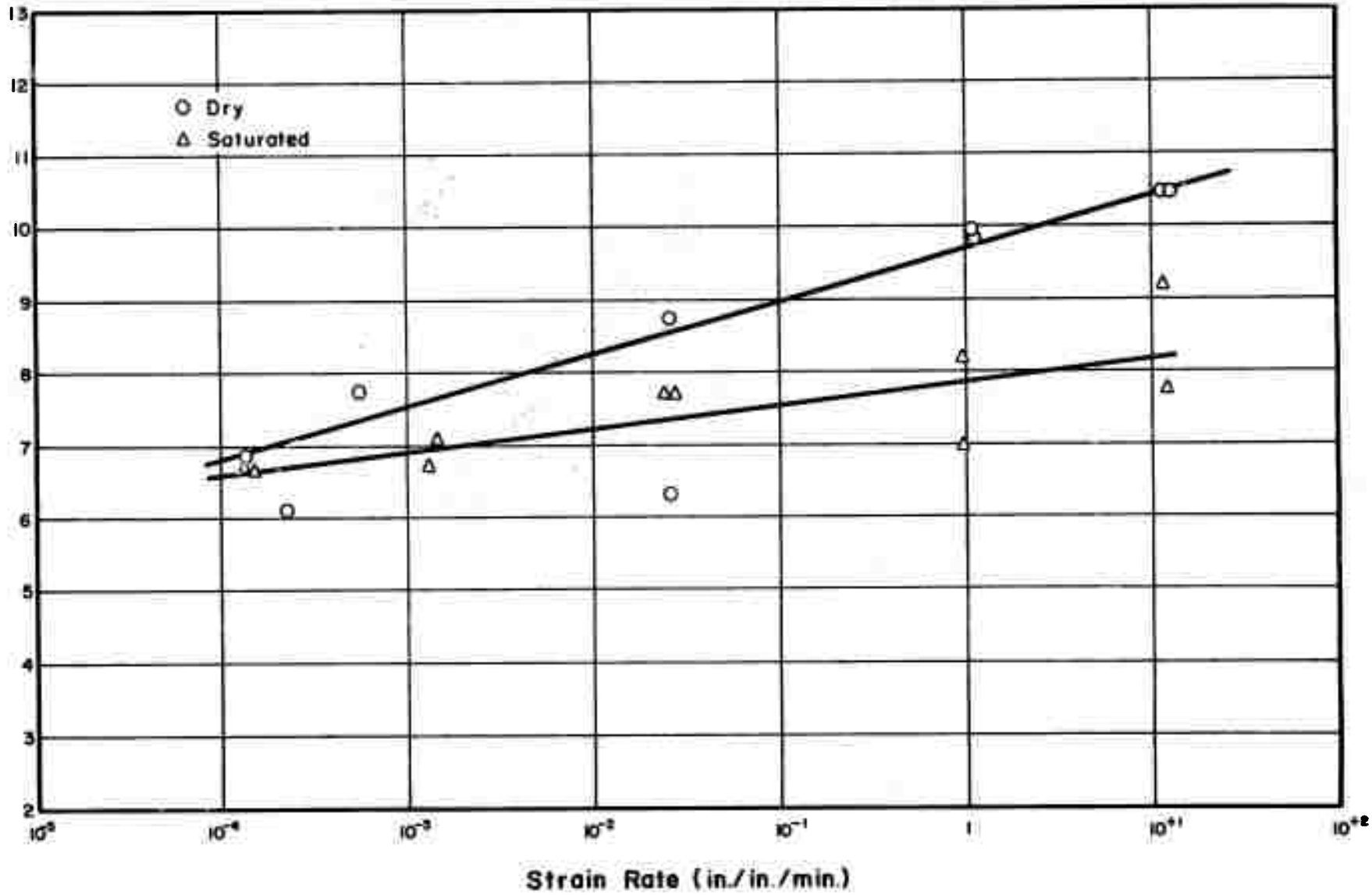

Fig. 3.6. Unconfined Compression Strength - Strain Rate Relation for Berea Sandstone

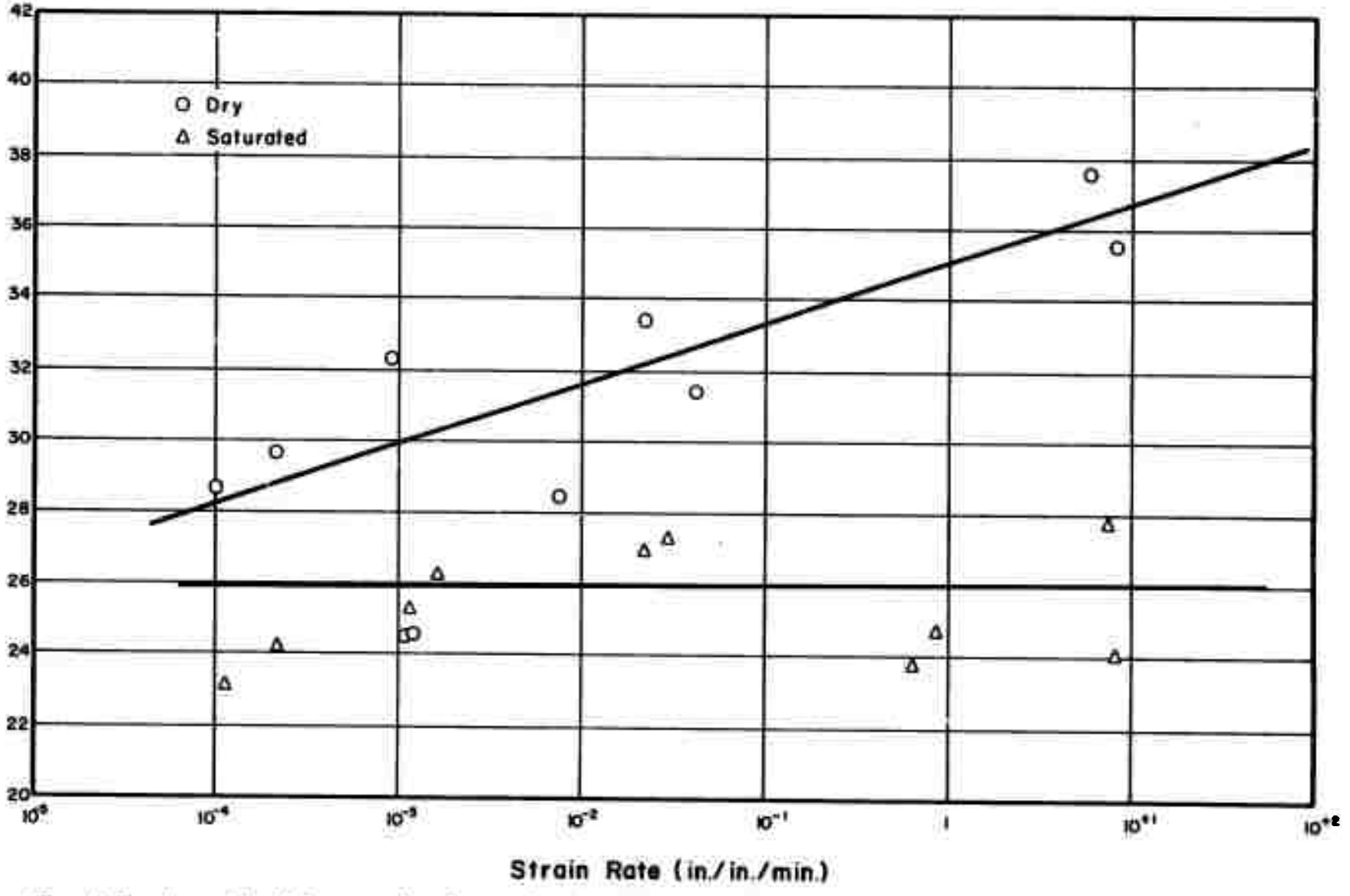

Fig. 3.7. Unconfined Compression Strength - Strain Rate Relation for Clinch Sandstone

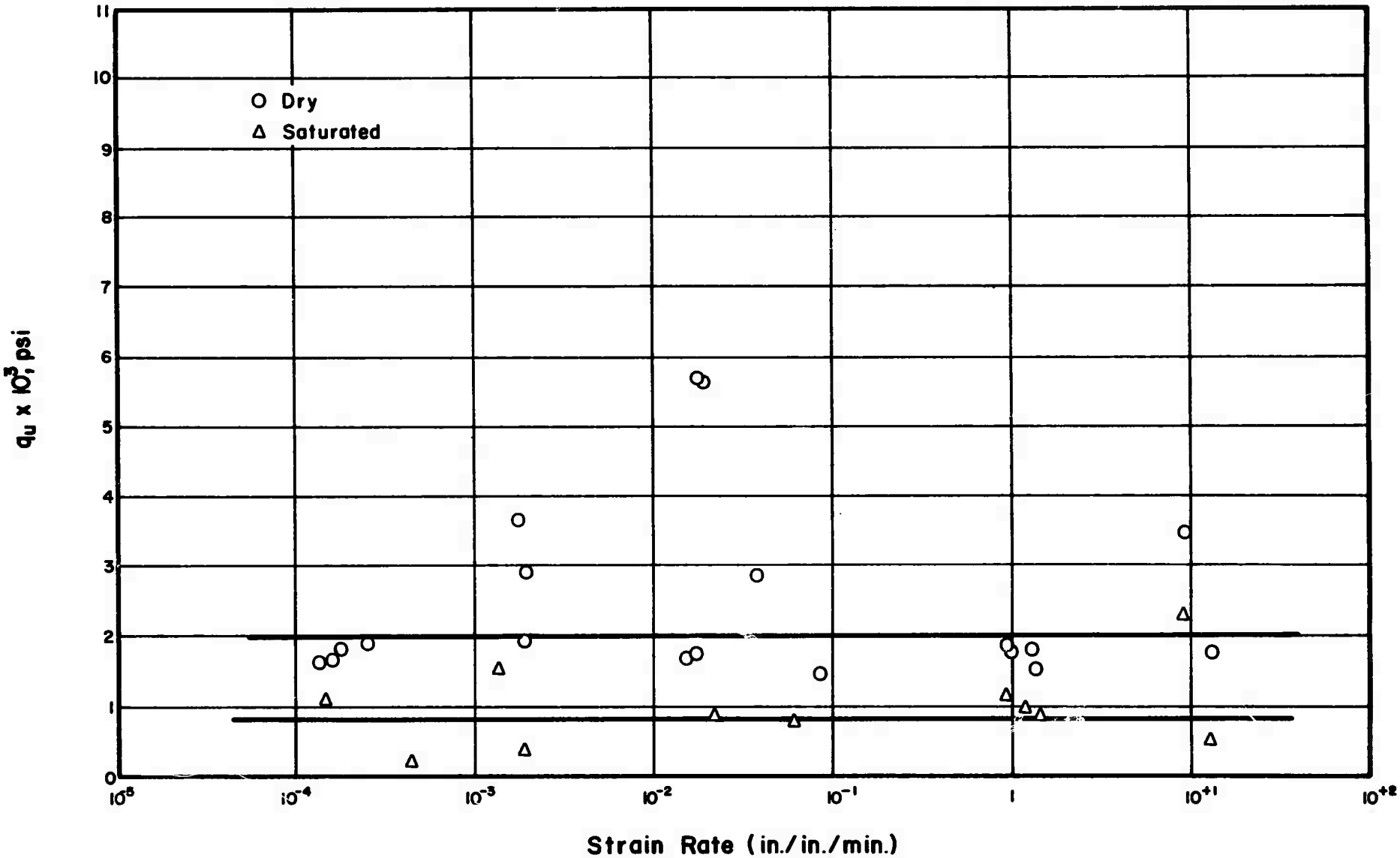

Fig. 3.8. Unconfined Compression Strength - Strain Rate Relation for Nevada Tuff

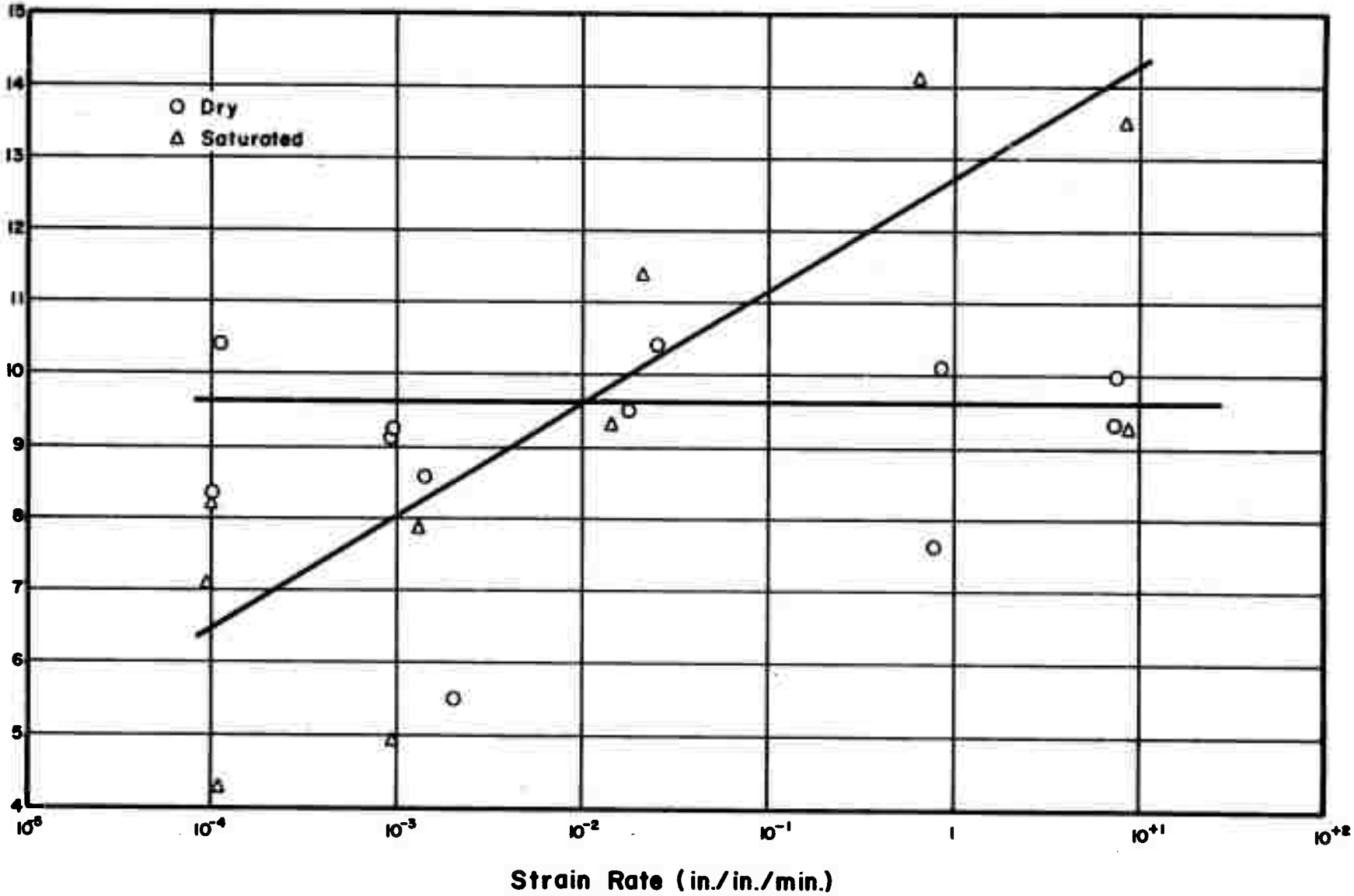

Fig. 3.9. Unconfined Compression Strength - Strain Rate Relation for Yule Marble

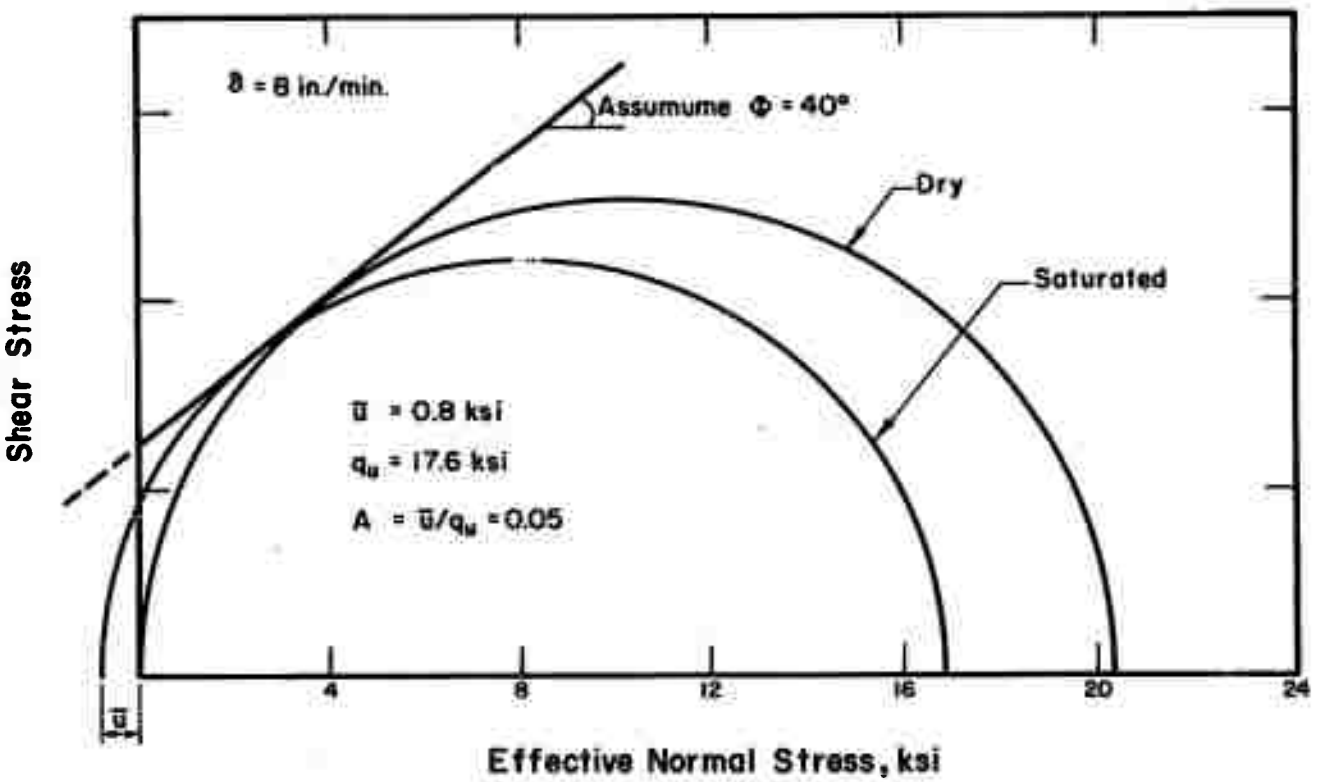

Fig. 3.10. Estimation of Excess Pore Water Pressure and A coefficient - From a Comparison of Unconfined Compression Strength of Dry and Saturated Rock Samples

SECTION 4

TRIAXIAL TESTS

4.1 Introduction

A 2000 psi capacity triaxial compression cell was designed and constructed. The triaxial cell was designed for 2 1/8-inch diameter and 4 1/2-inch long rock specimens and can be used for:

(1) saturation of rock specimens,

(2) measurement of permeability of rock,

(3) measurement of the B coefficient,

(4) drained and undrained triaxial compression tests with pore water pressure control.

The triaxial cell has been successfully used to saturate, measure permeabilities, and measure the B coefficient of four different rock types.

4.2 Design of the Triaxial Cell

The triaxial cell is constructed from stainless steel and has many special features. The pore pressure and drainage lines are made of continuous stainless steel tubing (O. D. = 0.125 inch, I. D. = 0.073 inch) with no sharp bends or any intermediate connections. This important feature substantially reduces the compressibility of the pore pressure measuring system and practically eliminates the possibility of trapping air bubbles in the pore pressure lines. The drainage tubings were connected to the pore pressure and drainage fittings using Ecco bond 51 Epoxy Adhesive supplied by Emerson and Cuming Inc., Canton, Massachsetts. In the pore water pressure measuring

system all of the connections are made through cone fittings, and as much as possible valves were eliminated from the pore pressure connections. This feature further reduces the compressibility of the system. There is only one 2000 psi capacity Circle Seal Valve in each pore pressure line, and this valve is absolutely necessary for back pressure control.

The confining pressure is applied through water which surrounds the sample. Compressed nitrogen bottles are used as the source of pressure. A specially designed gas-mercury-water transfer system connects gas pressure to water pressure which is used in the triaxial cell. This eliminates the possibility of gas diffusion into the rock specimen through the rubber membrane, and also increases the safety of the operation. The rock specimen is encased in a rubber membrane which is sealed to the top loading cap and base pedestal by means of 4 rubber O-rings.

All of the O-ring grooves have been designed for minimum volume change during cell pressure change, and all of the stainless steel surfaces which act as seals are highly polished. These provisions reduce the compressibility of the cell and practically eliminate leakage of the cell fluid. This feature will allow accurate control and measurement of the total volume of the rock samples under various loading conditions, in the second and third phases of the study. Two cross sections of the triaxial cell are shown in Figures 4.1 and 4.2 and photographs of the cell are shown in Figures 4.3 and 4.4. The detailed design drawings of the parts of the cell are included in the Appendix.

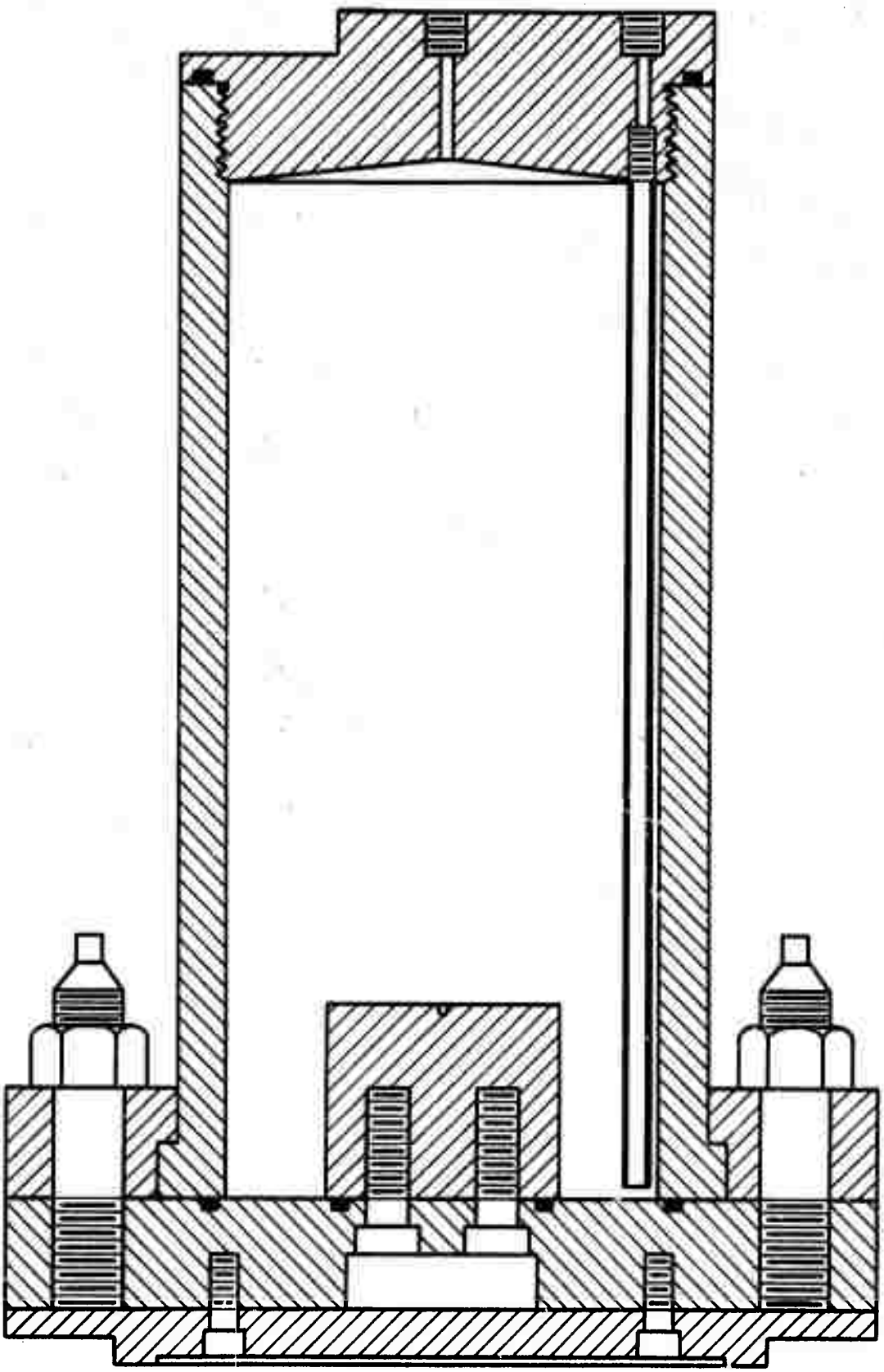

Triaxial Cell (Permeameter), Cross Section A–A

Fig. 4.1. Triaxial Cell, Cross Section 1

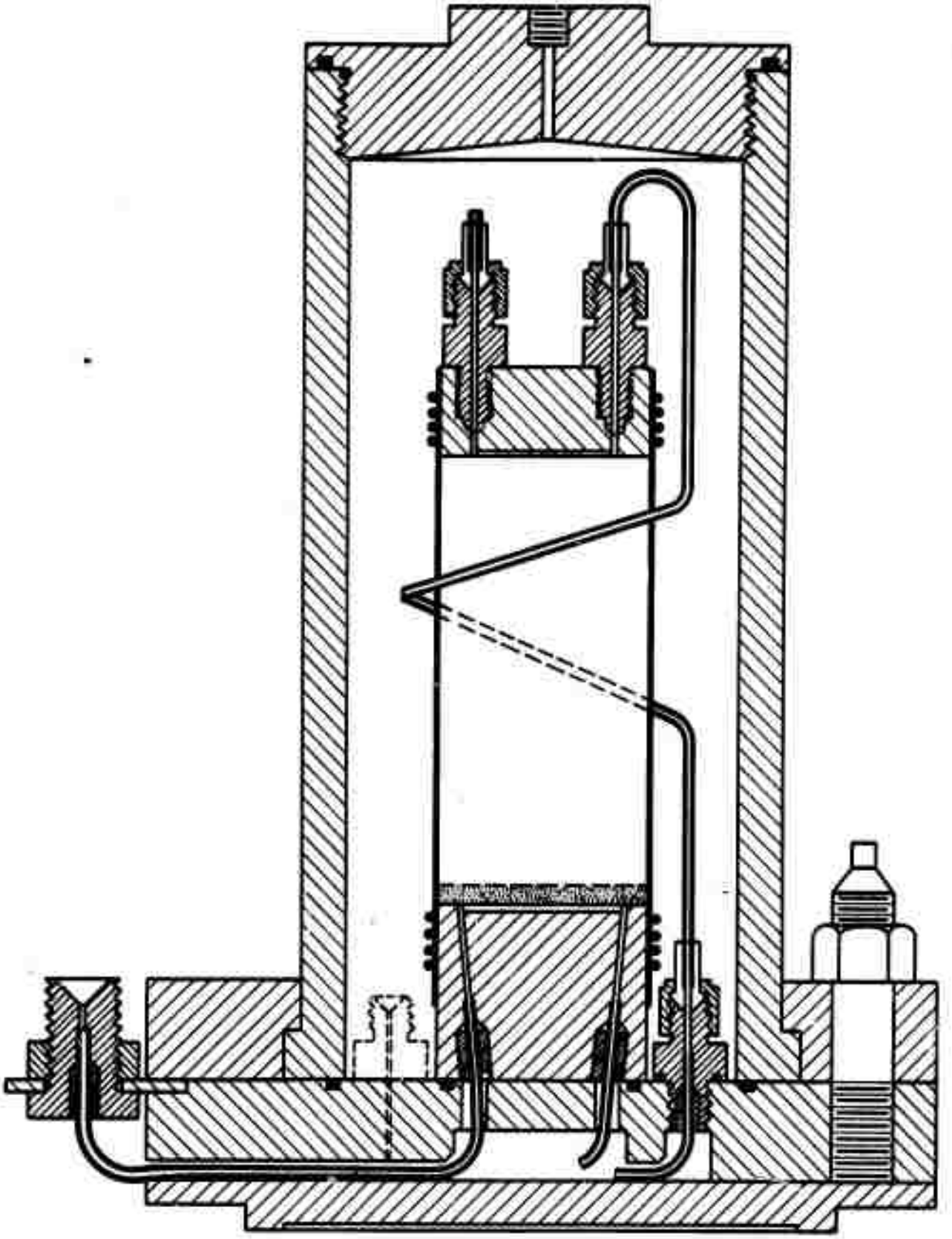

Fig. 4.2. Triaxial Cell, Cross Section 2

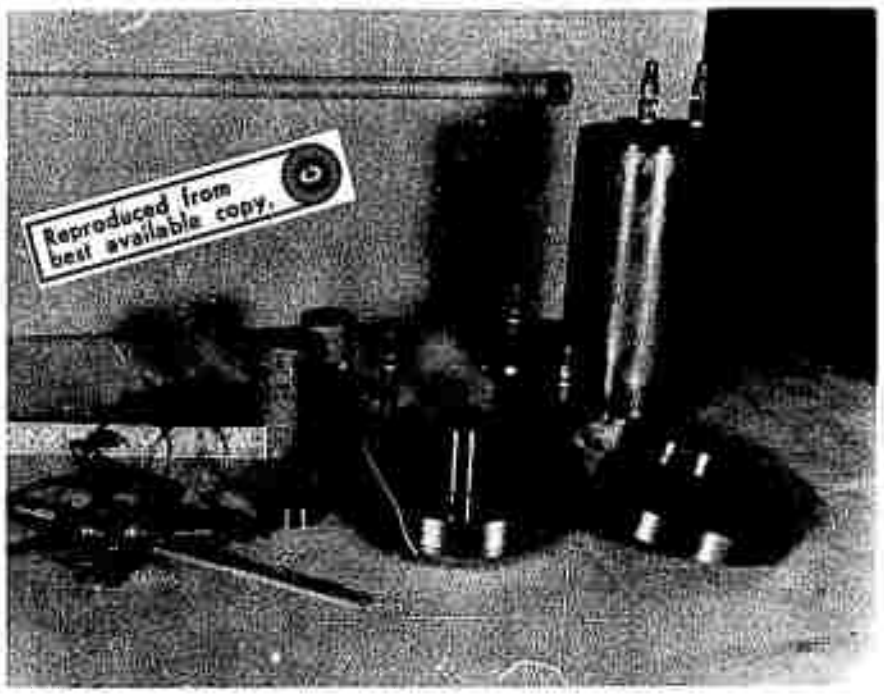

Fig. 4.3. Triaxial Cell Unassembled, View 1

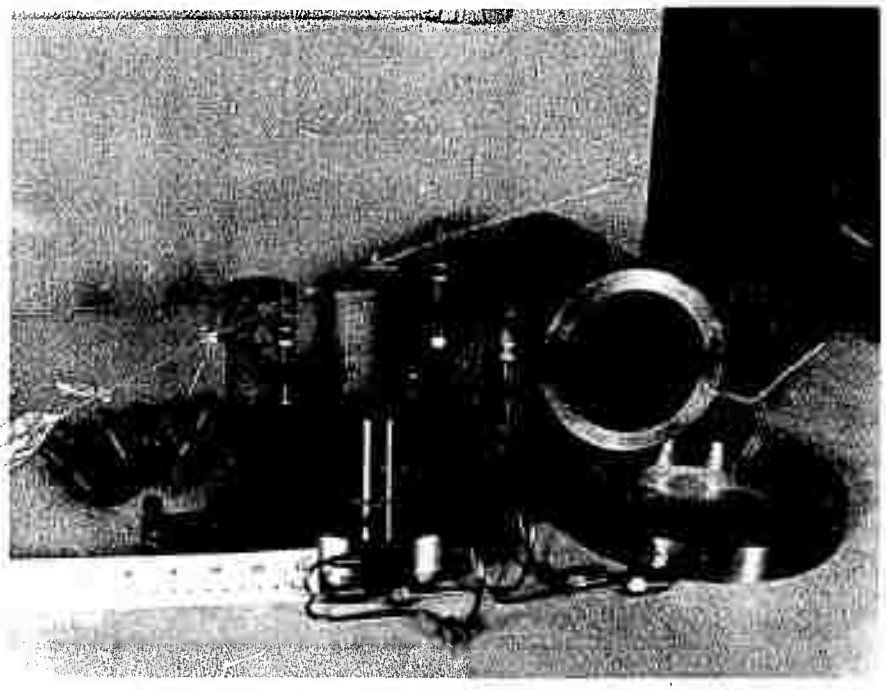

Fig. 4.4. Triaxial Cell, Unassembled, View 2

4.3 Testing Procedure

The testing procedure consisted of setting up rock specimens in the triaxial cell, saturating the rock specimens, measuring permeability, and finally measuring the B coefficient under increase in cell pressure.

4.3.1 Specimen set up

All of the drainage lines were saturated prior to specimen set up with deaired distilled water. The rock specimen was placed between the base pedestal and the loading cap and was encased in a 0.012-inch thick rubber membrane. The membrane was sealed to the loading cap and base pedestal by means of four rubber O-rings at each end. A thin layer of high-vacuum silicon grease was used on the highly polished loading cap and base pedestal in order to provide a better seal under the O-rings. In order to minimize the possibility of water flow around the rock specimen during rock specimen saturation, several O-rings were also placed on the membrane over the rock specimen. Figure 4.5 shows a specimen set up with the top drainage connections in place. Next the cell was assembled and filled with water, Figures 4.6 and 4.7.

4.3.2. Saturation of rock specimens and permeability measurements

The rock specimens were oven-dried for 48 hours before set up in the triaxial cell. The specimens were cooled in a vacuum-dessicator and set up in the triaxial cell. The jacketed specimen was subjected to a cell pressure which sealed the membrane against the sample surface, and the specimen was saturated with deaired, distilled water which was forced to flow under a pressure gradient from the bottom up through the specimen. A cell pressure in the range of 150 psi to 200 psi was applied

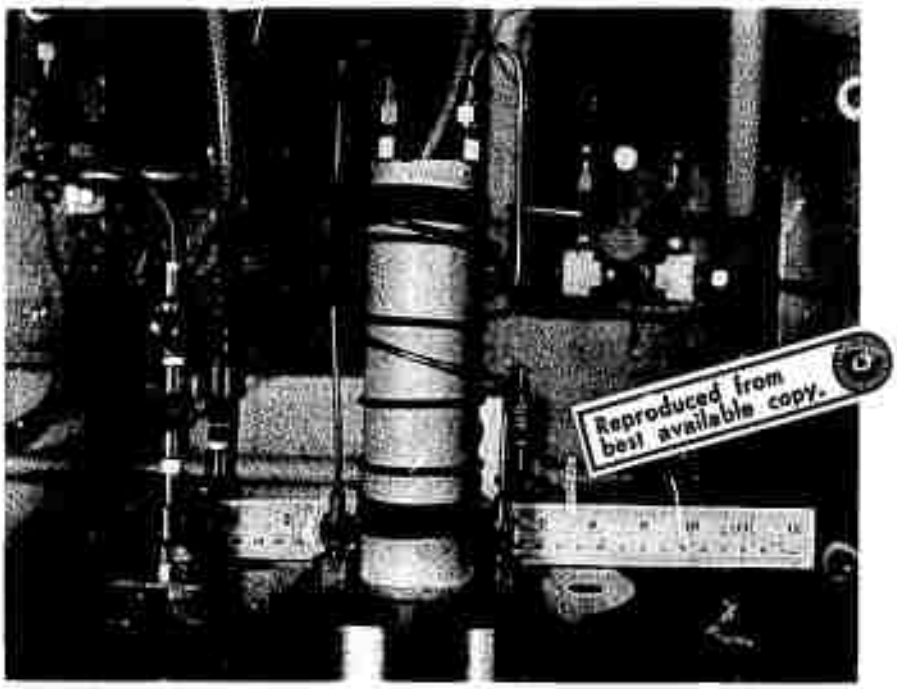

Fig. 4.5. Triaxial Specimen Set-Up

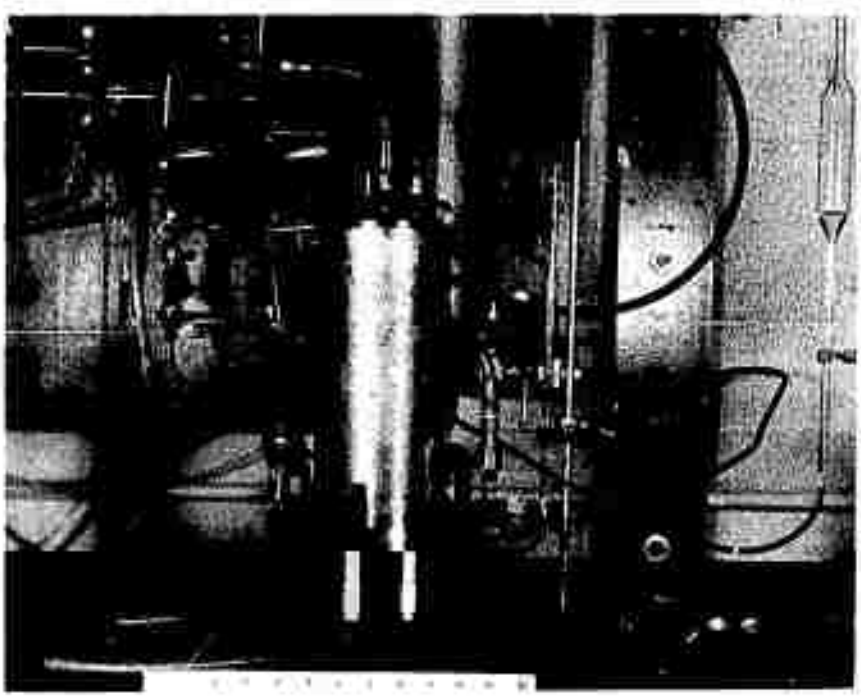

Fig. 4.6. Triaxial Cell, Unassembled

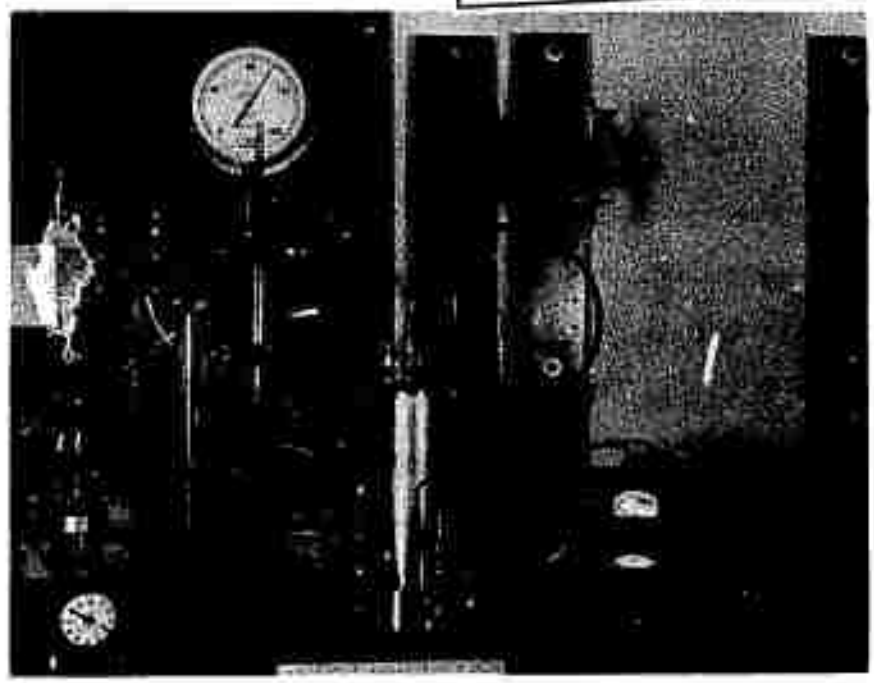

Fig. 4.7. Triaxial Cell, Back Pressure Apparatus, and Pore Pressure Measurement System

which resulted in the best seal of membrane against rock samples and prevented water flow around the sample. This pressure range was found by trial and error by measurement of the rate of flow of water through the specimen. The procedure was as follows: A cell pressure was applied to the specimen and a back pressure less than cell pressure was applied to the base of the specimen to result in a reasonable rate of flow through the specimen (i.e., 1 cc/hour). After a constant rate of flow was established for a particular cell pressure, the cell pressure was incrementally increased and rate of flow again measured. In general the rate of flow decreased, Figure 4.8, as the cell pressure was increased. Increased cell pressure resulted in decreased flow of water between the rock specimen and membrane. Finally after a certain cell pressure, the seal was adequate and no decrease in rate of flow was observed. The minimum rate of flow, the corresponding hydraulic gradient, and dimensions of the specimen were used to compute the coefficient of permeability of the rock specimen. The process was repeated for different hydraulic gradients and in general the computed coefficient of permeability remained constant.

4.3.3 B coefficient measurements

After the rock sample was saturated, one of the drainage lines at the base of the triaxial cell was connected to a 1000 psi capacity pore water pressure transducer. All of the saturated drainage lines were turned off, the cell pressure was increased by an increment, and pore water pressures were observed. If the measured B coefficient was less than unity, a back pressure was applied in order to get a B coefficient equal to unity. The cell pressure was again increased,

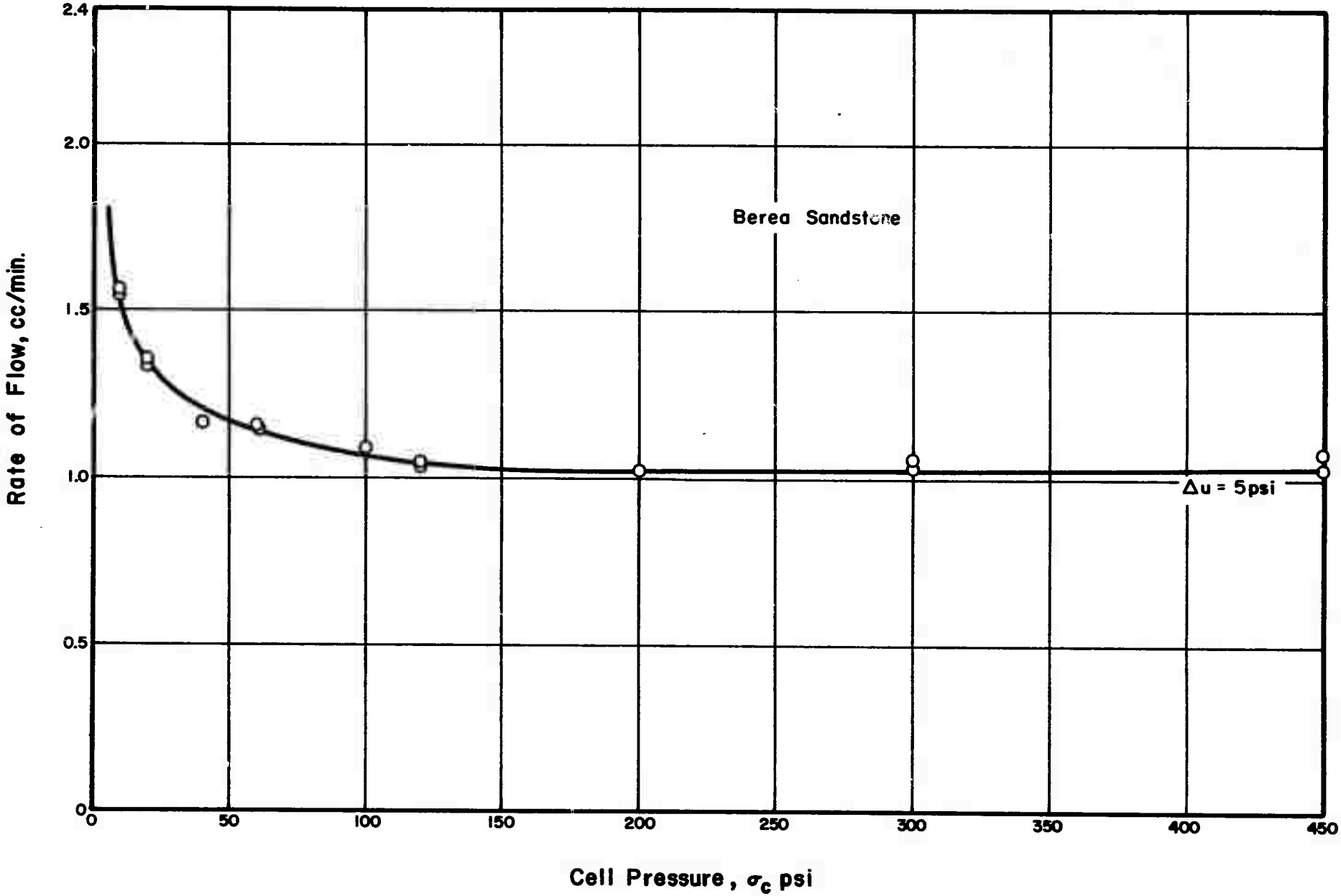

Fig. 4.8. Relation of Cell Pressure to Rate of Flow as an Indicator of Effectiveness of Membrane Seal

pore pressure changes were observed, and the process was continued until the increment of cell pressure resulted in a B coefficient of unity.

4.4 Experimental Results

Permeability and B coefficient measurements were made on Berea sandstone, Clinch sandstone, Yule marble, and Barre granite. The triaxial cell performed very satisfactorily and more tests have been planned for the second phase of the study. Table 4.1 summarizes the results of the permeability measurements.

Rock Type	Porosity, %	Permeability, (cm/sec)
Berea sandstone	18.30	2.4×10^{-3}
Yule marble	0.77	7.8×10^{-10}
Clinch sandstone	5.75	5.1×10^{-9}
Barre granite	1.92	1.1×10^{-9}

Table 4.1 Results of Permeability Measurements

The results of the B coefficient measurements are summarized in Figure 4.9. The values reported correspond to measured pore pressure six seconds after the application of the cell pressure increment. In general after the six second measurement, either the pore pressure remained practically constant or it decreased slightly, Figures 4.10-4.12. In one case (Clinch sandstone) the pore pressure decreased substantially after the initial peak value, Figure 4.13. The decrease in pore pressure is attributed to compression and expansion of the air bubbles either in the sample or pore pressure measuring

system. The pore pressure fluctuations also could be due to slight temperature fluctuations. Future tests will be performed in a constant temperature water bath.

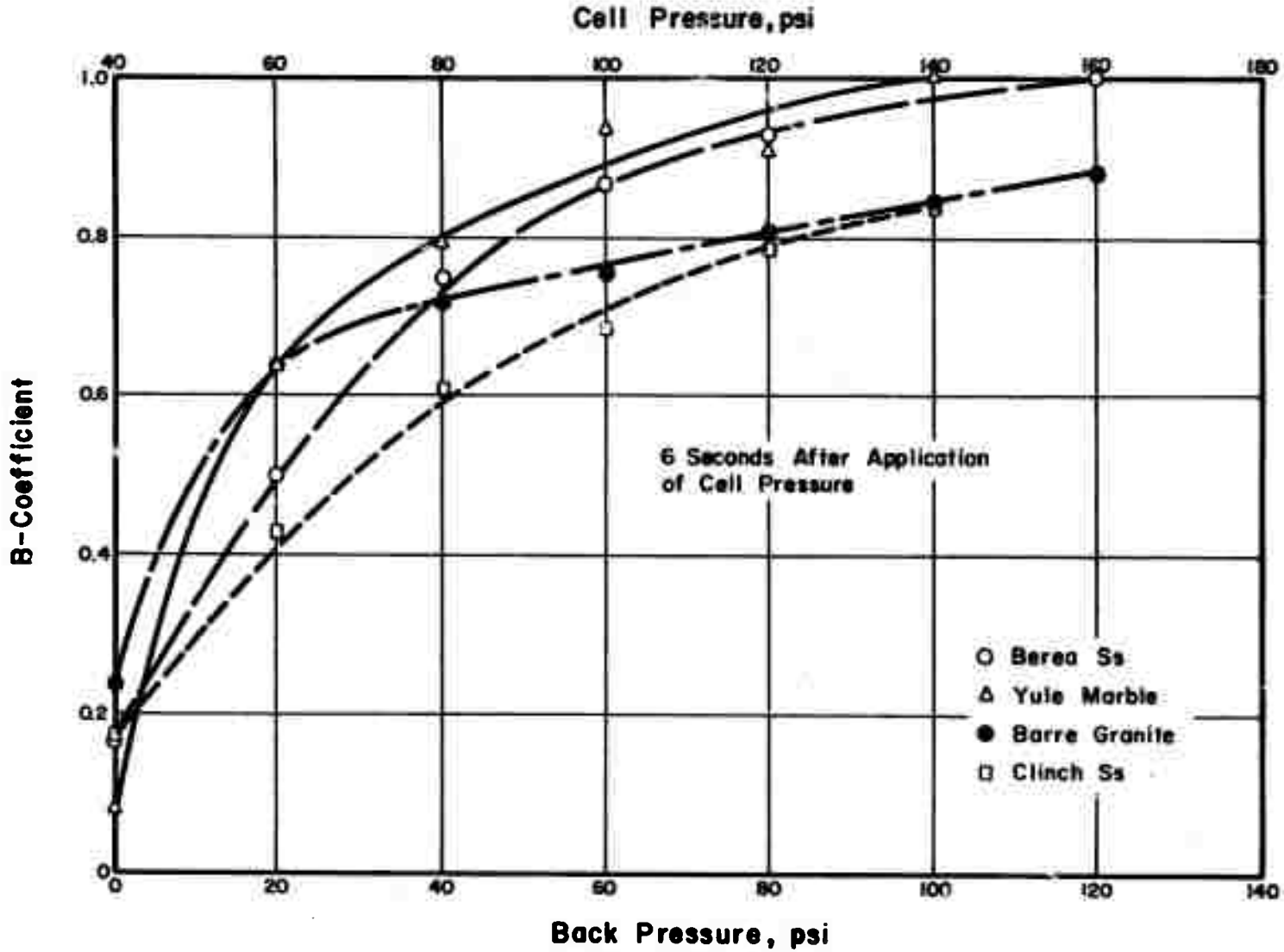

Fig. 4.9. Summary of B Coefficient Measurements

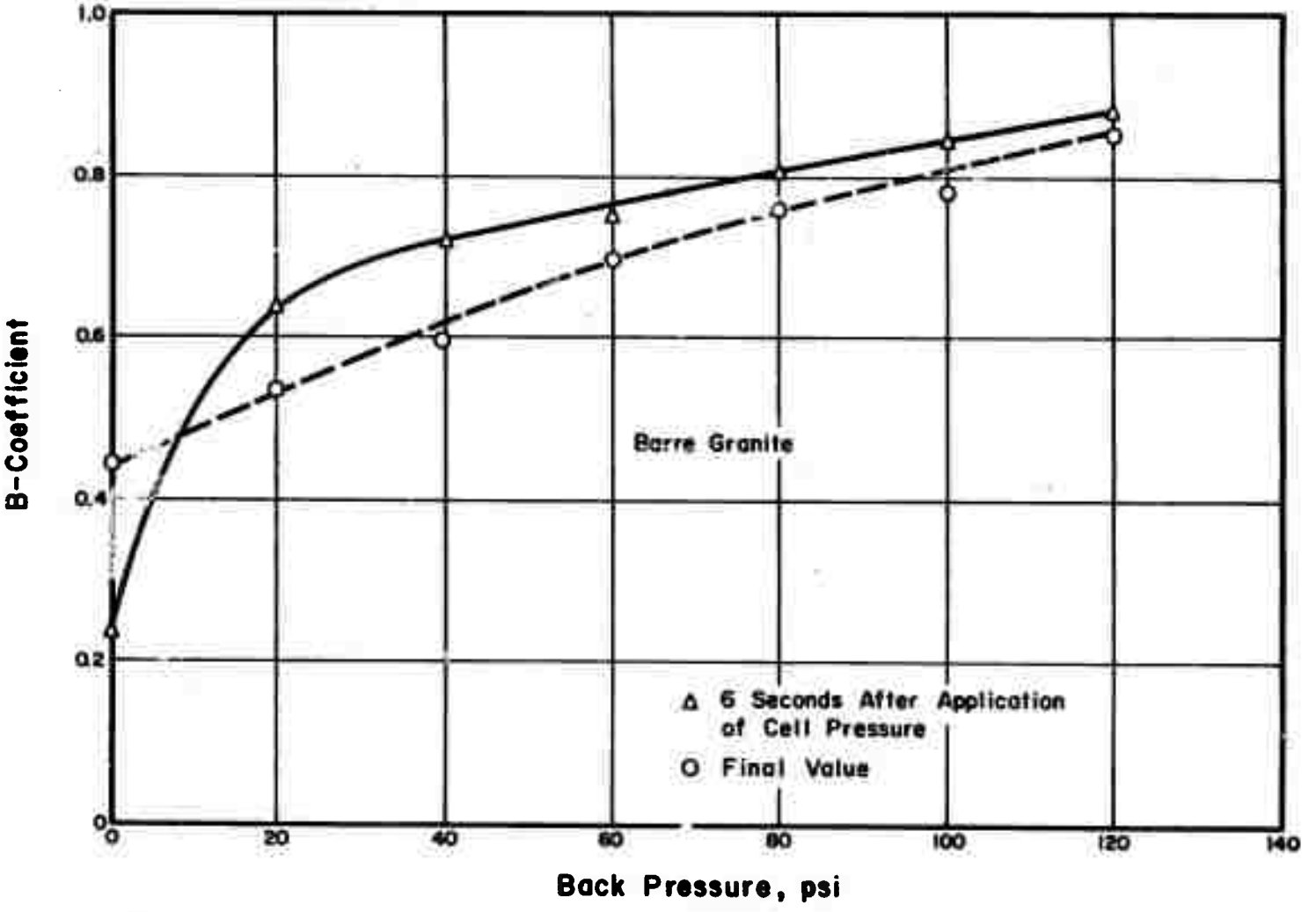

Fig. 4.10. B Coefficient Measurements for Barre Granite

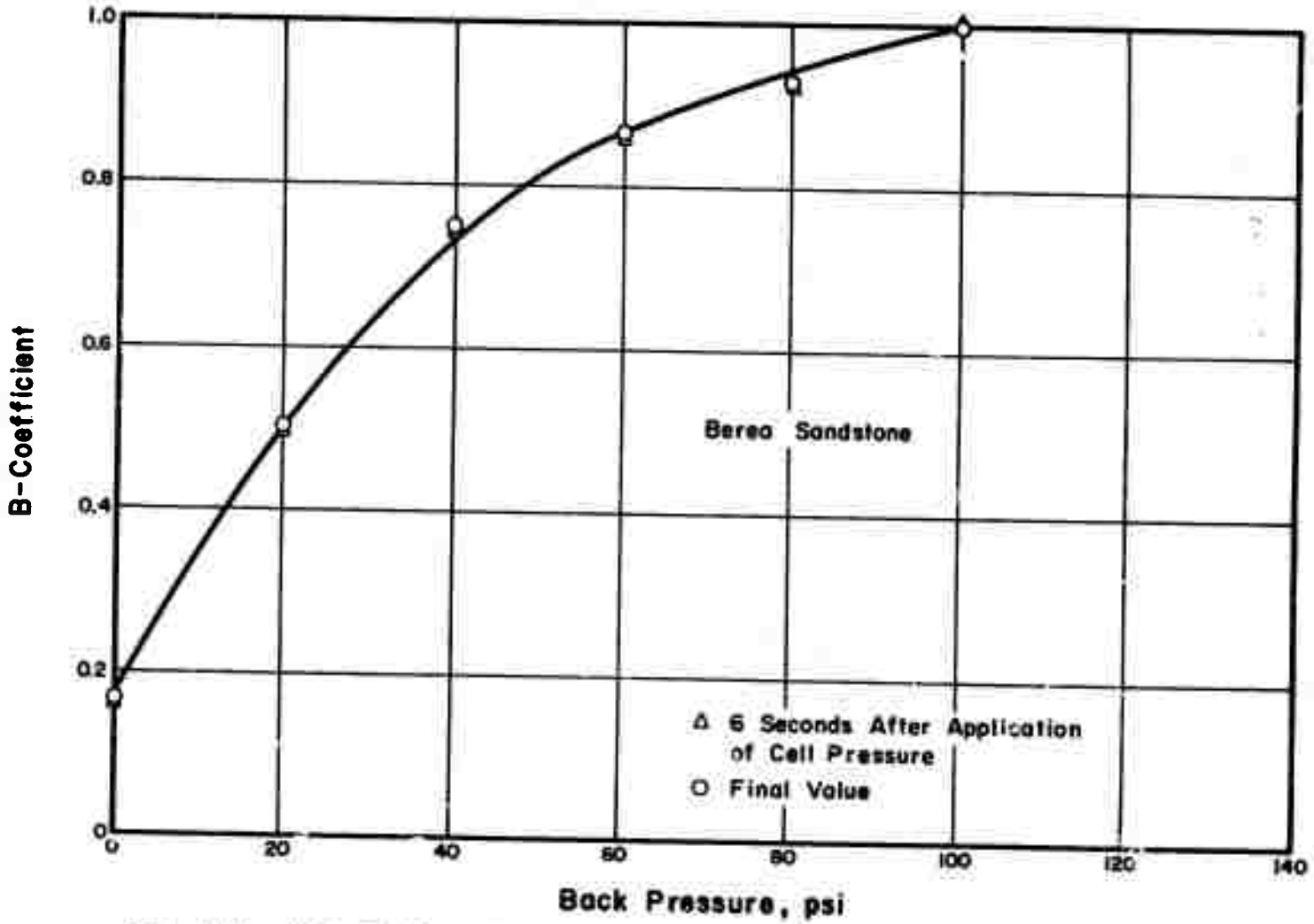

Fig. 4.11. B Coefficient Measurements for Berea Sandstone

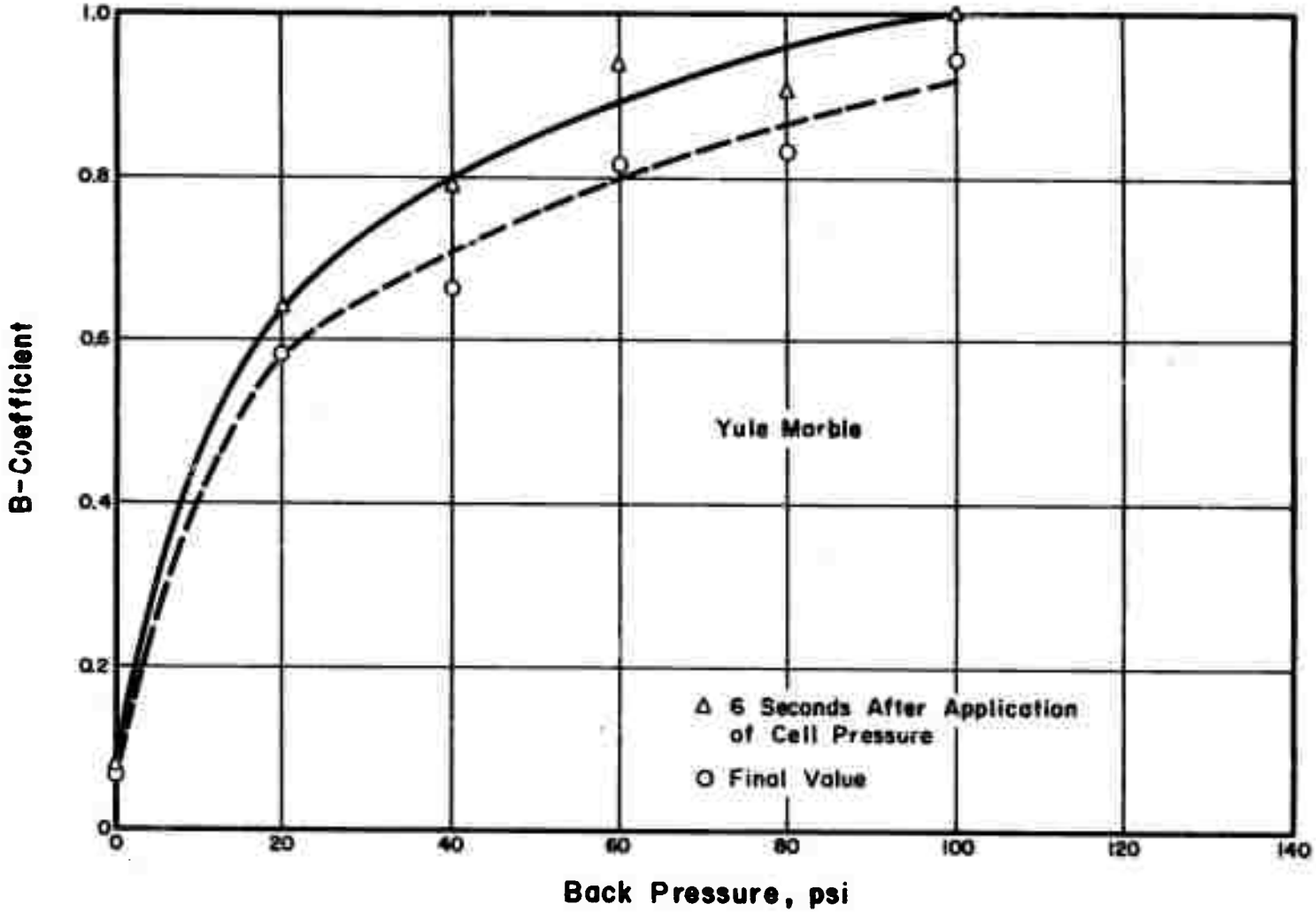

Fig. 4.12. B Coefficient Measurements for Yule Marble

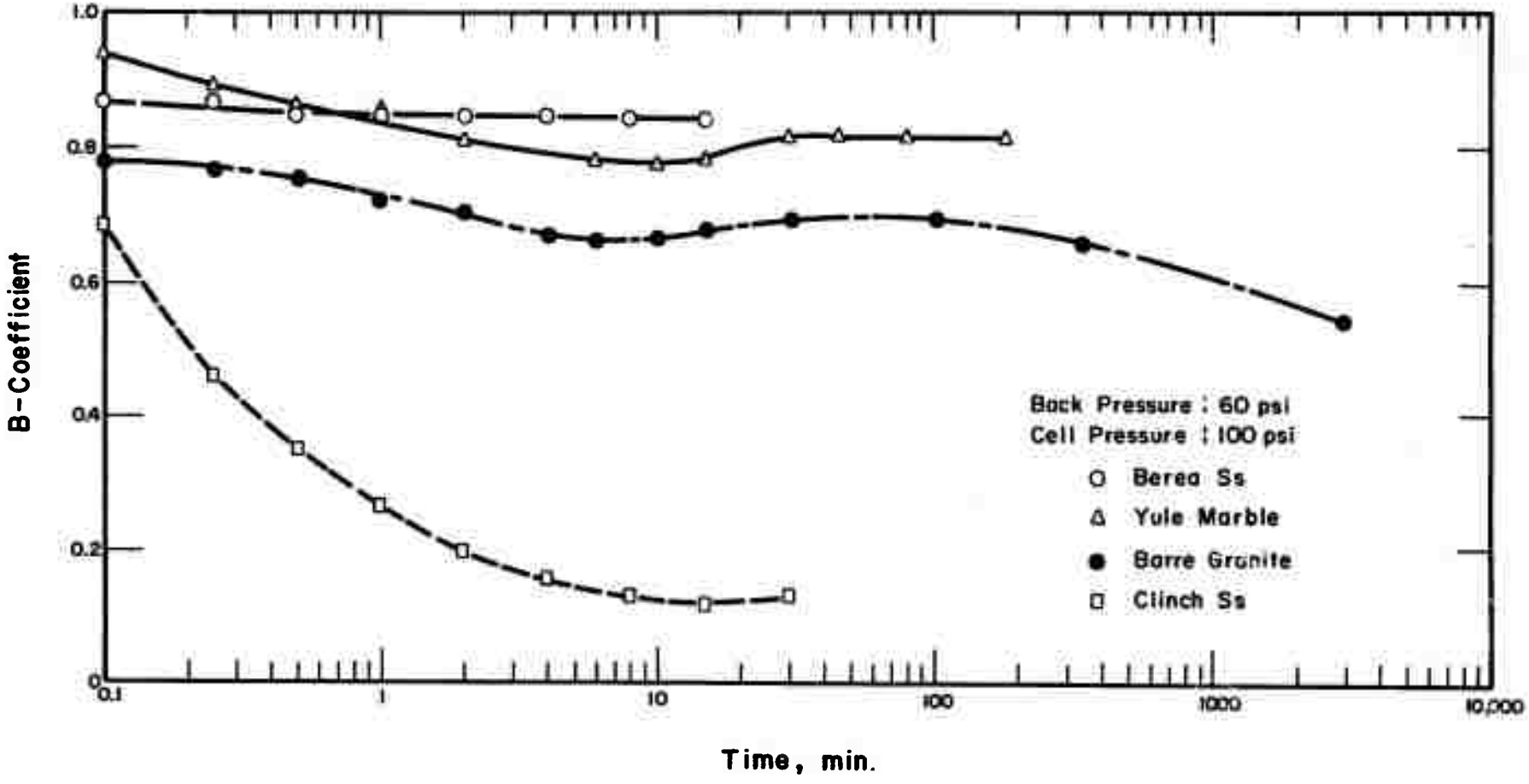

Fig. 4.13. B Coefficient Measurements Indicating Pore Pressure Fluctuation with Time

SECTION 5

DISCUSSION

5.1 Unconfined Compression Tests

Five series of unconfined compression tests were performed on Barre granite, Clinch sandstone, Nevada tuff, Yule marble, and Berea sandstone, with rates of strain varying from 0.0001 inch/inch/min. to 10.0 inch/inch/min. Tests were performed on dry and saturated specimens. The purpose of these tests was to study the influences of the load induced pore pressures on the strength of rock.

If the rock aggregate structure tends to decrease in volume during axial compression, it would be expected in saturated specimens that positive pore water pressures would develop during shear, thereby decreasing the rock strength. The positive pore pressures reduce the effective normal stress at grain contacts in the rock, thus reducing shear resistance which is frictional in nature. If the rock aggregate structure tends to dilate during axial compression, negative pore pressures would develop and the specimen would be stronger when saturated. The pore pressure effects would be more pronounced at higher rates of strain where the rate of generation of excess pore pressure exceeds the rate at which pore water can flow through the rock and dissipate.

If the strength of saturated specimens is less than the strength of dry specimens, even at slow rates of strain, this would indicate that the presence of water in the voids has some deleterious effect on the strength of the rock. The pore fluid could be adsorbed to the surfaces of mineral grains and change the frictional character-

istics of the mineral surfaces. If the interaction of pore fluid with mineral surface reduces the frictional characteristics of the surface, this interaction would result in reduced shear resistance at grain contacts and thus reduced strength for the rock. From a different mechanistic point of view, it could be considered that part of the effective normal stress at mineral contacts is carried by highly adsorbed fluid molecules, such that this portion of the effective normal stress does not contribute to shear resistance at the contacts.

For all five rock types which were tested in this investigation, even at the slowest rates of strain, the strength of saturated samples were less than the strength of the samples which were tested dry. For Berea sandstone and Clinch sandstone, where the strengths of dry and saturated specimens appear to approach each other as strain rate decreases, all or most of the observed difference in strength could be due to pore pressure effects. In the case of Yule marble, there appears to be a definite deleterious effect of water on the strength of rock, since for slowtests saturated specimens were weaker, but became stronger as the rate of strain increased (see later discussion of pore pressure effect). For Barre granite and Nevada tuff, the saturated specimens are weaker than the dry specimens and the difference in the strength of the dry and saturated specimens is not influenced by the strain rate. This could either indicate that for these rocks the only effect of water is physico-chemical in nature or even the slowest tests were not slow enough for excess pore pressure dissipation. This latter effect seems likely for the very low porosity granite. Initially plans had been made to perform a limited number of unconfined compression tests using an inert pore fluid such as benzene which does not interact with the mineral surfaces. These tests were not performed for two

reasons. First the extensive literature survey partly answered the question of the deleterious effects of pore fluids on rock strength. Pore fluids such as water, which are strongly adsorbed to the mineral surfaces, can influence surface friction. On the other hand fluids such as benzene, which are chatacterized by low dielectric constant and surface tension, most likely do not influence surface properties. The nature of the interaction and the magnitude of the effects are mainly determined by the minerology of the rock. A careful study of the question, particularly physico-chemical interaction, would require an extensive study in itself and is not within the scope of this investigation. A limited number of tests would be rather inconclusive and not very useful in delineating these complex interactions. There was another reason for not performing a few tests with inert fluids. Initially plans had been made to test ten samples of each rock type. The first series of unconfined compression tests on dry and water-saturated specimens gave results with a relatively large scatter. Therefore no useful conclusions could be drawn based on the initial series of tests. In order to obtain a better picture of the average behavior of the rocks, the decision was made to test from ten to twenty more rock samples of each rock type.

In the case of Barre granite, the strength of samples tested dry increased with increasing strain rate. The dry specimens of Yule marble and Nevada tuff did not show any significant change in strength with change in strain rate. The increase in strength with increased strain rate could be due to better interlocking effect between rock grains, since grain deformation and relocation could be viscous (time-dependent) in nature.

It appears that Berea sandstone and Clinch sandstone had a tendency to experience volume reduction during compression. Therefore positive excess pore water pressures were generated which resulted in decreased strength for the saturated specimens. The difference between the strengths of dry and saturated specimens becomes more pronounced as strain rate increases, thus reinforcing the assumption of a significant pressure effect. On the other hand for Barre granite and Nevada tuff, the difference in the strength of dry and saturated specimens remains practically constant at all strain rates. This would either indicate that pore water pressures were not of any significance in these rock types, or most likely, even the slowest rate of strain used in this investigation was too fast for pore pressure dissipation.

The results of tests on Yule marble indicate that this rock had a tendency to dilate during compression. The strength of saturated specimens is significantly lower than the strength of dry specimens at slow rates of strain. As rate of strain increases, the strength of saturated specimens increases (negative pore pressures increase the effective confining pressure), while the strength of dry specimens remains approximately constant.

Using the values of unconfined compressive strength of dry and saturated specimens, and assuming a value for the effective angle of friction and a linear failure envelope, Skempton's A coefficients were computed. It should be noted that these computations are based on the assumption that differences in strength of dry and saturated specimens are caused entirely by pore water pressure effects.

During the planning stage of the investigation the possibility of performing a very limited number of tests on artificially jointed

rock was suggested. For reasons similar to those given for eliminating the tests using inert fluids, no tests were performed on jointed rock. It is practically impossible to perform unconfined compression tests on jointed rock and a few tests would be of no significant value in studying the several important parameters. Furthermore it appears certain that along joint surfaces, Terzaghi's effective stress equation will be fully applicable, and Skempton's B coefficient will be unity. Finally it should be noted that unconfined compression tests were performed on five rock types rather than on four types as originally planned.

5.2 Triaxial Tests

Skempton's B coefficients were measured for Barre granite, Clinch sandstone, Yule marble, and Berea sandstone in a specially designed triaxial cell. The B coefficient is defined as the ratio or the change in pore pressure to the change in all around confining pressure under undrained conditions. Skempton's equation for B coefficient includes the compressibilities of the pore fluid and aggregate structure and is based on the assumptions that solids are relatively incompressible and that Terzaghi's effective stress equation is applicable.

The literature survey indicates that there have been extensive studies dealing with the applicability of the effective stress equation to rock. For this purpose, the compressive strength of jacketed and unjacketed rock specimens have been compared under dry and saturated conditions. The conclusion appears to be that the effective stress equation will hold true for all rock types except those of very low porosity (boundary porosity less than unity), particularly if the pores

are disconnected. Also as the effective confining pressure increases beyond the yield strength of the rock grains, the individual grains of rock undergo plastic deformation, thus reducing boundary porosity and rendering the effective stress equation less applicable. Rocks which are composed of minerals with low yield strength obviously will undergo plastic deformation under relatively small confining pressures. It should also be noted that under conditions where failure takes place by the progressive formation of microcracks, pore fluid pressure will have access to all of the fracture surface at the time of failure and the effective stress equation will be applicable.

The value of the B coefficient will be close to unity whenever the compressibility of the rock aggregate structure is much larger than the compressibility of the pore water. In cases where the compressibility of the rock is close to or even smaller than the compressibility of water, Skempton's equation for B coefficient does not apply and the compressibility of rock solids has to be taken into account in any equation for the B coefficient. Of course in cases where the compressibility of the rock aggregate structure is less than the compressibility of water and approaches the compressibility of its mineral solids, Terzaghi's effective stress equation most likely will not be applicable.

The test results on Berea sandstone, Yule marble, Barre granite, and Clinch sandstone are very interesting and rather surprising in some respects. At a back pressure of about 100 psi and a cell pressure of about 140 psi Berea sandstone and Yule marble gave B coefficients of unity. Under the same conditions Barre granite and Clinch sandstone gave a B value of about 0.85. In all rocks, B coefficients were low under small back pressures and continuously increased as the back

pressure was increased. It appear that it was not possible to saturate the specimens under pressure gradients without applying a back pressure, and the degree of saturation increased as back pressure increased. A more detailed analysis and discussion of B coefficient measurements are referred to the second phase of study where this problem will be considered in detail along with triaxial compression tests.

5.3 Summary and Recommendations

The objective of this research program is to determine the influence of pore water pressure on the engineering properties of rock. The research program for the first year of the investigation consisted of performing unconfined compression tests with different rates of strain on five rock types having a range of compressibilities and permeabilities, under dry and saturated conditions. The purpose of these tests was to determine the nature of the effects of excess pore water pressures which may develop in rock when it is subjected to shear stresses. Also a special triaxial cell was designed and constructed. The triaxial cell was used to saturate rock specimens, to measure rock permeabilities, and to measure rock pore water pressures under changes in all-around confining pressure (isotropic compression).

A comprehensive literature survey was made in order to review and summarize published theoretical and experimental studies of pore pressure and effective stress in rock and other similar porous materials. There have been extensive studies dealing with the application of the effective stress equation to rock. For this purpose, the compressive strength of jacketed and unjacketed rock specimens have been compared under dry and saturated conditions. The conclusion appears to be

that the Terzaghi effective stress equation will hold true for rocks, except for those of very low porosity, particularly if the pores are disconnected. Also as the effective confining pressure increases beyond the yield strength of the rock grains, the individual grains of rock undergo plastic deformation, thus reducing boundary porosity. For this condition, the effective stress equation is less applicable. The literature survey also indicated that pore fluids which have a high dielectric constant and are strongly adsorbed to the mineral surfaces, such as water, can influence the surface properties of rock grains and the shear resistance at contacts. The nature of the interactions and the magnitude of these effects are mainly determined by the mineralogy of the rock.

Five series of unconfined compression tests were performed on Barre granite, Berea sandstone, Clinch sandstone, Nevada tuff, and Yule marble. In all, a total of 112 unconfined compression tests were performed with rates of strain varying from 0.0001 inch/inch/min. to 10.0 inch/inch/min. Tests were performed using 2 1/8-inch diameter and 4 1/2-inch long rock specimens under dry and saturated conditions. Pore water had some influence on the strength of all rock types tested. For Berea sandstone and Clinch sandstone, the strengths of the saturated samples were less than the strength of the samples which were tested dry. But as the rate of strain was decreased, the difference in the strength of dry and saturated specimens decreased. This behavior seems to suggest that the decrease in the strength of saturated specimens would be explained by positive pore pressure effects (positive A coefficients). In the case of Yule marble, both the deleterious effects of water and pore pressure effects were apparent. The saturated specimens were weaker than the dry specimens at slow rates of loading, but as the

rate of strain was increased, the saturated specimens increased in strength, while the strength of dry specimens remained practically constant. The increase in the strength of the saturated specimens of Yule marble with increase in strain rate is attributed to dilation of the rock during compression, producing the generation of negative pore water pressures (negative A coefficients). For Barre granite and Nevada tuff, the saturated specimens were weaker than the dry specimens and the difference in the strength of the dry and saturated specimens remained constant at all strain rates. In the case of Nevada tuff the strength and reduction could be due to deleterious effects of water, whereas for Barre granite the reduction in the strength of saturated specimens is more likely due to positive pore pressure effects which were not appreciably influenced by the rate of strain.

A special triaxial compression cell was designed and constructed. The triaxial cell was successfully used to saturate, measure permeabilities, and measure B coefficients of rock. This cell will also be used in the second phase of the study to perform undrained and triaxial compression tests with pore water pressure control.

Skempton's B coefficients were measured for Barre granite, Clinch sandstone, Yule marble and Berea sandstone. Skempton's equation for B coefficient includes the compressibilities of the pore fluid and aggregate structure and is based on the assumption that solids are relatively incompressible and Terzaghi's effective stress equation is applicable. According to Skempton's equation, the value of B coefficient will be close to unity whenever the compressibility of the rock aggregate structure is much higher than the compressibility of the pore water. In cases where the compressibility of rock is close to or even smaller than the compressibility of water, Skempton's equation for B

coefficient does not apply and in this case the compressibility of rock solids has to be included in any equation for prediction of B coefficients.

Rather interesting and, in some respects, surprising results were obtained in the B coefficients measurements. At a back pressure of about 100 psi, and a cell pressure of about 140 psi, Berea sandstone and Yule marble gave B coefficients of unity. Under the same conditions, Barre granite and Clinch sandstone gave a B value of approximately 0.85. In all rocks, B coefficients were low under small back pressures and continuously increased as back pressure increased.

It is recommended that B coefficient measurements be continued during the second phase of the study to include more samples and a variety of rock types and a higher range of pressures. This could be easily done without additional expense during the second phase of the study since triaxial compression tests are to be performed in the same triaxial cell which was used for B coefficient measurements.

SECTION 6

APPENDIX

DETAILED DESIGN DRAWINGS OF THE TRIAXIAL CELL

Cell Base (A)

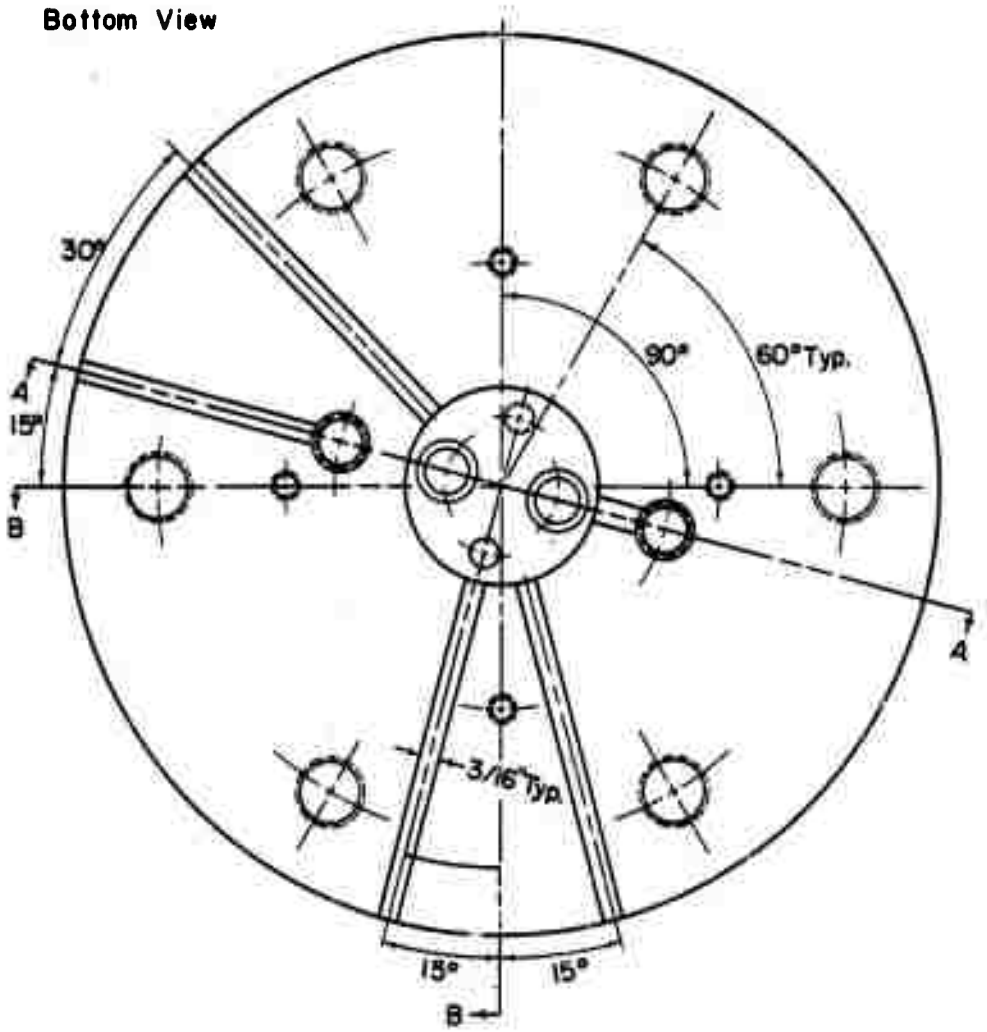

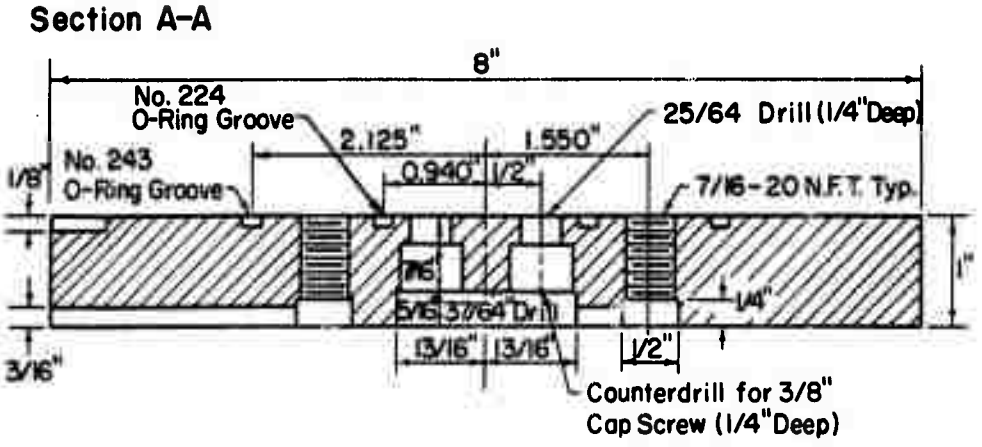

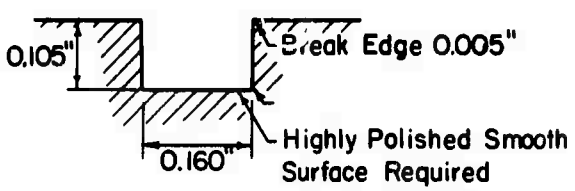

Material : Stoinless Steel

Fig. 6.1. Cell Base A, Plan and Section A-A

Cell Base (A)

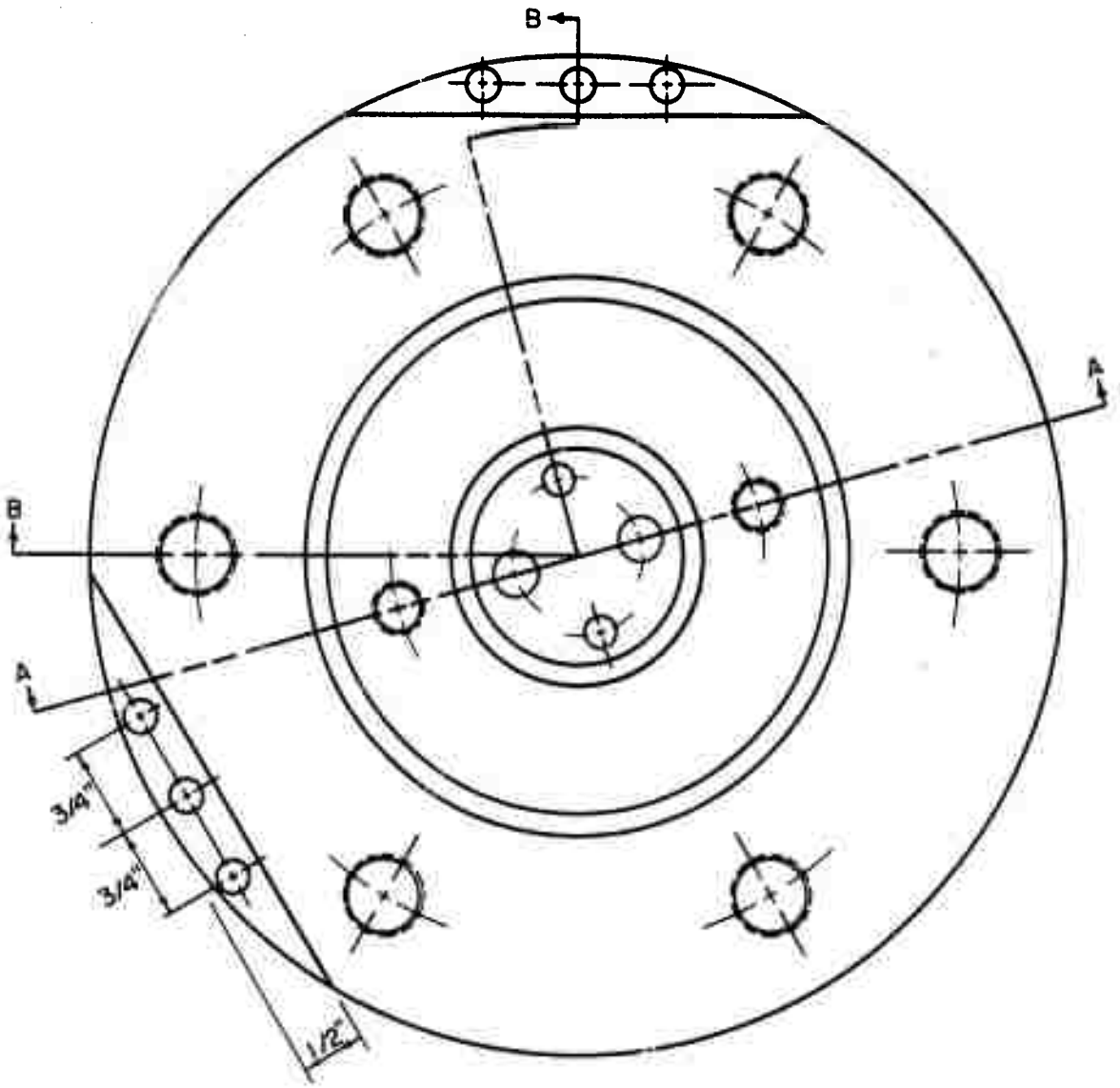

Top View

Material: Stainless Steel

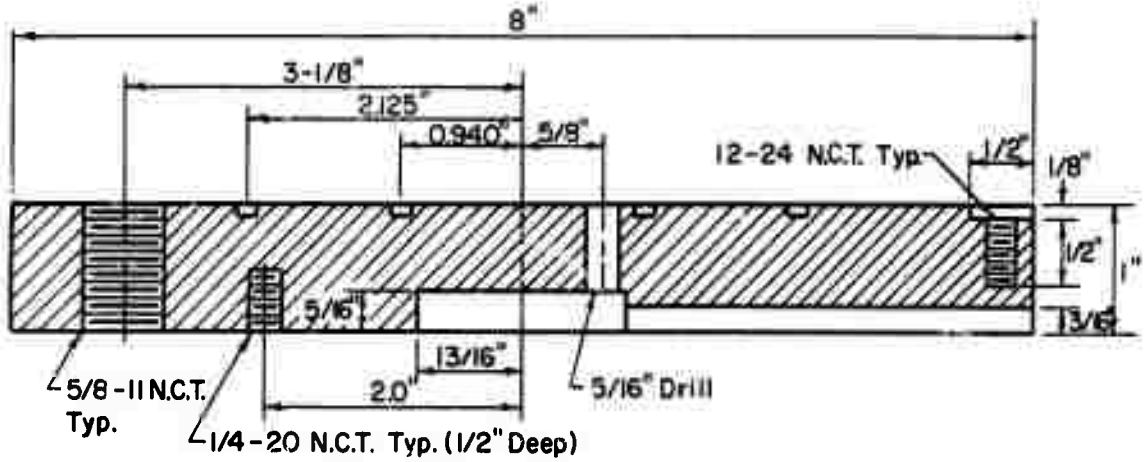

Section B-B

Fig. 6.2. Cell Base A, Plan and Section B-B

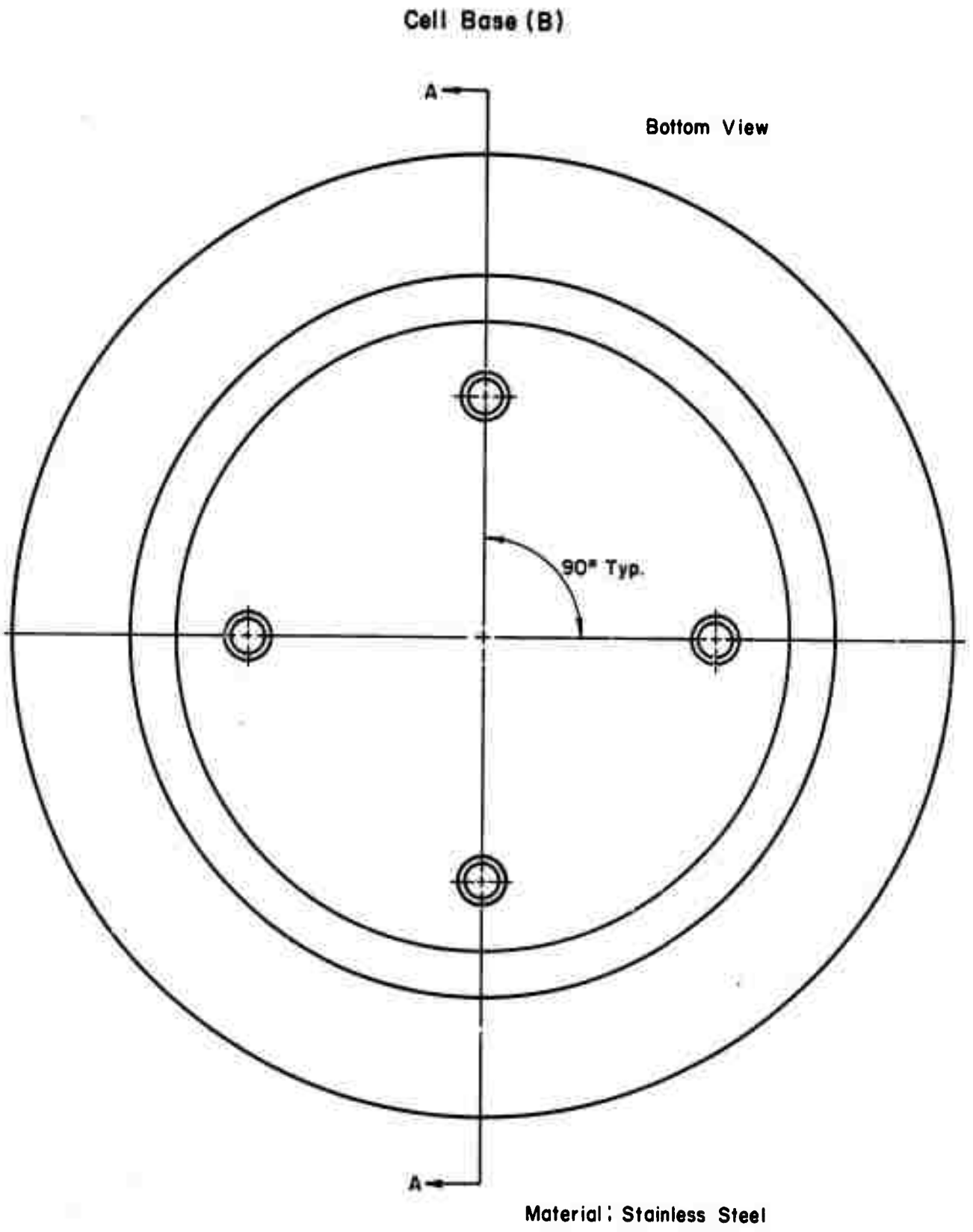

Fig. 6.3. Cell Base B, Plan

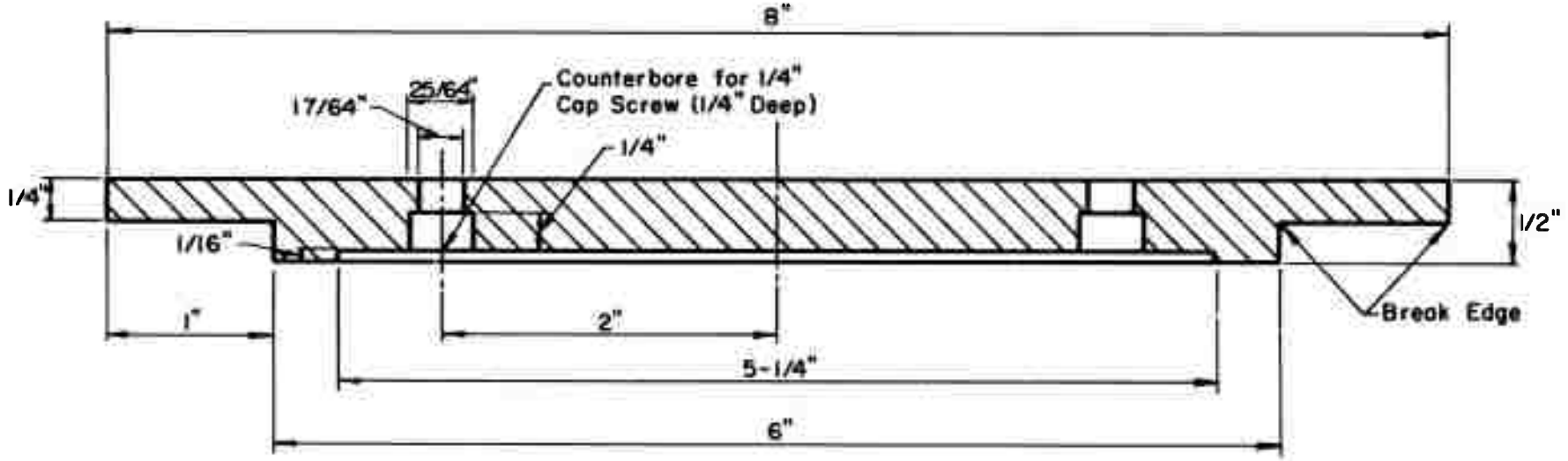

Material : Stainless Steel

Base — (B), Cross Section A-A

Fig. 6.4. Cell Base B, Section A-A

Cell Body

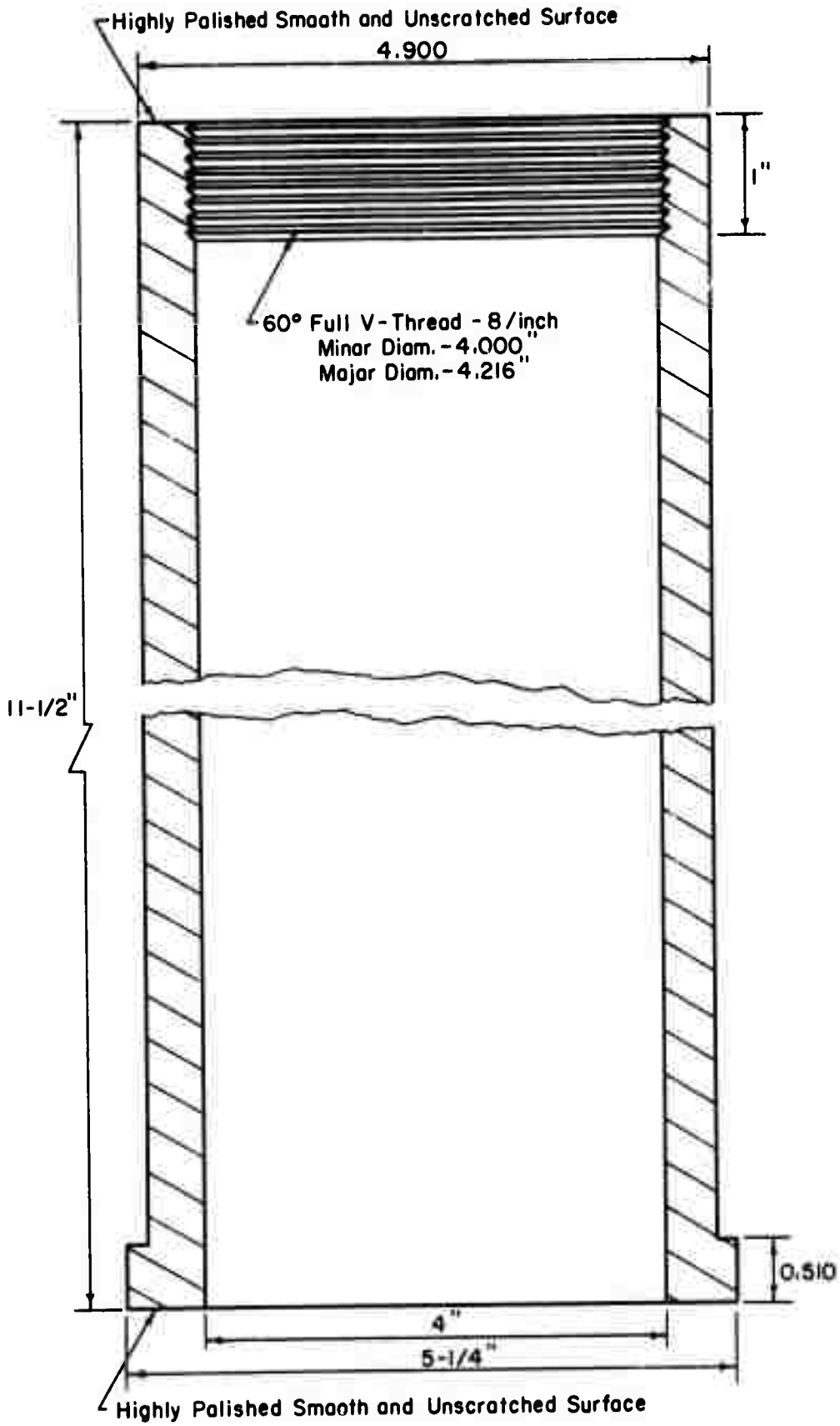

Material: Cold Drawn Steel Seamless Tubing, 5-1/4" O.D. 5/8" Wall Thickness
All Dimensions In Inches

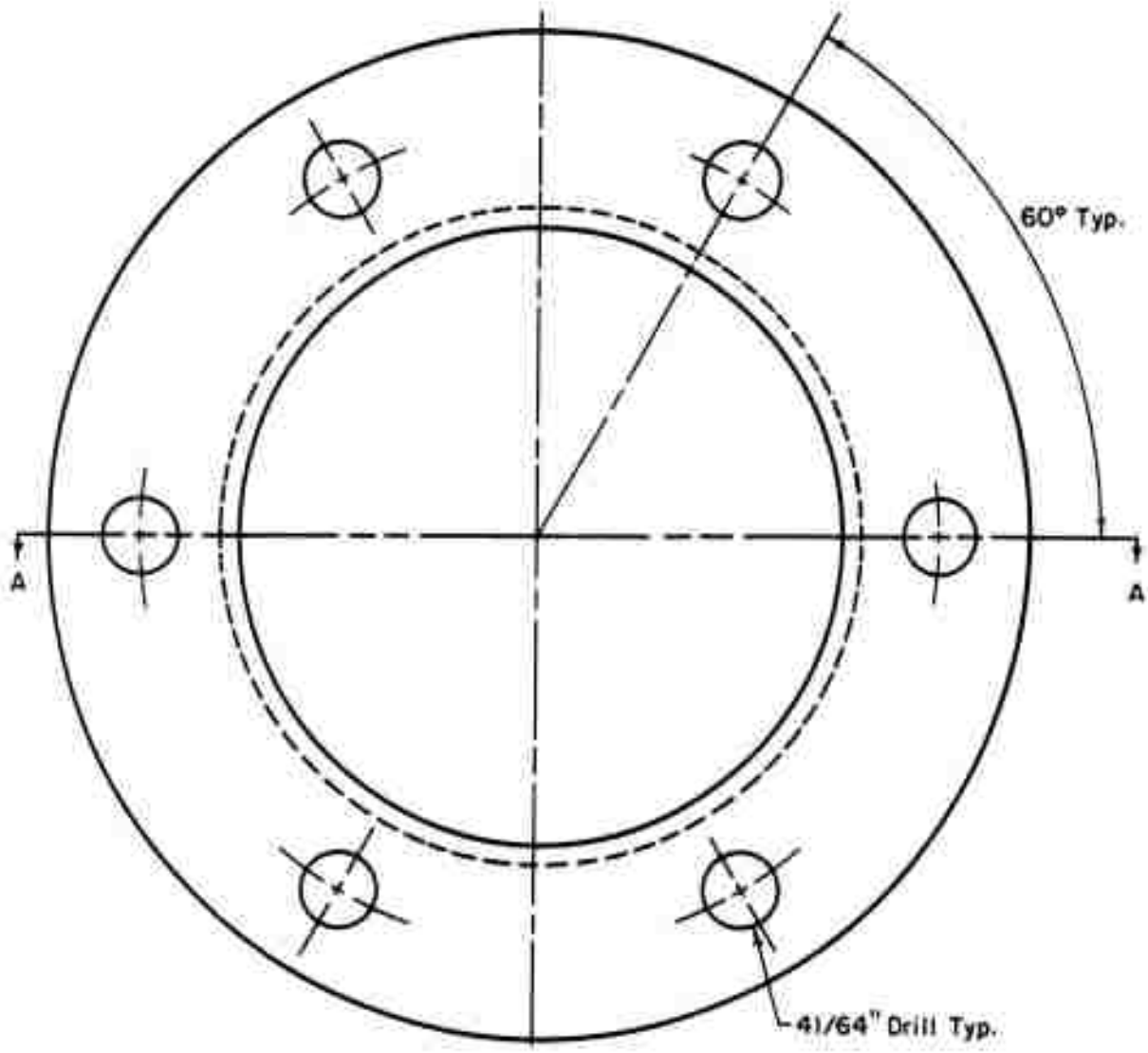

Cell Body Flange - Top View

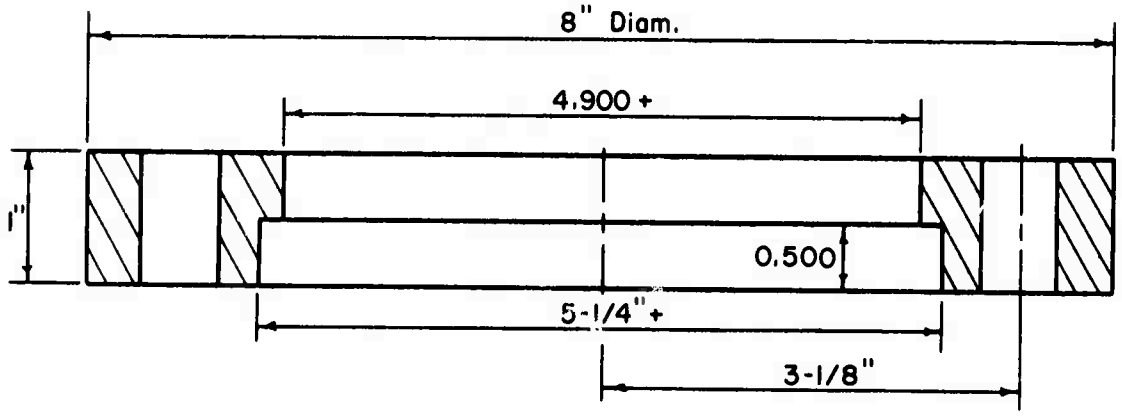

Section A—A

Material: Stainless Steel
All Dimensions In Inches

Fig. 6.6. Cell Body, Top View and Section A-A

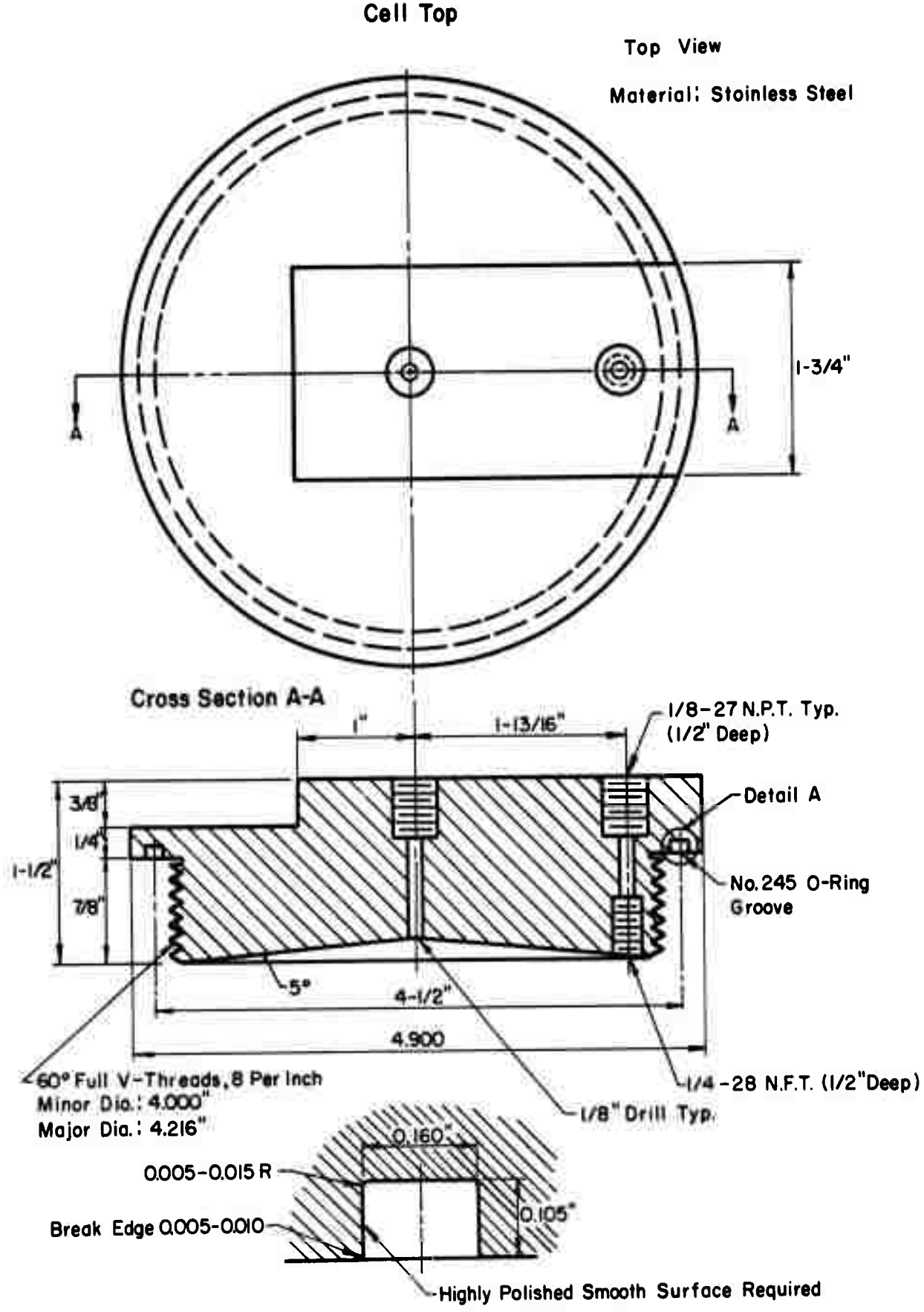

Fig. 6.7. Cell Top; Top View, Section A-A, and Detail A

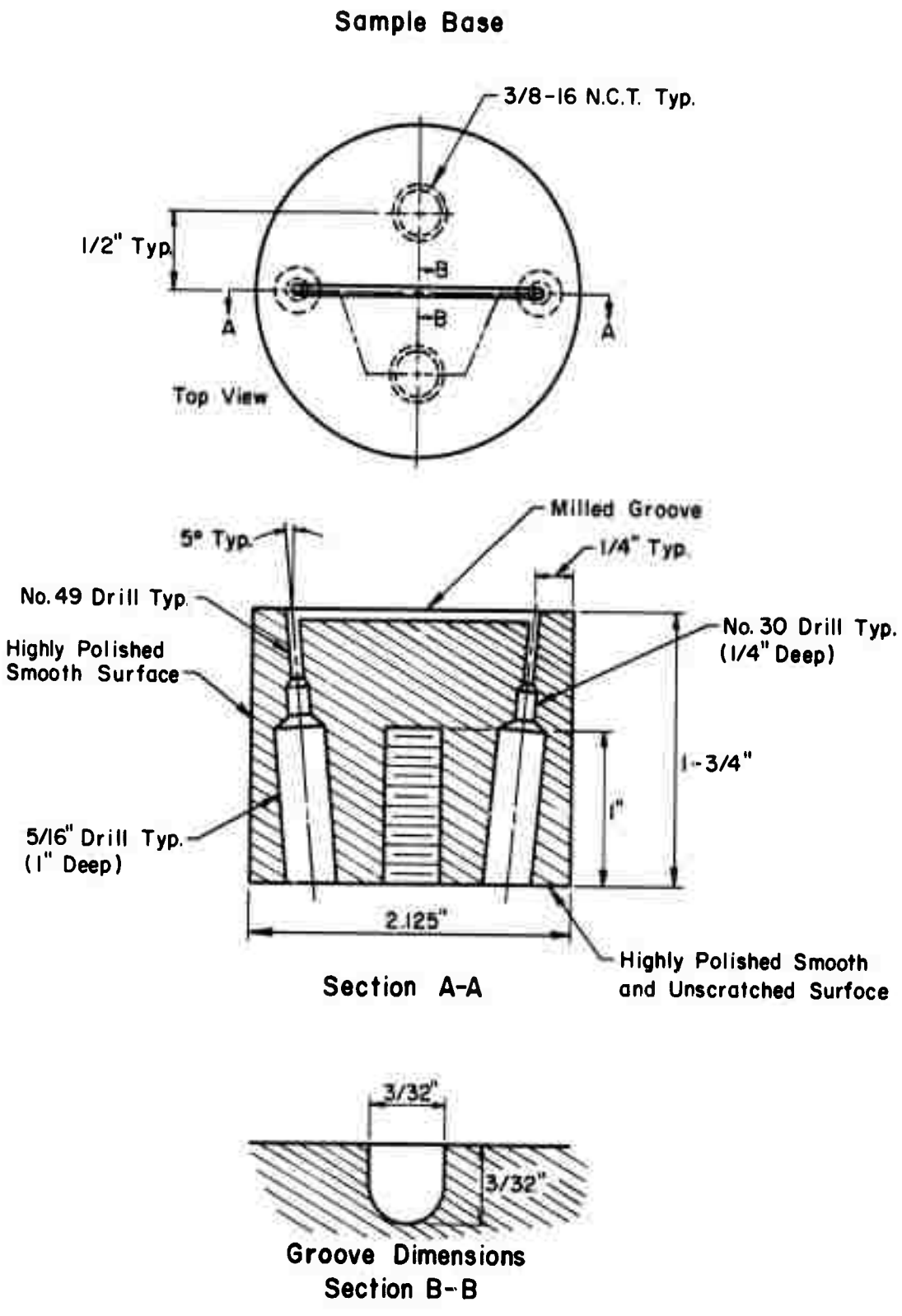

Fig. 6.8. Sample Base, Top View and Sections A-A and B-B

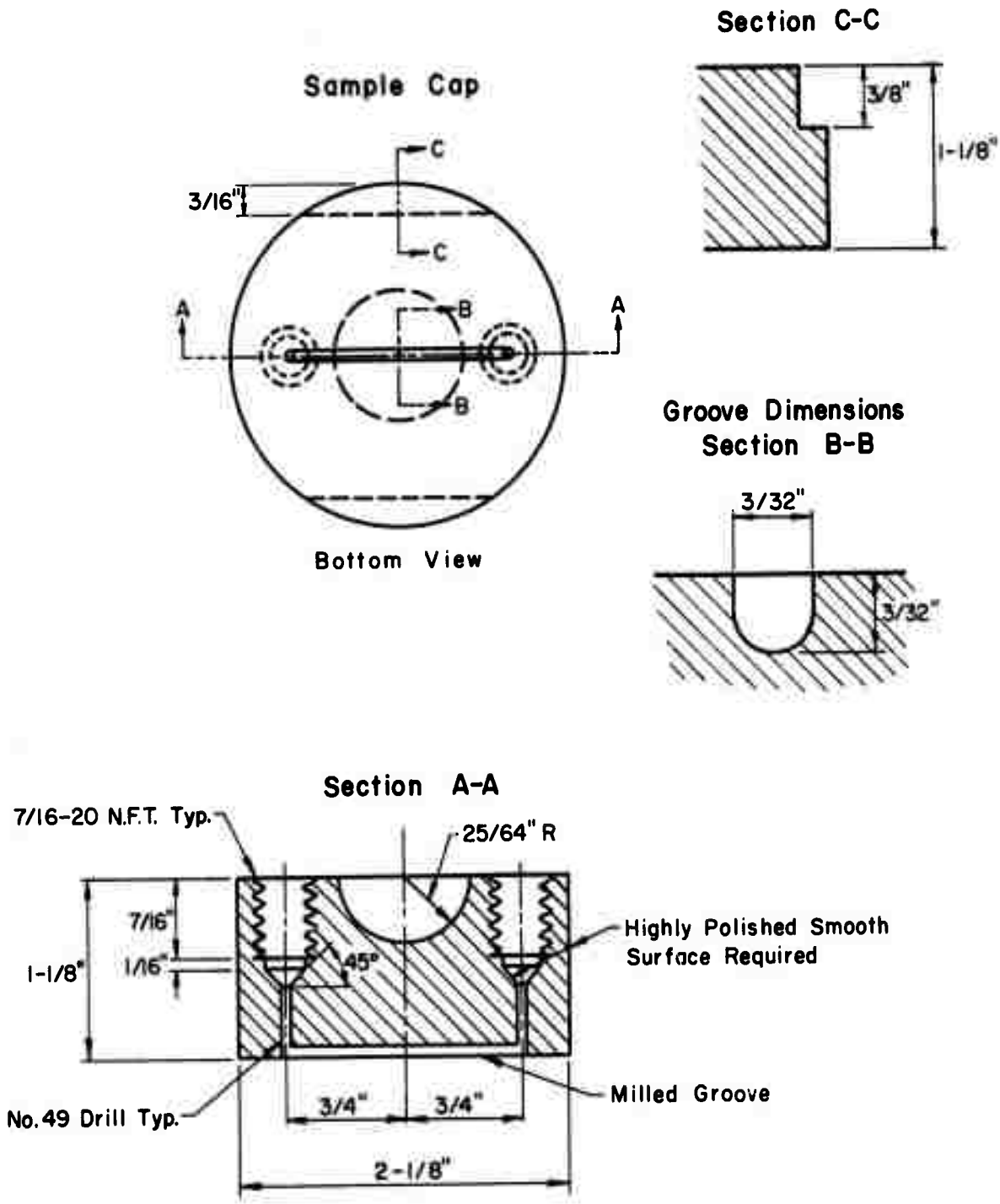

Fig. 6.9. Sample Cap; Bottom View and Sections A-A, B-B and C-C

Fixing Plate for Fittings

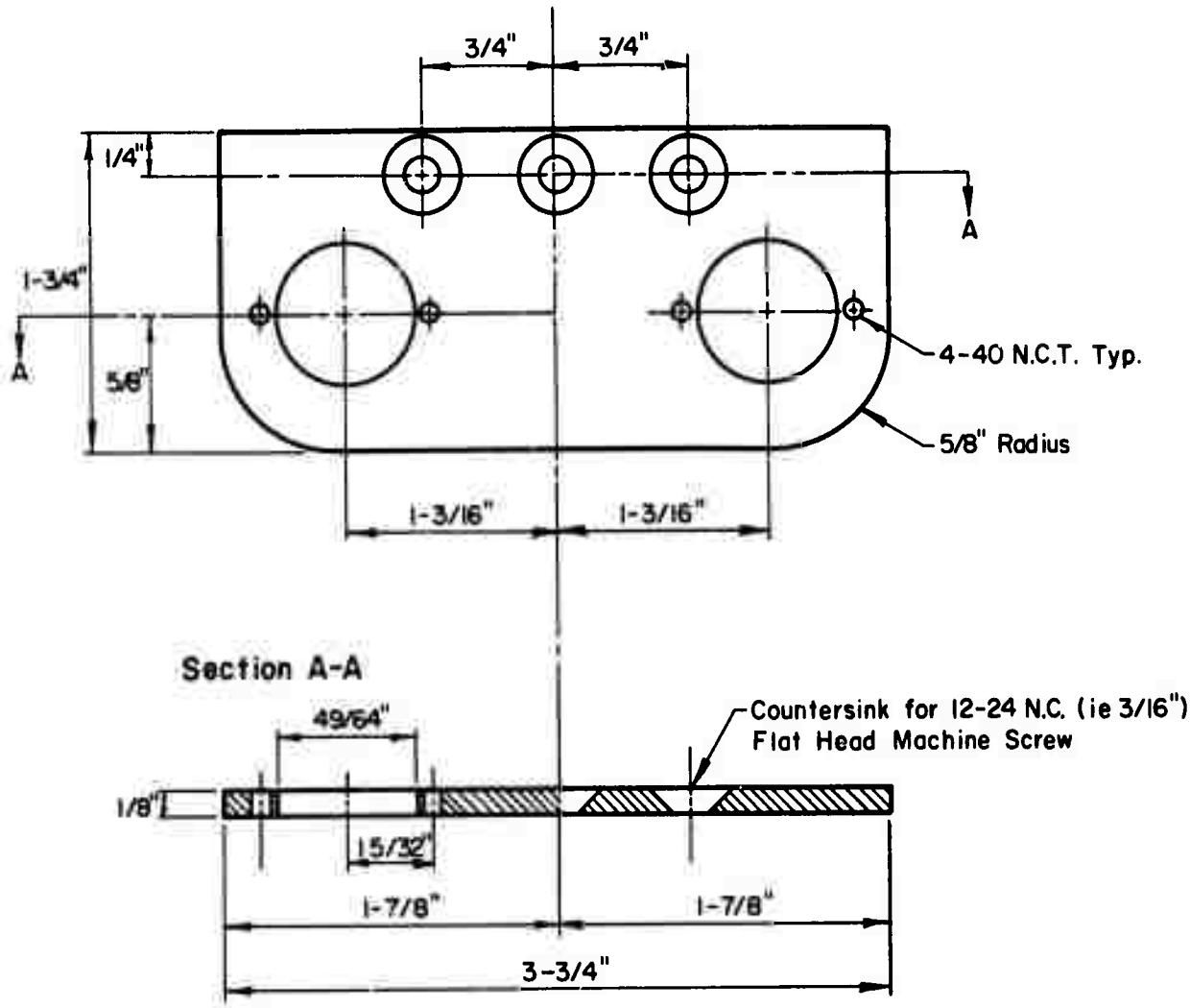

Material : Stainless Steel

Fig. 6.10. Fixing Plate for Fittings, Plan and Section A-A

Cell Base Fixing Rod

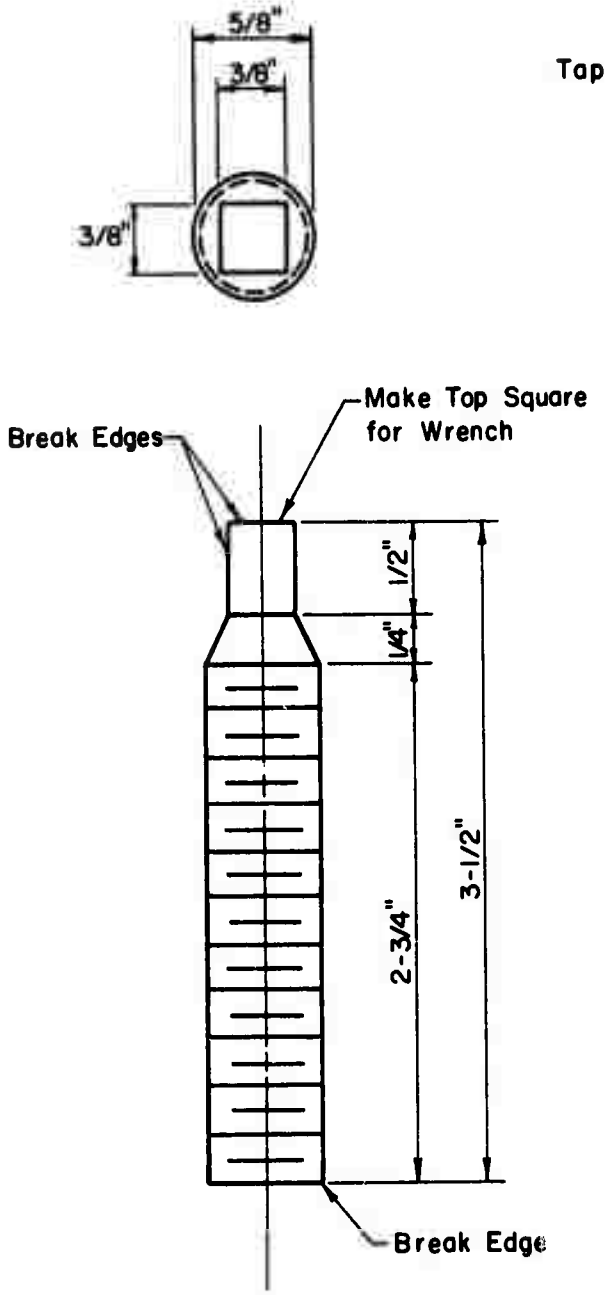

Material : Heat Treated Stainless
Threaded Bar, 5/8 - 11 N.C.T.

Drain Tube

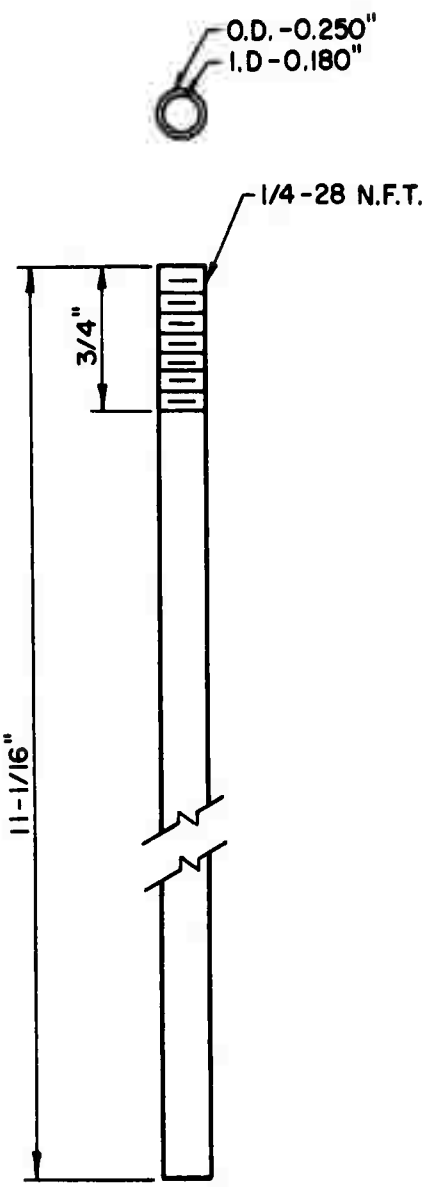

Material: Stainless Tubing

Fig. 6.11. Cell Base Fixing Rod and Drain Tube

Sample Cap Drainage Fitting (B)

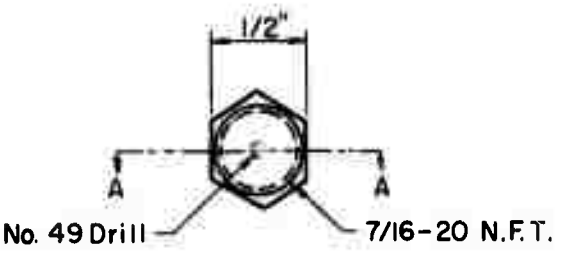

Top View

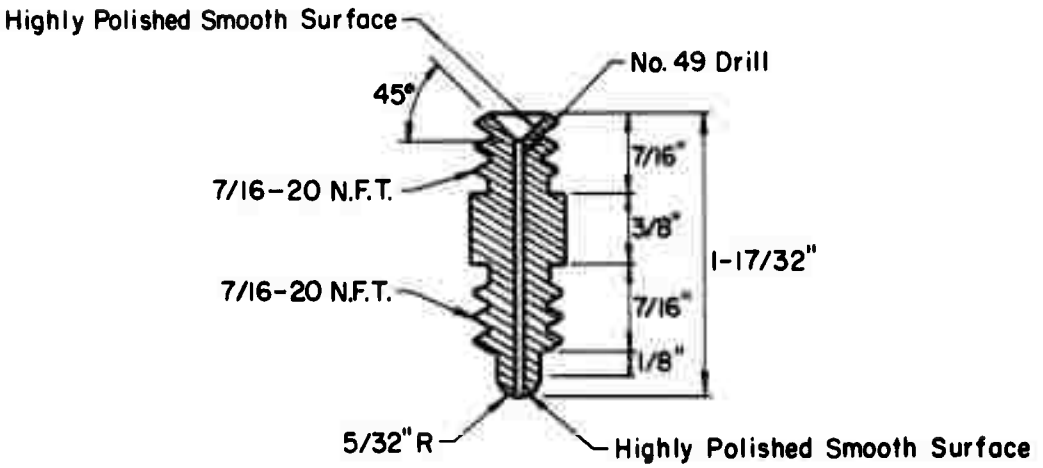

Section A-A

Material: 1/2" Hexagonal Stainless Stock

Fig. 6.12. Sample Cap Drainage Fitting B, Top View and Section A-A

Pore Pressure and
Volume Change Fittings

Fixing Nuts

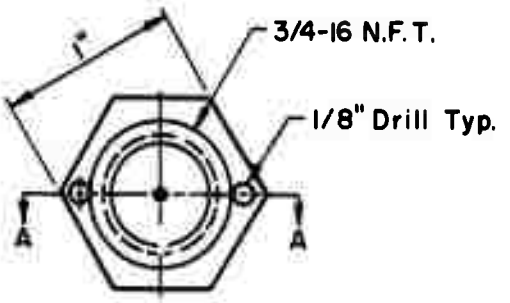

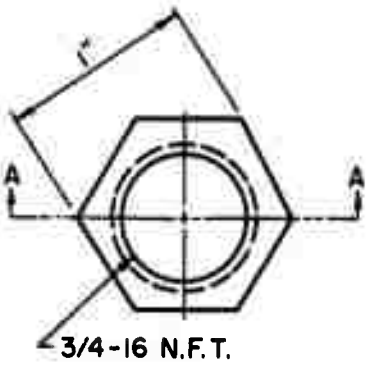

Top View

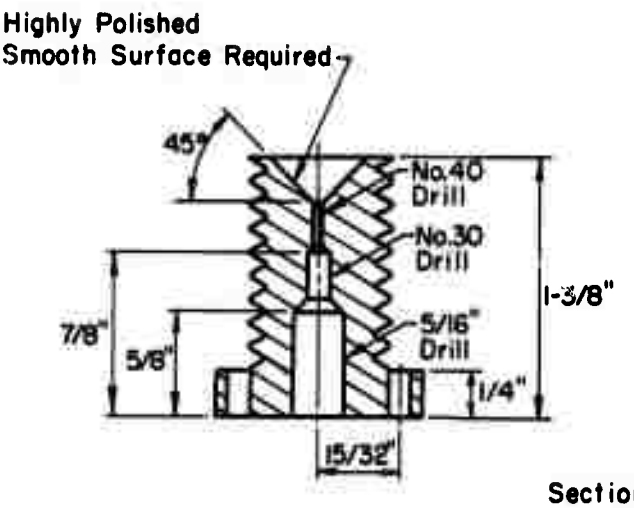

Section A-A

Material: 1" Hexagonal Stainless Steel Stock

Fig. 6.13. Pore Pressure and Volume Change Fittings and Fixing Nuts

Loading Cap Drainage Fittings (A)

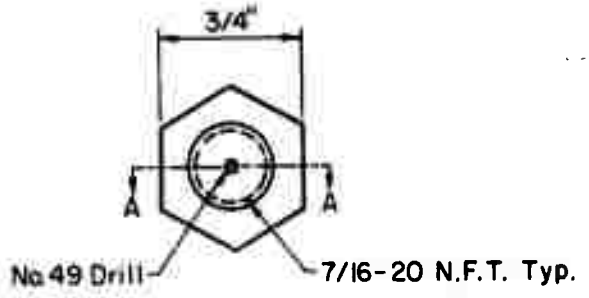

Top View

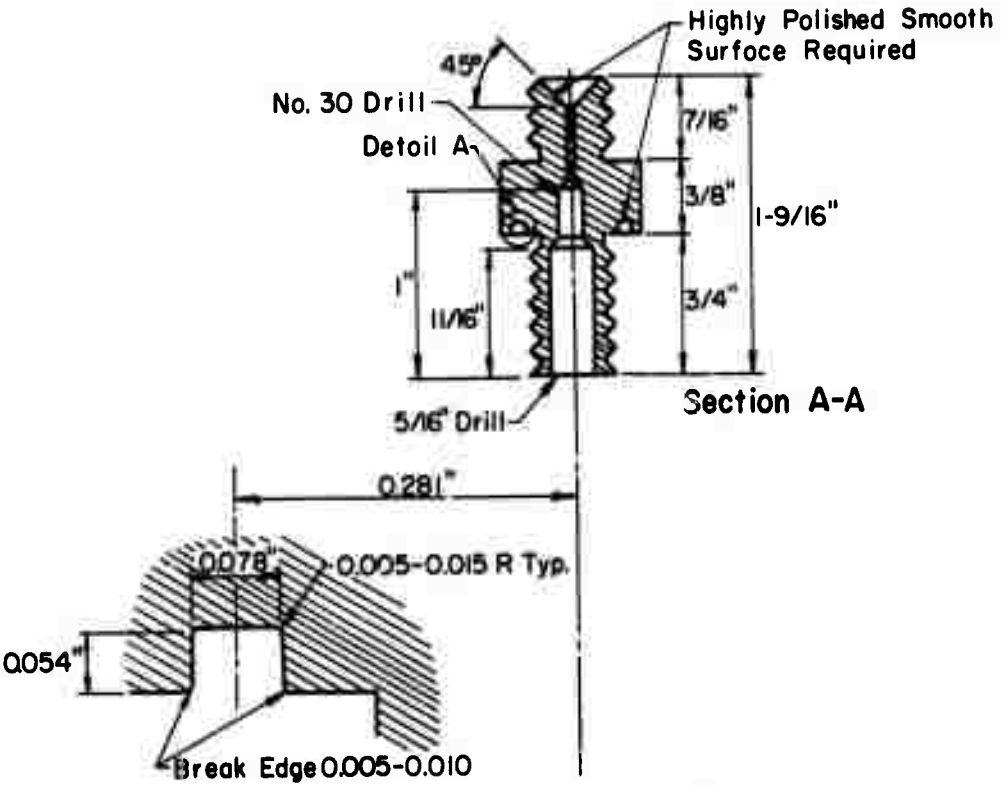

014 O-Ring Groove

Detail A

Material : 3/4" Hexagonal Stainless Steel

Fig. 6.14. Loading Cap Drainage Fittings A; Top View, Section A-A, and Detail A

Connection for Drainage Fittings

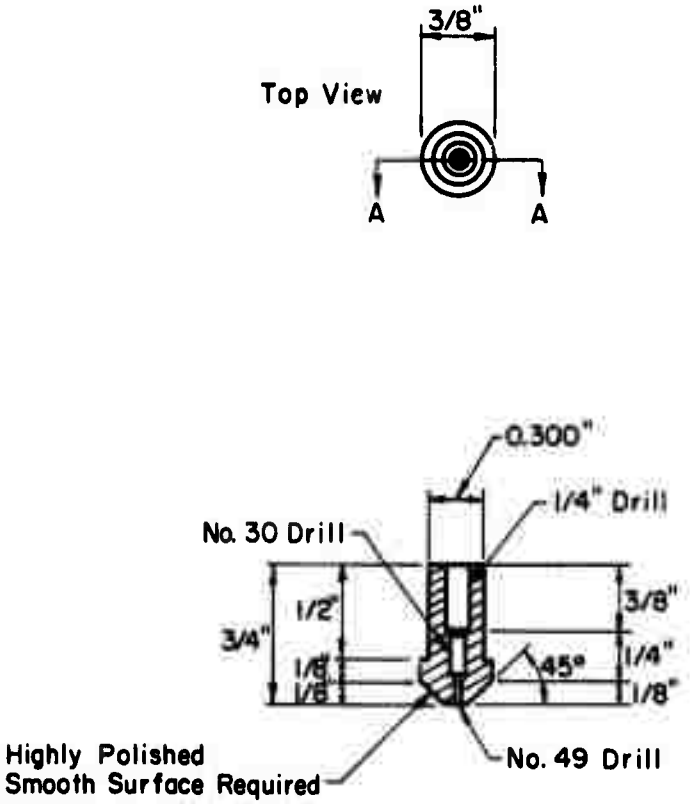

Material: Stainless Stock

Fig. 6.15. Connection for Drainage Fittings, Top View and Section

Drainage and Back-Pressure Fittings

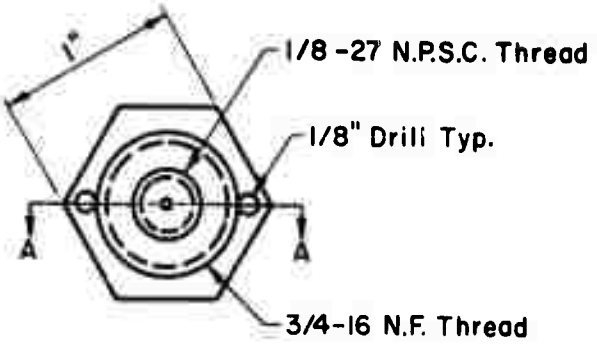

Top View

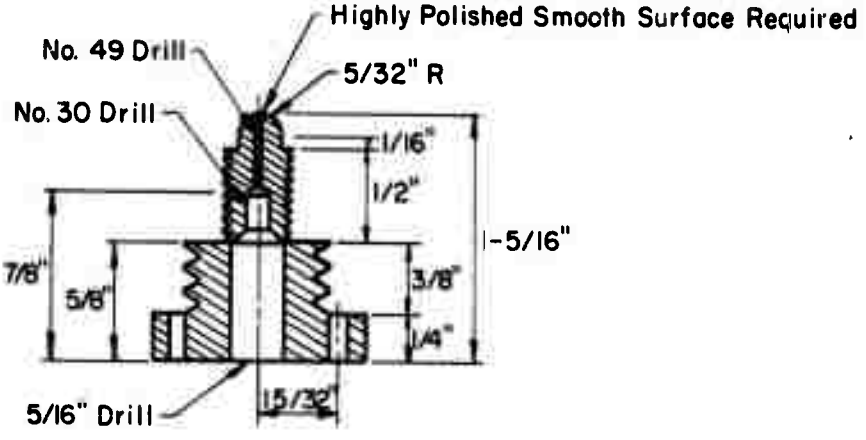

Section A-A

Material : 1" Hexagonal Stainless Stock

Fig. 6.16. Drainage and Back Pressure Fittings, Top View and Section

SECTION 7

BIBLIOGRAPHY

Bieniawski, Z. T. (1967), "Mechanism of Brittle Fracture of Rocks," International Journal of Rock Mechanics and Mining Sciences, Parts 1 and 2, October.

Biot, M. A. (1941), "General Theory of Three Dimensional Consolidation," Journal Applied Physics, Vol. 12, pp. 155-164.

Boozer, G. D., K. H. Hiller, and S. Serdengecti (1963), "Effects of Pore Fluids on the Deformation Behaviour of Rocks Subjected to Triaxial Compression," Rock Mechanics, Pergammon Press, pp. 579-625.

Brace, W. F. (1968), "The Mechanical Effects of Pore Pressure on Fracturing of Rocks," Proceedings, Conference on Research in Tectonics, Geological Survey of Canada, Paper 68-52.

Brace, W. F. and J. D. Byerlee (1966), "Recent Experimental Studies of Brittle Fracture of Rocks," 8th Symposium of Rock Mechanics, Minnesota, pp. 58-81.

Brace, W. F. and R. J. Martin, III (1968), "A Test of the Law of Effective Stress for Crystalline Rocks of Low Porosity," International Journal of Rock Mechanics & Mining Sciences, Vol. 5, p. 415.

Bredthauer, R. O. (1957), "Strength Characteristics of Rock Samples Under Hydrostatic Pressure," Trans. American Soc. of Mechanical Engineers 79, pp. 695-708.

Carlson, R. W. (1956), "Permeability, Pore Pressure and Uplift in Gravity Dams," Trans. American Society of Civil Engineers, December, pp. 587-613.

Colback, P. S. B. and B. L. Wiid (1965), "The Influence of Moisture Content on the Compressive Strength of Rocks," Proceedings of Rock Mechanics Symposium, Dept. of Mines, Ottawa.

Deere, D. U. and R. P. Miller (1966), "Engineering Classification and Index Properties for Intact Rock," Air Force Weapons Laboratory Technical Report No. AFWL-TR-65-116.

Geertsma, J. (1957), "The Effect of Fluid Pressure Decline on Volumetric Changes of Porous Rocks," Trans. A.I.M.E., Vol. 210, pp. 331.

Griggs, D. T. (1936), "Deformation of Rocks under High Confining Pressures," Journal of Geology, Vol. XLIV, pp. 541-577.

Handin, J. R., V. Hager, Jr., M. Friedman and J. N. Feather (1963), "Experimental Deformation of Sedimentary Rocks under Confining Pressure: Pore Pressure Tests," Bulletin of the American Association of Petroleum Geologists, Vol. 47, No. 5.

Harza, L. F. (1947), "The Significance of Pore Pressure in Hydraulic Structures," Trans. American Society of Civil Engineers, pp. 1507-1528.

Heard, H. C. (1960), "Transition from Brittle Fracture to Ductile Flow in Solenhofen Limestone as a Function of Temperature, Confining Pressure and Interstitial Fluid Pressure," Fluid Pressures in Rock Deformation, Geological Socl. of America Memoir 79, pp. 193-226.

Horn, H. M. and D. U. Deere (1962), "Frictional Characteristics of Minerals," Geotechnique, Vol. 12, pp. 319-335.

Hubbert, M. K. and W. W. Rubey (1959), "Role of Fluid Pressure in Mechanics of Overthrust Faulting," Bulletin of the Geological Soc. of America, Vol. 70, pp. 115-166.

Kjaernsli, B. and A. Sande (1966), "Compressibility of Some Coarse Grained Material," Norwegian Geotechnical Institute, pp. 245-251.

Kowalski, W. C. (1966), "The Interdependence between the Strength and Void Ratio of Limestones and Marls in Connection with Their Water Saturating and Anisotropy," 1st International Conference on Rock Mechanics, Lisbon, pp. 143-144.

Lane, K. S. (1969), "Engineering Problems Due to Fluid Pressure in Rock," 11th Symposium of Rock Mechanics, pp. 501-537.

Lee, K. L., R. A. Morrison and S. C. Haley (1969), "A Note on the Pore Pressure Parameter B," Seventh International Conference on Soil Mechanics and Foundation Engineering, Vol. 1. pp. 231-238.

McHenry, D. (1948), "The Effect of Uplift Pressure on the Shearing Strength of Concrete," 3rd Congress on Large Dams, Stokholm, paper R48.

Murrel, S. A. F. (1963), "A Criterion for Brittle Fracture of Rocks and Concrete under Triaxial Stress, and the Effect of Pore Pressure on the Criterion," Rock Mechanics, Ed., C. Fairhurst, Pergammon Press, pp. 563-577.

Neff, T. L. (1966), "Equipment for Measuring Pore Pressure in Rock Specimens Under Triaxial Load," Special Technical Publication 402, American Society for Testing and Materials.

Rebinder, P. A. and V. Likhtman (1957), Proc. Second International Congress Surface Activity, Vol. III, pp. 563-580. Academic Press, New York.

Richart, F. E., Brandtzaeg and R. L. Brown (1928), "A Study of the Failure of Concrete under Combined Compressive Stresses," Publication of the Engineering Experiment Station, University of Illinois, Bulletin No. 185.

Robinson, L. H. (1959), "Effects of Pore and Confining Pressure on Failure Characteristics of Sedimentary Rocks," Quarterly Colorado School of Mines, Vol. 54, No. 3, (Incorporated in 1959 Rock Mechanics Symposium).

Robinson, L. H. and W. E. Holland (1969), "Some Interpretations of Pore Fluid Effects in Rock Failure," Rock Mechanics-Theory and Practice, 11th Symposium on Rock Mechanics.

Ros, M. and A. Eichinger (1928), "Versuche zur Klarung der Frage der Bruchgefahr. II. Nichtmetcallische Stoffe," Zurich, Eidgenossische Materialprofungsanstalt an der Eidgenossischen Technischen Hochscule, June, p. 57. (Diskussionsbericht Nr. 28).

Schwartz, A. E. (1964), "Failure of Rock in Triaxial Shear Test," 6th Symposium on Rock Mechanics, Rolla, pp. 109-131.

Skempton, A. W. (1954), "The Pore Pressure Coefficients A and B," Geotechnique, December, pp. 143-152.

Skempton, A. W. (1960), "Effective Stress in Soils,Concrete and Rocks," Proceedings, Conference on Pore Pressure and Suction in Soils, Butterworth, London, pp. 4-16.

Terzaghi, K. (1923), Die Berechnung der Durchlassikeitsziffer des Tones aus dem Verlauf der Hydrodynamischen Spannungserscheinungen: Sitz. Akad. Wiss. Wien, v. 132, p. 105-124.

Terzaghi, K. (1934), "Die Wirksame Flachen porositat des Betons," Zietschrift Osters. Ing. u. Arch.-ver., Heft 2.

Terzaghi, K. (1945), "Stress Conditions for the Failure of Saturated Concrete and Rock," reproduced in From Theory to Practice in Soil Mechanics, pp. 181-197.

Trollope, D. H. and E. T. Brown (1966), "Effective Stress Criteria of Failure of Rock Masses," 1st International Congress on Rock Mechanics, Lisbon, Vol. 1, pp. 515-519.

Von Karman, Theodor (1911), "Festigkeitsversuche unter allseitigem Druck," Mitt. Forschungsarb. d. V. D. I., Heft.

Walsh, J. B. and W. F. Brace (1966), "Cracks and Pores in Rocks," 1st International Conference on Rock Mechanics, Lisbon, pp. 643-646.

Weinbrandt, R. M. and I. Fatt (1969), "Scanning Electron Microscope Study of the Pore Structure of Sandstone," 11th Symposium of Rock Mechanics, pp. 629-640.

Wissa, A. E. (1969), "Pore Pressure Measurement in Saturated Stiff Soils," Journal of Soil Mechanics and Foundations Div., ASCE, July, pp. 1063-1073.

Zisman, W. A. (1933), "Compressibility and Anisotropy of Rocks at and near the Earth's Surface," Proc. N.A.S., Geology, Vol. 19.